NASA CR- 159,648

NASA-CR-159648
1979 0023170

LIQUID OXYGEN/LIQUID HYDROGEN BOOST/VANE PUMP for the Advanced Orbit Transfer Vehicle Auxiliary Propulsion System

ENGINEERING REPORT

SUNDSTRAND CORPORATION
SUNDSTRAND AVIATION FLUID PUMPING

PREPARED FOR

NATIONAL AERONAUTICS AND SPACE ADMINISTRATION

NASA LEWIS RESEARCH CENTER
CONTRACT NAS3-20401

1. Report No.
CR159648

2. Government Accession No.

3. Recipient's Catalog No.

4. Title and Subtitle
Liquid Oxygen/Liquid Hydrogen Boost/Vane Pump for the Advanced Orbit Transfer Vehicle Auxiliary Propulsion System.

5. Report Date
September, 1979

6. Performing Organization Code

7. Author(s)
F. Gluzek I. H. To J. Wollschlager
R. G. Mokadam J. D. Stanitz

8. Performing Organization Report No.

9. Performing Organization Name and Address
Sundstrand Corp.
Sundstrand Aviation - Fluid Pumping
2421 11th Street
Rockford, Illinois 61108

10. Work Unit No.

11. Contract or Grant No.
NAS 3-20401

12. Sponsoring Agency Name and Address
NASA - Lewis Research Center
Cleveland, Ohio 44135

13. Type of Report and Period Covered

14. Sponsoring Agency Code

15. Supplementary Notes

16. Abstract

A rotating, positive displacement vane pump with an integral boost stage was designed to pump saturated liquid oxygen and liquid hydrogen for APS of orbit transfer vehicle. This unit is designed to ingest 10% vapor by volume, contamination-free liquid oxygen and liquid hydrogen. The final pump configuration, predicted performance, and the major design work performed under this contract are included in this publication.

17. Key Words (Suggested by Author(s))
Material Selection
Leakage & Performance Estimation
Centrifugal Boost Stage
Vane Stage

18. Distribution Statement

19. Security Classif. (of this report)

20. Security Classif. (of this page)

21. No. of Pages

22. Price*

* For sale by the National Technical Information Service, Springfield, Virginia 22161

N79-31341

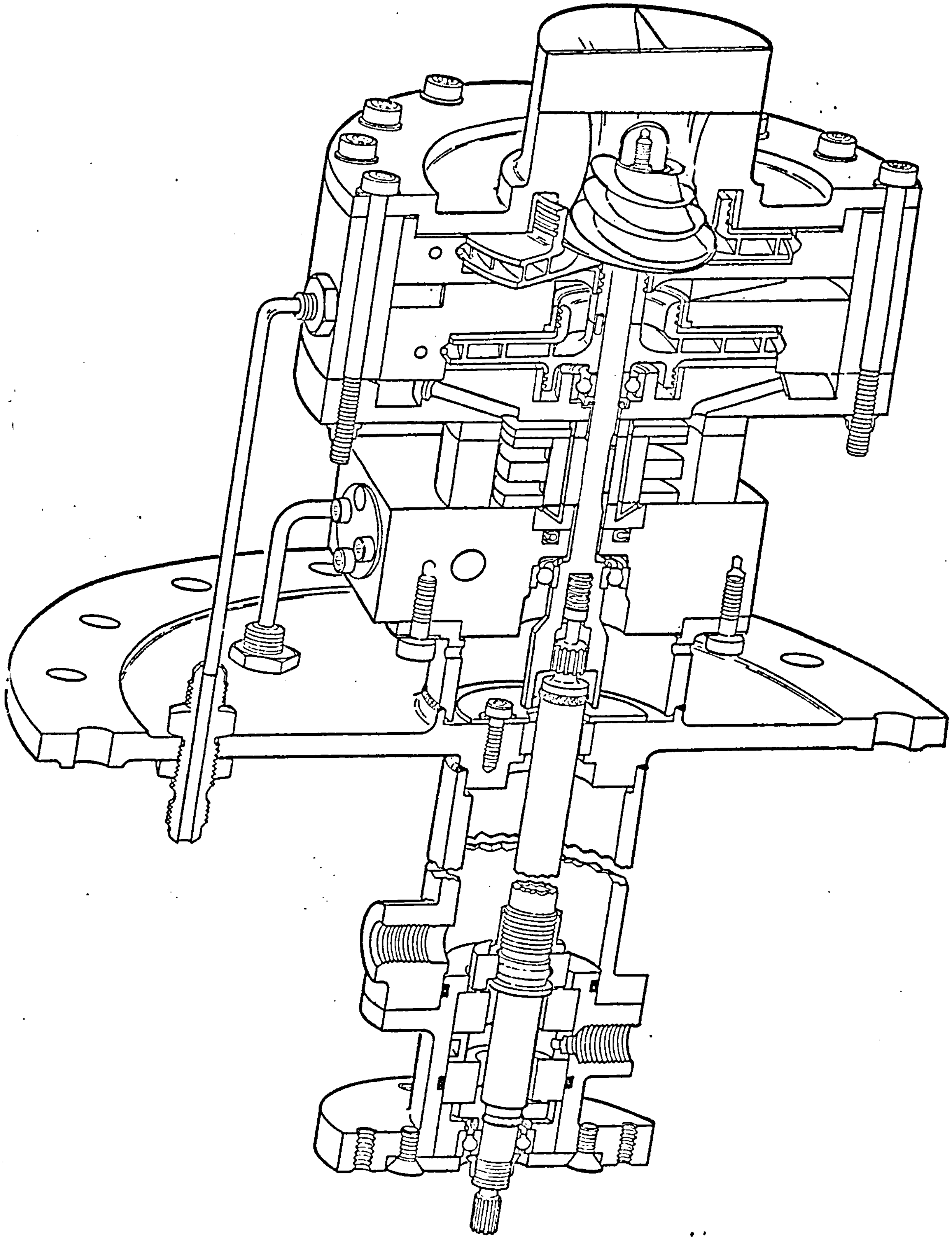

CONTENTS

ILLUSTRATIONS

ILLUSTRATIONS (continued)

1. SUMMARY

A rotating, positive displacement vane pump with an integral boost stage was designed to pump liquid oxygen and liquid hydrogen with the following requirements:

	LIQUID HYDROGEN	LIQUID OXYGEN
Overall Efficiency	75%	75%
NPSP	"0" - 10% Vapor	"0" - 10% Vapor
Life	125 Hours	125 Hours
Cycles (starts)	6000	6000
Fluid Inlet Temp. (^oK)	20.2^o (37^oR)	90.2^o (163^oR)
Flow Rate (gr/sec)	28.6 (.063 lb/sec)	86.2 (.19 lb/sec)
Pressure Rise (N/M^2)	1.49×10^6 (216psi)	2.23×10^6 (323psi)

Preliminary studies led to the conclusion that engineering effort was to concentrate on the liquid hydrogen pump and adapt the configuration to pump liquid oxygen. The two pumps were to be built from different material to meet the material compatability with the fluids.

Analyses indicated that the LH_2 vane pump required two matching boost stage while the LOX vane pump took only one.

Analysis work done included vane stage cam profile, vane dynamics, thermal leakages, stresses, and various design calculations.

2. INTRODUCTION

Cryogenic fluid pumping is a newly developing technology in the field of fluid transfer. Up to the present, no successful attempt in building a cryogenic vane pump has been recorded. Both PESCO and General Motors have ventured into this field but their effort have been unrewarding. Nevertheless, PESCO liquid hydrogen vane pump test data has been proven to be an invaluable calibration tool for the mathematic model developed by Sundstrand's engineers in this conquest.

The objective of this program is to design and fabricate a boost vane pump package which will serve as a test vehicle for the technology development of small positive displacement pumps for liquid oxygen and liquid hydrogen for APS Feed System. Since this is a technology development program, neither weight nor size has been treated as a design constraint. In order to reduce the manufacturing cost, the displacement for the liquid hydrogen pump was used for both fluids.

3. DESIGN GUIDELINES

1. The preliminary design effort was to be guided toward, but not limited to:

   a. Stress analysis
   b. Bearing loads, life, and cooling requirements
   c. Seal leakage and life
   d. Internal leakage analysis
   e. Thermal analysis
   f. Rubbing speeds and loads
   g. Materials selection and heat treatment
   h. Oxygen and hydrogen compatibility of materials.

2. The boost/vane pump package was a self contained unit with its own seals and bearings. A mounting flange and coupling was to be provided for mounting and driving the unit from an external power source.

3. The pump displacement was to be selected so that the flow conditions was to be met at nominal pump speeds of either 4000, 6000, 8,000, 12000, or 24000 RPM. The oxygen pump and hydrogen pump requirements were such that, for the same displacement, they would require different operating speeds, but the speed selected for each fluid was to be one of those listed.

4. If a single pump design could not meet the flow rate requirements of both fluids, with the speed constraints listed above, a compromise must be made in the selection of the pump displacement. The displacement selected would be that which would provide for the greatest technology gain when considering both material selection and boost pump performance.

5. The ability of the pump to expel gas and recover nominal performance would be more critical than a momentary reduction in flow or pump efficiency.

6. The pump would be designed so that both the vane pump and boost pump components could be tested separately.

7. The vane pump would be designed so that material changes could be made in the area that rubbing contact occurs between the vanes and the pump housing.

4 . MATERIAL SELECTION

MATERIAL SELECTION
LH_2 AND LO_2 CRYOGENIC VANE PUMPS

Evaluation of materials for usage at cryogenic temperatures was conducted taking into account the basic low temperature characteristics of materials. This constituted the rating of materials using the following basic parameters as applicable:

1) Low temperature mechanical strength
2) Low temperature impact strength
3) Low thermal contraction differential
4) Wear resistance

More importantly, material compatibility with LO_2 was established using what is termed as the "burn factor"(1) for selected materials.

The material selections are summarized in Table 4.1a and 4.1b and described below.

An attempt has also been made to fabricate the vane stage parts from similar, if not the same, materials in each respective pump. This is due to areas in the vane stage requiring tight tolerances. Similar materials thus similar contraction rates alleviate loss of these tolerances at cryogenic temperatures.

LH_2 Pump Vane Stage

The low lubricity characteristics of LH_2 dictates a wear resistant base material or coating for the rubbing surfaces. Most hardenable steels have been discounted due to their low temperature embrittlement effects or poor impact strength at cryogenic temperatures as exhibited by 4340 steel in Fig.4.1.(2) The 300 series stainless steels would not possess adequate wear resistance even though their hardness and strength increases at low temperatures (Fig.4.2).(2)

Investigation into suitable wear resistance led to the Ferro-TiC materials (Div. of Sintecast). The Ferro-TiC materials are a family of steel or alloy bonded carbides utilizing extremely hard TiC grains uniformly distributed through a hardenable metal matrix. A variety of metal matrices are available. The selected grade was HT-6 which is composed of a nickel alloy (Inconel 718) matrix with a 45% TiC particle content.

The nickel alloy matrix provides excellent low temperature strength (Fig.4.3)(2) while the TiC particles provide the essential wear resistance. (Similar Ferro-TiC grades (Ferro-TiC SK, CM) have exhibited excellent wear resistance for vane stage parts). Alternate material selection for the vane stage parts necessitated the use of dissimilar metals due to the low temperature embrittlement of hardenable conventional steels. The dissimilar combination (Table4.1a) utilizes a hard on soft material approach. A-286 stainless steel exhibited the optimum low temperature properties for the rotor and vanes while maintaining similar thermal contraction rates with the leaded bronze port plates and liner. To insure adequate wear resistance, the rotor ends and vanes will be electroless nickel plated. This combination insures that all rubbing contact will be composed of hard (60 RC) electroless nickel against the self lubricating leaded bronze.

The inducer, impeller and housings were originally to be cast from C355 aluminum although to provide for interchangeability with the LO_2 pump, K Monel will be used. Similarly the shaft has been changed from 304L CRES to K Monel. These changes also provide for a closer match of thermal contractions on the inducer, impeller and shaft.

The labyrinth seal rings for the LH_2 pump will be P5N carbon and 70/30 Brass will be an alternate choice.

The ball bearings will be made from 440C stainless steel with one piece rulon retainers which have shown excellent performance on the space shuttle LH_2 and Centaur LO_2 pumps.

LO_2 Pump Vane Stage

Compatibility with LO_2 was used as the primary basis of material selection for the LO_2 pump. Rubbing metal to metal contact of the vane stage elements require materials possessing high ignition temperature, high thermal diffusivity and low heat of oxidation while maintaining wear resistance.

A few of the alloys used as preliminary candidates in the LO_2 pump study are listed in Table 4.II [1] Some thermodynamic properties of each of the alloys are also shown. The first column lists the density of the material. The second column presents the calculated heat evolved from each alloy assuming complete combustion of 100 grams of the material. The heat of oxidation was calculated by taking the concentration of each of the major constituents in the alloy multiplying the weight present by the standard heat of oxidation for each constituent and summing the component values to obtain a calculated heat of alloy oxidation. A large value for ΔH_f, the standard heat of oxidation, implies large amounts of heat evolved in the oxidation of 100 grams of the alloy.

The third column in the table presents a calculated value of the diffusivity of each material. The diffusivity is defined by the following expression:

$$\alpha = \frac{k}{\rho c} \quad \text{where } \alpha = \text{thermal diffusivity}$$

$$k = \text{thermal conductivity}$$

$$\rho = \text{density}$$

$$c = \text{specific heat}$$

The diffusivity is a value representing the ability of a material to diffuse heat away from a heat source.

The fourth column in the table is the ratio of the heat of oxidation divided by the diffusivity and is referred to as the "burn factor". This number provides a relative ranking of each material in terms of the amount of heat produced when a fixed amount of material oxidizes divided by the diffusivity, the ability of the base metal to diffuse heat away. The high value of $\frac{\Delta H_f}{\alpha}$ implies either a high heat of oxidation or a low diffusivity, or a high ratio of the two factors.

Table III lists the materials of interest according to the burn factor, $\frac{\Delta H_f}{\alpha}$. The materials at the top of the list are considered to be more resistant to burning because of either a low heat of oxidation or a high diffusivity or both. Materials appearing lower in the list have either a high heat of oxidation or low diffusivity and are expected to be less resistant to both ignition and combustion.

The prime and alternate materials selected for the LO_2 pump are shown in Table 4 lb. The Ferro-TiC CN-5 material to be used as the rotor, port plates, liner and vanes is composed of 45 V/O, tungsten carbide and 55 V/O, 70/30 brass. The tungsten carbide is present as interspersed particles in the 70/30 brass matrix. This combination of hard and soft constituents has provided excellent wear resistance in conventional aircraft fuel pumps. Compatibility of the Ferro-TiC CN-5 with LO_2 was estimated by calculating the "burn factor" for the alloy. (Appendix).

The alternate materials selected for the LO_2 vane stage all appear high on the list in Table 4.III. This combination, as in the LH_2 version will provide a hard on soft approach and utilizes electroless nickel against leaded bronze as the mating materials.

The shaft, inducer, impeller and housings will be fabricated from K Monel due to its low burn factor and excellent mechanical properties at cryogenic temperatures. S Monel will be used if the parts are to be casted.

The bearing, as with the LH_2 pump, will be made from 440C stainless steel as used on the Centaur LO_2 and space shuttle LH_2 pumps.

The following calculation is performed to estimate the "burn factor" of Ferro-TiC CN-5. The heats of oxidation (ΔH_f^o) for 100g of each constituent material (Cu, Ni, W, + C) is calculated initially. From the percentages of constituents present, a heat of alloy oxidation is arrived at $\Delta H_{f_{CN-5}}^o$) for 100g of Ferro-TiC CN-5. The diffusivity (α) is then calculated similarly.

The ratio of the heat of oxidation and the diffusivity yields the "burn factor". ($\frac{\Delta Hf}{\alpha}$).

Property data for Ferro-TiC CN-5 is given below:
Density: $11.8 g/cm^3$
Composition: 45 V/O, WC

55 V/O, Cu-Ni alloy (similar to CA 715)

Since the Cu-Ni alloy matrix is similar to copper alloy 715, property data for this alloy will be used in calculation of the burn factor.

CA 715

$$K = \frac{17\ BTU\ (ft)}{(ft^2)(hr)(^oF)} = \text{thermal conductivity}$$

$$C = \frac{.09\ BTU}{lb^oF} = \text{specific heat}$$

WC

$$K = \frac{57.8\ BTU\ (ft)}{(ft^2)(hr)(^oF)} = \text{thermal conductivity}$$

$$C = \frac{.049\ BTU}{lb\ ^oF} = \text{specific heat}$$

Since the density of Ferro TiC CN-5 is 11.8g/cc the amount of the constituent elements in 100g of the alloy is calculated as follows, keeping in mind that there is 45 V/O WC and 55 V/O CA 715.

$$100g\ CN\text{-}5 \times \frac{cm^3}{11.8g} = 8.47 cm^3\ CN\text{-}5$$

$$45\ V/O\ of\ 8.47 cm^3 = 3.81 cm^3\ WC$$

$$55\ V/O\ of\ 8.47 cm^3 = 4.66 cm^3\ CA\ 715$$

Using the following densities the amount of constituent materials is found.

$$\rho_{CA\ 715} = 8.94 g/cm^3$$

$$\rho_{WC} = 14.99 g/cm^3$$

CA 715

$$4.66 cm^3 \times \frac{8.94}{cm^3} = \boxed{41.66 g\ CA\ 715}$$

WC

$$3.81 cm^3 \times \frac{14.99 g}{cm^3} = \boxed{57.11 g\ WC}$$

Therefore in 100g of Ferro-TiC CN-5 we have ~ 40 W/O CA 715 and 60 W/O WC.

We can now calculate the heat of oxidation for a 100 gram sample of the material. To do so we start with calculating the amount of each constituent element in the material:

For 40g CA 715 (approx. 70% Cu, 30% Ni)

$$70\% \text{ of } 40 g = \boxed{28 g\ Cu}$$

$$30\% \text{ of } 40 g = \boxed{12 g\ Ni}$$

For 60g WC

$$60 g \times \frac{1 \text{ mole WC}}{195.86 g} \times \frac{183.85 gW}{\text{mole WC}} = \boxed{56.32 g\ W}$$

$$60 g \times \frac{1 \text{ mole WC}}{195.86 g} \times \frac{12.01 gC}{\text{mole WC}} = \boxed{3.68 g\ C}$$

If we now calculate the amount of heat evolved in oxidizing 100 grams of the constituents, we will arrive at the heat of oxidation of the Ferro-TiC CN-5 by multiplying these results by the percent of constituent present and then adding them.

For complete oxidation of 100g of Cu the amount of heat evolved is calculated below. Since the oxidation of $Cu \rightarrow CuO$ (-37.1Kg cal/mole) evolves more heat than any oxide product of copper, it will be used.

$$100g\ Cu \times \frac{mole}{63.54g} \times \frac{-37.1\ kg\ cal}{mole} = \boxed{-58.39Kg\ cal}$$

For complete combustion of 100g Ni the oxidation reaction; $Ni \rightarrow NiO$ (-58.4Kg cal/mole) will be used again because it produces the most heat when formed.

$$100g\ Ni \times \frac{mole}{65.37g} \times \frac{-58.4Kg\ cal}{mole} = \boxed{-89.34Kg\ cal}$$

Similarly for W and C the heat evolved in the following reactions are used respectively: $W \rightarrow WO_3$ (-200.84Kg cal/mole) and $C \rightarrow CO_2$ (-94.05K cal/mole).

$$100g\ W \times \frac{mole\ W}{183.85g} \times \frac{-200.84Kg\ cal}{mole} = -109.24Kg\ cal$$

$$100g\ C \times \frac{mole\ C}{12.01g} \times \frac{-94.05Kg\ cal}{mole} = -783.10Kg\ cal$$

For 100g of Ferro-TiC CN-5 the expected heat evolved is calculated:

$$28g\ Cu \times \frac{-58.39Kg\ cal}{100g\ Cu} = 16.35Kg\ cal$$

$$12g\ Ni \times \frac{-89.34Kg\ cal}{100g\ Zn} = -10.72Kg\ cal$$

$$56.32g\ W \times \frac{-109.24}{100g\ W} = -61.52Kg\ cal$$

$$3.68g\ C \times \frac{-783.10Kg\ cal}{100g\ C} = -28.82Kg\ cal$$

Total = -117.41Kg cal

i.e. heat of oxidation for Ferro TiC CN-5

$$\boxed{\Delta H_{f_{CN-5}} = -117.41Kg\ cal/100g}$$

The thermal diffusivities of CA 715 and WC are now calculated as below:

CA 715 $\longrightarrow$ diffusivity $= \dfrac{k}{\rho c}$

$$K = \frac{17\ \text{BTU ft}}{\text{ft}^2\ \text{hr}\ ^{o}\text{F}} \times 4.135 \times 10^{-3} = \frac{.07\ \text{cal cm}}{\text{sec}\ \ \text{cm}^2\ \ \text{K}}$$

$$C = \frac{.09\ \text{BTU}}{\text{lb}\ ^{o}\text{F}} = \frac{.09\ \text{cal}}{\text{g}\ ^{o}\text{K}}$$

$$\rho = \frac{.323\ \text{lb}}{\text{in}^3} \times \frac{454\text{g}}{\text{lb}} \times \left(\frac{\text{in}}{2.54\text{cm}}\right)^3 = 8.949\text{g/cm}^3$$

$$\alpha = \frac{K}{\rho c} = \frac{.07\ \frac{\text{cal cm}}{\text{sec cm}^2\ ^{o}\text{K}}}{(8.949\text{g/cm}^3)(.09\ \text{cal/g}\ ^{o}\text{K})}$$

$$\boxed{\alpha_{\text{CA 715}} = \frac{8.6 \times 10^{-2}\ \text{cm}^2}{\text{sec}}}$$

WC diffusivity at $(212\ ^{o}\text{F})$

$$K = 57.8\ \frac{\text{BTU}}{\text{hr ft ft}^2\ ^{o}\text{F}} \times 4.135 \times 10^{-3} = .239\ \frac{\text{cal cm}}{\text{sec cm}^2\ ^{o}\text{K}}$$

$$C = .049\ \frac{\text{BTU}}{\text{lb}\ ^{o}\text{F}} = \frac{.049\ \text{cal}}{\text{g}\ ^{o}\text{K}}$$

$$\rho = \frac{.54\ \text{lb}}{\text{in}^3} \times \left(\frac{\text{in}}{2.54\text{cm}}\right)^3 \times \frac{454\text{g}}{\text{lb}} = 14.99\text{g/cm}^3$$

$$\boxed{\alpha_{\text{WC}} = \frac{.239\ \frac{\text{cal cm}}{\text{sec cm}^2\ ^{o}\text{K}}}{(14.99\text{g/cm}^3)(.049\ \text{cal/g}\ ^{o}\text{K})} = .325\ \frac{\text{cm}^2}{\text{sec}}}$$

Since there is 45 V/O WC and 55 V/O 70/30 brass the thermal diffusivity for the alloy is calculated as follows:

$$.45 \times \frac{.325\text{cm}^2}{\text{sec}} = 0.146\frac{\text{cm}^2}{\text{sec}}$$

$$.55 \times \frac{8.6\text{x}10^{-2}\ \text{cm}^2}{\text{sec}} = \frac{0.047\ \text{cm}^2/\text{sec}}{0.193\ \text{cm}^2/\text{sec}} = \text{Total}$$

i.e. the thermal diffusivity of Ferro TiC CN-5 is:

$$\boxed{\alpha_{CN-5} = 0.193\text{cm}^2/\text{sec}}$$

The burn factor can now be calculated for the alloy.

$$\text{Burn factor} = \frac{\Delta H^o_f\ CN-5}{\alpha\ CN-5} = \frac{121.96}{.193}$$

$$\boxed{\text{Burn factor} = 631.92}$$

Comparison of this number with Table II indicates that the Ferro-TiC CN-5 has a burn factor in the neighborhood of the bronze alloys + pure aluminum as anticipated and should be quite safe in liquid oxygen. Concurrently, the material will provide excellent wear characteristics based on the 45 V/O WC content.

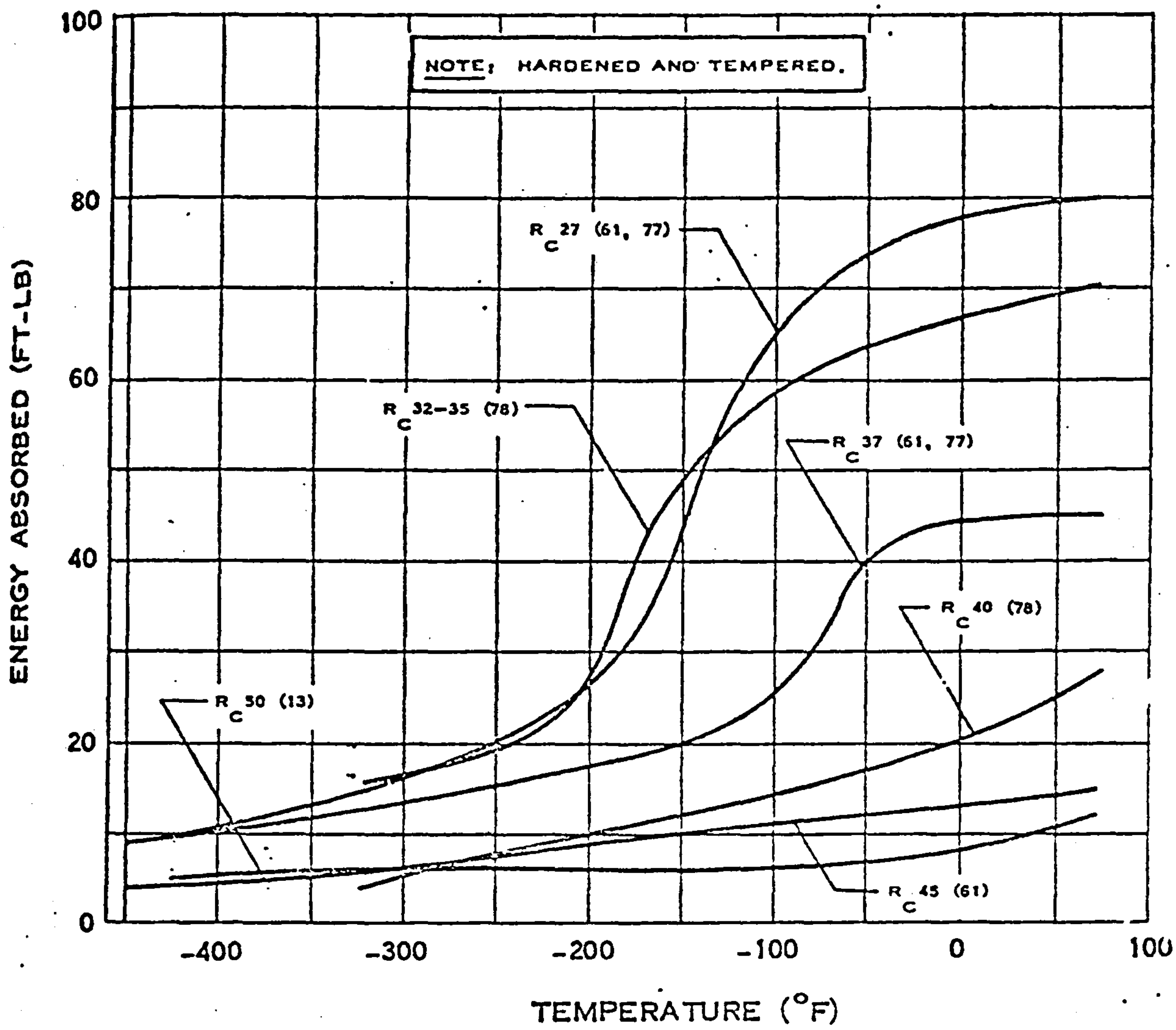

Fig. 4.1-IMPACT STRENGTH OF 4340 STEEL

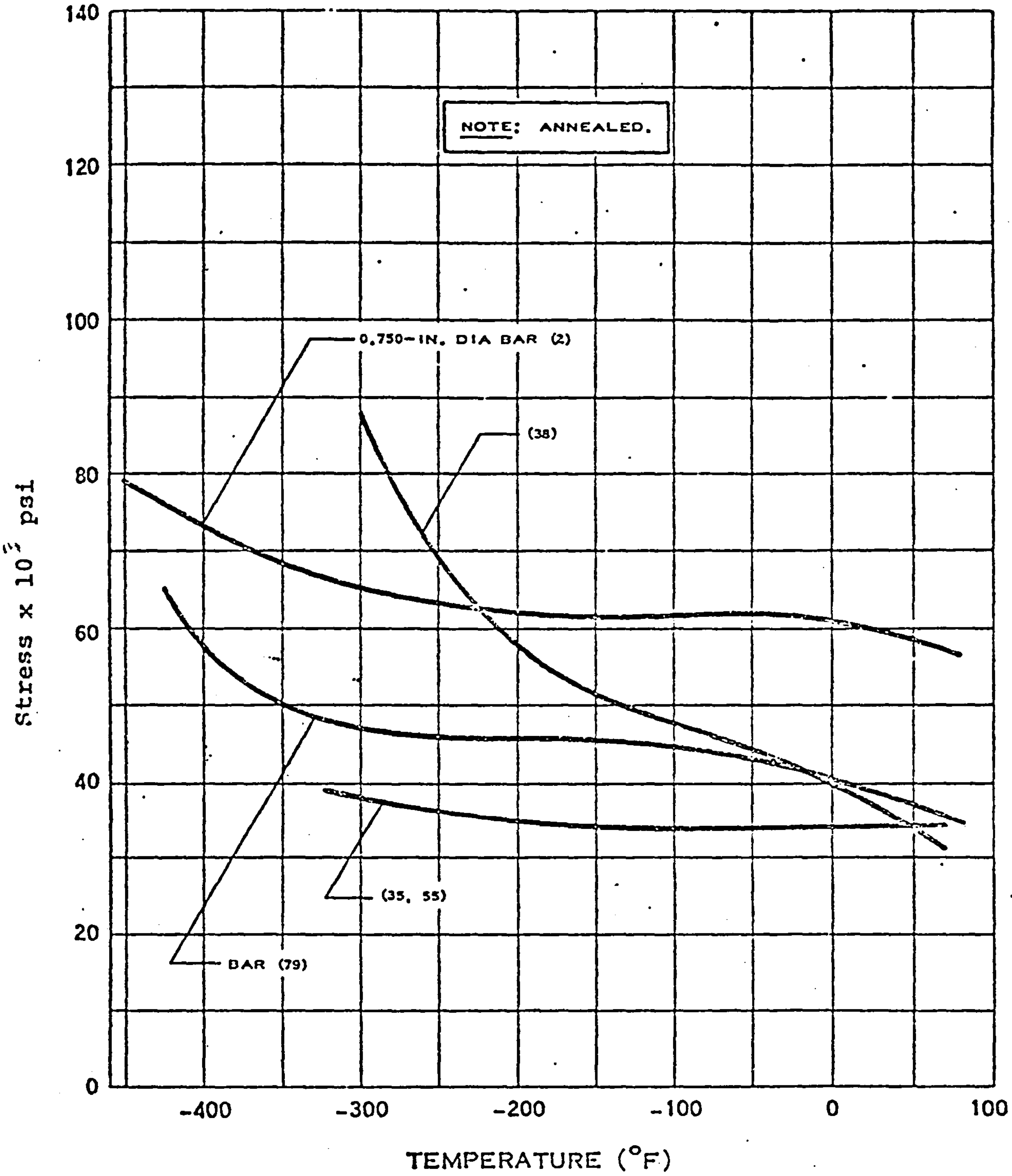

Fig. 4.2 - YIELD STRENGTH OF 304 STAINLESS STEEL

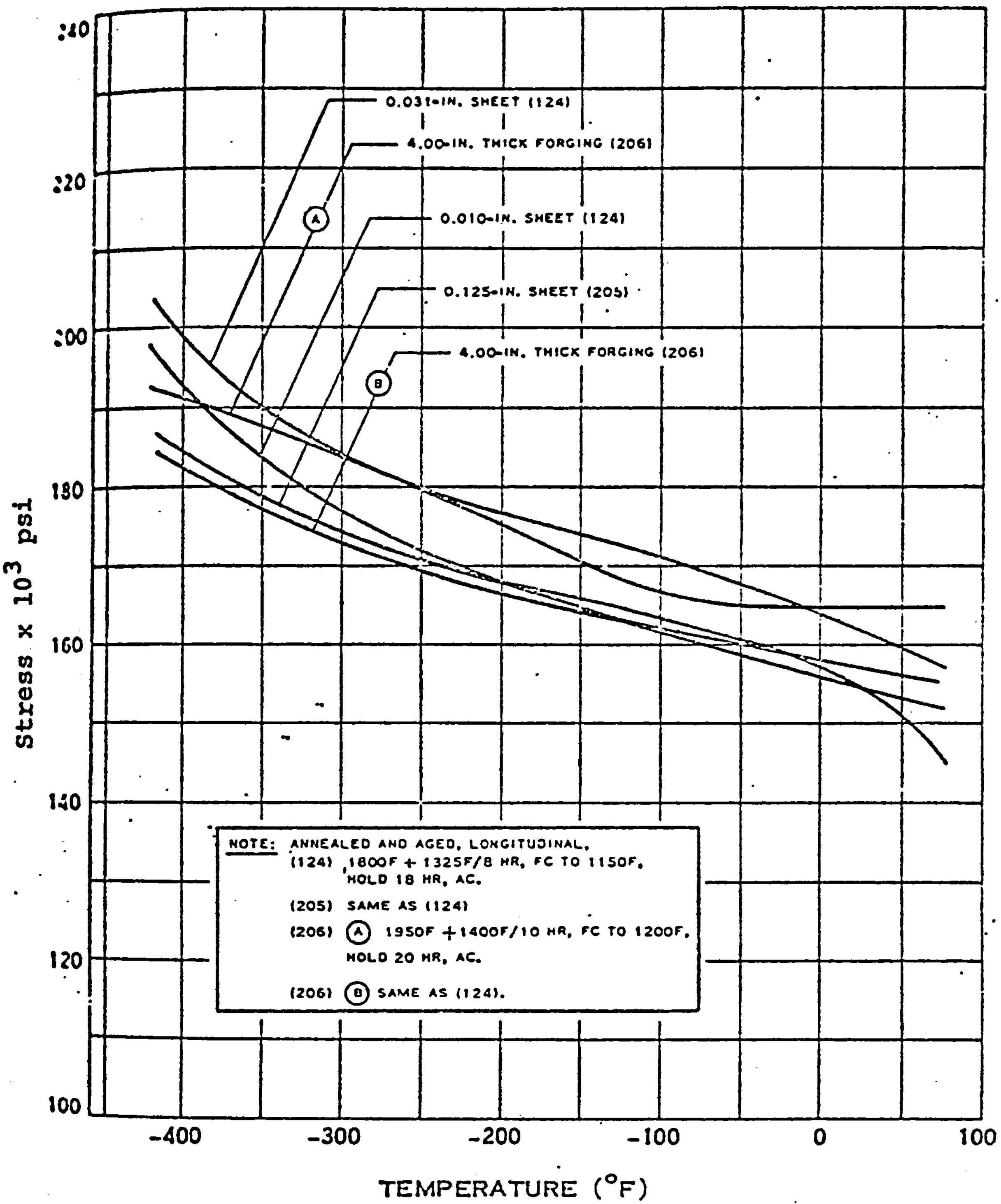

Fig. 4.3-YIELD STRENGTH OF INCONEL 718

CRYOGENIC VANE PUMP MATERIAL SELECTION

Table 4.1a

LH_2 Prime Candidates		Alternates
Rotor	Ferro-TiC HT-6	A-286 (Ni Plated Ends)
Liner	Ferro-TiC HT-6	Leaded Bronze
Port Plates	Ferro-TiC HT-6	Leaded Bronze
Vanes	Ferro-TiC HT-6	Nickel Plated A-286
Shaft	←	K Monel *
Inducer	←	S Monel
Impeller	←	S Monel
Labyrinth	←	P-5NR
Bearings	←	440C Rulon Cage
Housings	←	K Monel
Bolts		Nitronic 60

Table 4.1b

LO_2 Prime Candidates		Alternates
Rotor	Ferro-TiC CN-5	Nickel Plated (End Faces) Be-Cu
Liner	Ferro-TiC CN-5	Leaded Bronze
Port Plates	Ferro-TiC CN-5	Leaded Bronze
Vanes	Ferro-TiC CN-5	Ni Plated Be-Cu
Shaft	←	K Monel
Inducer	←	S Monel
Impeller	←	S Monel
Labyrinth	←	Nickel Plated Be-Cu
Bearings	←	440C Rulon Cage
Housings	←	K Monel
Bolts		Nitronic 60

*Monel material will be Ni Strike ~.001" Cu Plated due to the hydrogen sensitive nature of the material.

TABLE 4.II

Calculated Heats of Oxidation and Ratios of Those Heats and the Thermal Diffusivity (α) of Alloys of Interest (at Room Temperature)

Type of Alloy	Density, g/cm^3	Heat of Oxidation ΔH_f, kgcal/100 gms, alloy	Diffusivity α, cm^2/sec	Burn factor $\Delta H_f/\alpha$
Iron Alloys				
Cast iron, plain	7.20	210.2	.129	1629
Cast iron, alloyed	7.20	207.8	.117	1776
Ductile iron	7.11	209.3	.085	2462
C-Steel, cast	7.83	179.9	.136	1323
1025 steel	7.83	179.9	.136	1323
15-5 PH	7.80	185.1	.045	4120
17-4 PH	7.75	185.7	.046	4040
CA-15	7.61	193.9	.071 (K,212F),(C_ρ,RT)	2630
4340	7.83	176.9	.107 (K,120F),(C_ρ,RT)	1650
4140	7.83	174.6	.120	1455
A286	7.92	157.4	.036	4370
8630	7.83	176.0	.107	1645
304 S.S.	8.03	189.9	.040	4740
410 S.S.	7.75	191.2	.070	2730
Ni-Resist (2B)	7.39	191.1	.118	1619
Copper Alloys				
Al-Si Bronze-638	8.28	65.3	.119	549
Phosphor Bronze-544	8.88	35.0	.260	135
Al-Bronze-610	7.78	82.2	.237	347
Leaded Bronze-314	8.83	29.9	.543	55
Copper Alloy-828	8.08	73.0	.365	200
Tin Bronze-937	8.86	40.8	.141	289
Be-Cu	8.26	72.0	.31447	229
Nickel Alloys				
Monel-400	8.83	80.9	.058	1390
Monel-K500	8.47	102.3	.049	2090
Inconel-600	8.41	128.8	.040	3220
Inconel-625	8.44	139.3	.028	4970
Inconel-702	8.41	177.2	.025	7100
Inconel-718	8.19	148.3	.032	4640
Inconel-X750	8.25	136.6	.034	4010
Hastelloy X	8.22	163.9	.023	7160
Hastelloy C	8.94	148.1	.033 (K,392F),(C_ρRT)	4500
Udimet 500	8.03	180.5	.032	5650
Udimet 700	7.92	172.6	.056	3082
713-C	7.92	167.9	.051 (K,1000F),(C_ρ,1000F)	3300
			.045 (K,200F),(C_ρ,1000F)	3730
IN-100	7.75	187.0	.046 (K,1000F),(C_ρ,1000F)	4070
B-1900	8.22	162.0	.047	3450
MAR-M-200	8.53	175.9	.020	8900
Duranickel	8.25	142.1	.049	2900
Other Metals				
Babbitt-SAE 14	9.69	33.2	.155	214
Lead	11.35	28.2	.231 (K,212F),(C_ρ,32F)	122
Copper	8.94	32.9	1.140	29
Silver	10.49	3.3	1.710 (K,212F),(C_ρ,RT)	2
Nickel 270	8.88	97.6	.210	46[illegible]
Aluminum 1100	2.71	742.0	.890	834

TABLE 4-III

Ranking of Alloys According to Burn Factor - $\Delta \dot{H}f/\alpha$

Alloy	$\Delta \dot{H}f/\alpha$
Silver	2
Copper	29
Leaded Bronze	55
Lead	122
Phosphor Bronze	135
CDA-828	200
Babbitt-SAE 14	214
Be-Cu	229
Tin Bronze	289
Al-Bronze	347
Nickel 270	465
Al-Si Bronze	549
Ferro-Tic CN5	631.29
Aluminum 1100	834
1025 Steel	1323
C-Steel, cast	1323
Monel 400	1390
4140	1455
Ni Resist	1619
Cast Iron, plain	1629
8630	1645
4340	1650
Cast Iron, alloy	1776
K-Monel	2090
Ductile Iron	2462
CA-15	2630
410 S.S.	2730
Duranickel	2900
Udimet 700	3082
Inconel 600	3220
B-1900	3450
713-C	3730
Inconel X750	4010
17-4 PH	4040
IN-100	4070
15-5 PH	4120
A286	4370
Hastelloy C	4500
Inconel 718	4640
304 S.S.	4740
Inconel-625	4970
Udimet 500	5650
Inconel-702	7100
Hastelloy X	7160
Mar M 200	8900

5. THERMAL LEAKAGE ANALYSIS

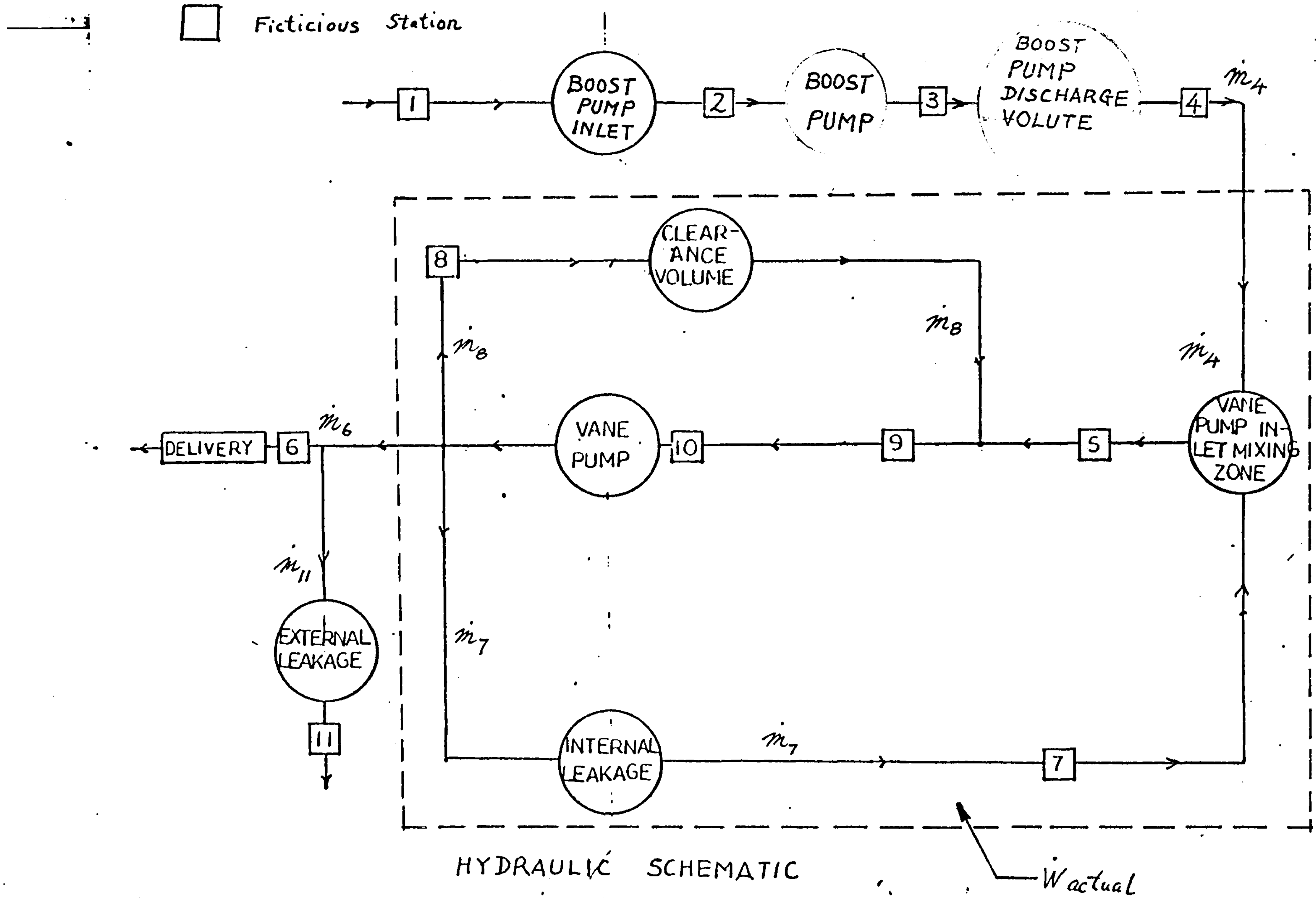

HYDRAULIC SCHEMATIC

Vane Pump shown in circle for representation only.
All work in compression, in leakage, in friction etc..
is designated by Wactual

A vane pump can be designed sucessfully for pumping cryogenic fluids, if clearances between moving and stationary components are maintained as low as possible. In cryogenic operation, leakage affects the pump performance adversely in two ways: (a) reduction in the volumetric efficiency, and (b) possibility of creating a two phase mixture at the inlet zone of the pump.

Two types of leakage occur in a vane pump: (1) internal, and (2) external. In internal leakage the fluid from the exit (or high pressure) port side is dumped into the inlet (or low pressure) port side of the pump. In external leakage the fluid flows from the exit (or the high pressure) port side to low pressure zones but not to the inlet port of the pump itself.

In the present analysis internal leakage has been considered at the following points:

(a) vane tips
(b) vane sides
(c) rotor sides
(d) kidney-to-kidney in port plates, and
(e) pressure plate sides;

and external leakage has been considered from kidneys to shaft spline.

Clearance or dead volume also reduces the pump performance. Figure 1 shows the flow diagram for a vane pump, and includes the boost pump components at the upstream as inlet side.

Analysis

Using time average values, the flow through the pump may be treated as steady-state. The pump is submerged in saturated liquid. Analysis shows that the variation in fluid temperature as it flows through various passages is small enough to preclude significant heat transfer. Hence the flows are assumed adiabatic to err or a safer side and obtain a conservative design. Variation in the kinetic and potential energy terms is in general negligible. The fluid density (particularly of hydrogen) may vary somewhat. However, momentum equations for incompressible fluids can be used here with an average density to account for its variation.

<u>Continuity</u>

$$\dot{m}_a = \dot{m}_b = \dot{m} \qquad \text{------------------------------} (1)$$

where a and b are the inlet and the exit stations of a control volume, and

$\dot{m}$ = fluid flow rate, kg per sec.

<u>Momentum</u>

$$\dot{m}(u_b - u_a) = \left\{ p_a A_a - p_b A_b + F_{sx} \right\} \qquad \text{--------------------} (2)$$

where

p = pressure, N/m^2

A = area, M^2

F_{sx} = "shaft" force exerted upon the fluid, Newtons

u = fluid velocity, ft per (sec), m/sec

<u>Energy</u>

Considering adiabatic flow, and neglecting the kinetic and the potential energy terms,

$$\frac{\dot{W}_m}{J} = \dot{m}\,(h_b - h_a), \qquad \text{------------------------------} (3)$$

where

$\dot{W}_m$ = work input rate, n. m per sec.

J = 778.16 n. m / kcal

h = specific enthalpy, kcal per Kg

<u>Entropy</u>

$$\dot{m}(S_b - S_a) = \Sigma \geq 0, \quad \text{-----} (4)$$

where

S = specific entropy, Kcal per Kg. ^0K

Σ = entropy production rate, kcal per sec

We also have

$$TdS = dh - \frac{dp}{J\rho} \quad \text{-----} (5)$$

which may be integrated to give

$$T_{ab}\ (S_b - S_a) = (h_b - h_a) - \frac{1}{J\rho_{ab}}\ (p_b - p_a) \quad \text{-----} (6)$$

where

T_{ab} = "Average" of T_a and T_b

ρ_{ab} = "Average" of ρ_a and $\rho_b = \frac{1}{2}\ (\rho_a + \rho_b)$

If a-b is an ideal pump, Σ is zero and from equations 3, 4 and 6 have

$$(\dot{W}_m)_{ideal} = \frac{\dot{m}}{\rho_{ab}}\ (p_b - p_a) \quad \text{-----} (7)$$

or

$$(\dot{W}_m)_{ideal} = \dot{Q}\,(p_b - p_a) \qquad (8)$$

where

$\dot{Q}$ = volume flow rate, m^3 per sec

<u>Internal Leakage</u>

Since the leakage paths have small gaps and a good design requires low leakage flows, these flow can be treated as laminar. A detailed analysis of such flow between parallel rectangular plates (with relative motion between them) shows that we have:

$$Q_j = \frac{v_{oj} b_j t_j}{2} + \frac{b_j^3\, t_j\,(p_{in,j} - p_{out,j})\, g_o}{12\, \mu l_j} \qquad (9)$$

<u>in the direction of v_o,</u>

where the subscript j is for the leakage path j, and

v_o = velocity of the moving plate, m per sec.

b = clearance between plates, m.

t = "thickness" of flow path (at right angles to flow), m

l = length of flow path, m

μ = fluid viscosity, average value, (lbm) per (ft) (sec), (kg) per (m)(sec)

Now

$$v_{oj} = \frac{2\pi r_j N}{60} \qquad (10)$$

where

r_j = "radius" or "location" of the moving element j from shaft center line, ft., m.

N = RPM

Since internal leakage includes only flows from high pressure to low pressure side of the pump, we also have

$$\left|\dot{Q}_j\right| = \alpha_j \dot{Q}_j \quad \text{-------------------------------} (11)$$

where

$$\alpha_j = 1.0, \text{ if } p_{inj} > p_{outj}$$

$$\alpha_j = 0.0, \text{ if } p_{inj} = p_{outj}$$

$$\alpha_j = 0.0, \text{ if } p_{outj} > p_{inj} \text{ and } \dot{Q}_j > 0$$

$$\alpha_j = -1.0, \text{ if } p_{outj} > p_{inj} \text{ and } \dot{Q}_j < 0$$

Thus some leakage paths may be "active" while the others are "inactive".

It can also be shown that the work transferred to the fluid by the moving element of the leakage path j is given by

$$\dot{W}_j = \left|\alpha_j\right| \left(2\pi \frac{N}{60}\right) \left[\frac{2\pi\mu N l_j t_j r_j^2}{60\, b_j g_o} + \frac{b_j r_j t_j (p_{outj} - p_{inj})}{2}\right]_j$$

$$\text{ft.lbf/sec} \quad \text{--------------} (12)$$

Following subscripts in Figure 1 (flow diagram), the total internal leakage flow m_7 is given by

$$\dot{m}_7 = \rho_{67} \sum_j \left|Q_j\right| \quad \text{kg per (sec)} \quad \text{-------------------------} (13)$$

where $\rho_{67} = 1/2\ (\rho_6 + \rho_7)$,

and the total work input to internal leakage flows is given by:

$$\dot{W}_{67} = \sum_j W_j \qquad \text{------------------------------------ (14)}$$

Clearance, Dead or Carry-around Volume

The flow returning to the inlet zone of the pump due to clearance volume is $\dot{m}_8$. It can be shown that

$$\dot{m}_8 = \rho_6 V_c N/60 \text{ kg per (sec)} \qquad \text{------------------------ (15)}$$

where

V_c = clearance volume per revolution, m^3

The clearance volume fluid expands from p_6, h_6 to p_8 (or P_4), h_8, and in so doing transfers work to the moving metals of the pump. To err on the safer side, it will be assumed that the work transfer is zero. From equation 3, we thus have

$$h_8 = h_6 \qquad \text{-- (16)}$$

External Leakage

This occurs between the kidneys in the rotor and the shaft spline. The flow may be assumed to have a line source at the kidney edge (bottom) radius and a line sink at the spline radius. The difference between these radii is not very large, and hence the flow equation in this case at zero rotor speed should reduce to equation 9 with ν_ρ equal to zero. Taking this into account and assuming the average tangential velocity of the fluid as equal to half of the rotor velocity, solution of the radial component of the momentum equation gives:

$$\dot{m}_{11} = \frac{2\rho_m \pi r m b_{ks}^3}{6\mu_m L_m} \left[go(p_6 - p_4) - \rho_m \left(\frac{\pi N}{60}\right)^2 l_m r_m \right], \qquad \text{-------- (17)}$$

kg per (sec),

with kidneys on either side of rotor. In the above equation

$\rho_m = \frac{1}{2} (\rho_6+\rho_{11})$, lbm per (cuft)

$r_m = \frac{1}{2} (r_{spline} + r_{kidney} - \frac{1}{2} t_{kidney})$, m

$\mu_m = \frac{1}{2} (\mu_6+\mu_{11})$, kg per (sec) m

$l_m = (r_{kidney} - \frac{1}{2} t_{kidney} - r_{spline})$, m

b_{ks} = kidney-side clearance, m

The work transfer to $\dot{m}_{11}$ was found to be a negligibly small quantity. Hence from equation 3, we have

$$h_{11} = h_6 \qquad (18)$$

Mixing Zone at Vane Pump Inlet

Applying continuity and the energy equations, we have

$$\dot{m}_5 = \dot{m}_4 + \dot{m}_7 \qquad (19)$$

$$\dot{m}_5 h_5 = \dot{m}_4 h_4 + \dot{m}_7 h_7 \qquad (20)$$

We also have

$$P_5 = P_4 = P_7 \qquad (21)$$

Junction 5-8-9

Here we have

$$P_5 = P_8 = P_9 \qquad (22)$$

$$\dot{m}_9 = \dot{m}_5 + \dot{m}_8 \qquad \text{-----(23)}$$

and

$$\dot{m}_9 h_9 = \dot{m}_5 h_5 + \dot{m}_8 h_8 \qquad \text{-----(24)}$$

Pump Efficiencies

The overall efficiency η_{ovp} is defined by

$$\eta_{ovp} = \frac{(\dot{W}_m)\,\text{ideal}}{(\dot{W}_m)\,\text{actual}} \qquad \text{-----(25)}$$

at the same fluid flow rate. Thus from equations 3,7 and 25,

$$\eta_{ovp} = \frac{(p_6 - p_4)}{\alpha\, J \rho_{46s} (h_6 - h_4)} \qquad \text{-----(26)}$$

where

$$\rho_{46s} \cong \frac{1}{2} (\rho_4 + \rho_{6s})$$

$$\rho_{6s} = \rho \text{ at } p = p_6 \text{ and } S_6 = S_4$$

The volumetric efficiency η_v of the pump is given by

$$\eta_v = \frac{(60)\ \dot{m}_6}{\rho_4 V_d\ N} \qquad \text{-----(27)}$$

where V_d is the displacement volume in cuft per revolution. Alternatively η_v is given by

$$\eta_v = \frac{60}{\rho_v V_d N} \left\{ \frac{\rho_4 (V_d + V_c)\ N}{60} - \frac{\rho_4 \dot{m}_c}{\rho_5} - \dot{m}_7 - \dot{m}_{11} \right\} \qquad \text{---(28)}$$

The $\dot{m}$ terms can be obtained from equations 13, 15 and 17. Substituting for $\dot{m}_8$ equation 15, we have

$$\eta_v = 1 - \frac{V_c}{V_d}\left(\frac{\rho_6}{\rho_5} - 1\right) - \frac{60}{\rho_4 V_d N}\left(\dot{m}_7 + \dot{m}_{11}\right) \quad \text{-----------------(29)}$$

as an alternative to equation 27.
With a constant density fluid, V_c has no effect of η_v (which of course should be the case).

The torque efficiency η_t of the pump is defined by

$$\eta_t = \frac{T_i}{T_a} = \left\{\frac{\rho_4 V_d N (p_6 - p_4)}{2\pi N \rho_{46s}}\right\} \Bigg/ \frac{\dot{m}_6 (h_6 - h_4) 60}{2\pi N J} \quad \text{----------(30)}$$

using equations 3 and 7. Thus from equations 26, 29 and 30

$$\eta_{vop} = \eta_t \eta_v \quad \text{--------------------------------------(31)}$$

as usual. Thus if η_t is known, η_{vop} can be obtained from η_v.

Fluid State at Various Locations

The state of the fluid at 4 is completely defined. Also p_6, η_t, N and pump geometry are prescribed.

Equation 26 can be used to determine h_6, T_6, ρ_6 etc.

From equations 3 and 26, we have

$$h_7 = h_4 + \frac{1}{J}\left\{\frac{(p_6 - p_4)}{\rho_{46s}\eta_{vop}} + \frac{\dot{W}_{67}}{\dot{m}_7}\right\} \quad \text{----------------------------(32)}$$

to obtain the properties at point 7. For $\dot{m}_7$ and $\dot{W}_{67}$ use equations 13 and 14.

From equations 19, 20, 26 and 32 we get

$$h_5 = h_4 + \frac{1}{\dot{m}_4 + \dot{m}_7} \left\{ \dot{m}_7 \ (h_6 - h_4) + \frac{\dot{W}_{67}}{J} \right\} \qquad \text{------------------}(33)$$

to obtain the properties at location 5.

From equations 19, 23, 24 and 33 we have

$$h_9 = h_4 + \frac{1}{\dot{m}_4 + \dot{m}_7 + \dot{m}_8} \left\{ (\dot{m}_7 + \dot{m}_8) \ (h_6 - h_4) + \frac{\dot{W}_{67}}{J} \right\} \qquad \text{----------}(34)$$

to obtain the properties at location 9.

From equations 26 and 34, we can also write

$$h_6 - h_9 = \frac{\dot{m}_4}{\dot{m}_4 + \dot{m}_7 + \dot{m}_8} \left\{ \frac{p_6 - p_4}{\rho_{46s} \eta_{vop}} - \frac{\dot{W}_{67}}{J\dot{m}_4} \right\} \qquad \text{------------------}(35)$$

From -

From figure 1 and equation 3, it is obvious that $h_6 > h_9$, and so

$$\frac{\dot{m}_4 \ (p_6 - p_4)}{\rho_{46s} \dot{W}_{67}} > \eta_{vop} \qquad \text{--}(36)$$

which can be used as a check in the calculation of various terms.

The location 10 in Figure 1 is a point at the proximity of the vane where the fluid at 9 has undergone an isentropic and adiabatic acceleration. Thus we have

$u_9 = 0$ but $u_{10} > 0$, and so

$$\left.\begin{aligned} h_9 &= h_{10} + \frac{U_{10}^2}{2\, g_o J} \\ &\text{and} \\ s_9 &= s_{10} \end{aligned}\right\} \text{------------------------------} (37)$$

where

$$u_{10} = \frac{2\pi R_{maj} N}{60} \quad \text{m per sec}$$

R_{maj} = Cam Ring major radius, m

Thus p_{10} and T_{10} can be obtained.

In a pump with a large number of vanes, it is possible that a leakage path j may actually be made up of more than one "leakage channel" in series. Calculations with "typical" cases show that a series combination of two channels can be considered as a single channel with twice the length and 0.98 of the thickness of one channel.

Programs for properties of hydrogen and oxygen (in liquid as well as the vapor phase) were obtained from NASA. After eliminating some errors from this material, subroutines have been made to obtain the fluid properties.

Evaluation Procedure

Dimensions of components and leakage paths are listed. Inlet conditions (location 4), p_G, η_t are N are specified.

From a sketch or a drawing showing vane positions, ports, kidneys etc., P_{inj} and P_{outj} for each leakage path j is determined.

Assuming $\dot{m}_4$ and $\dot{m}_{11}$, η_v and η_{ovp} are calculated from equations 27 and 31. Properties at locations 6, 8 and 11 are obtained from equations 26, 16 and 18 respectively.

Using equation 17, $\dot{m}_{11}$ is calculated and checked against the assumed value. Assumed $\dot{m}_{11}$ is altered until agreement is obtained.

Assuming h_7, $\dot{m}_7$ and $\dot{W}_{67}$ are obtained from equations 13 and 14. Using equation 32, h_7 is calculated. Iteration is necessary to make the assumed h_7 equal to the calculated h_7.

Properties at 5 are calculated using equation 33. The η_v is calculated from equation 29 and checked against the value based on assumed $\dot{m}_4$ and $\dot{m}_{11}$. Iteration is necesssary to obtain correct $\dot{m}_4$ resulting in the same η_v from equations 27 and 29.

Properties at 9 and 10 are evaluated from equations 34 and 37. Equation 36 is used as a check.

The quality of the fluid is checked at various locations. In a properly designed pump, the fluid should be subcooled at location 10.

In the event of a two phase flow through a leakage path, the flow is assumed homogeneous. The density of the fluid is the density of the mixture; whereas the liquid viscosity is used in the flow equations. Choking of a two phase flow through a passage is possible. The problem is complicated by the two phase fluid and the passage with moving boundaries. Choking, if it should occur, limits the flow and as a result, the error caused by not taking it into account will be on the safer side.

Conclusion

A computer program of the analysis has been made. A cryogenic pump made and tested ~~a few years ago~~ was used as a sample to check the program. The agreement between the measured and the calculated values has been found to be quite good. As a result liquid H_2 and O_2 vane pumps may be designed with the help of this program. The program may also be used for non-cryogenic operations such as fuel pumps.

The computer program output consists of the fluid condition (including its quality) at all locations, the volumetric efficiency, and the pump capacity, as a function of the inlet condition, delivery pressure, speed, torque efficiency and the pump geometry. The computer printout is shown in Fig. 5.2.

RGM/gn

Fig. 5.2 THERMAL LEAKAGE PROGRAM LISTING


```
**WRITE PRINT,ZAD10
C           DATA SET ZAD10      AT LEVEL 004 AS OF 11/10/78
C
C   ANALYSIS OF THE PERFORMANCE OF VANE PUMPS WITH REFERENCE TO
C   LEAKAGE IN PUMPING LIQUID HYDROGEN AND LIQUID OXYGEN
C
C
C
      REAL LM,MDOT6,MDOT11,MU68
      REAL LVT,LVS,LRS,LCS,LKS
       REAL MU,L,MDOT4,MDOT7,MDOT8
      LOGICAL VAPOR
      LOGICAL VP7,VP8,VP6
      INTEGER ERROR,ENTRY
      DIMENSION PROPS(8)
      DIMENSION POUTVT(200),PINVT(200)
      DIMENSION TITLE(20)
      COMMON L(200),B(200),T(200),R(200),PIN(200),POUT(200),P4,P6,PI,
     1     RPM,MU,NVANES,NROTOR,NKID,NCAM
       COMMON/FLUIDC/GAMMA,WL,WG,DENSL,DENSG,ENTL,ENTG,ENTHL,ENTHG
C
10000 CONTINUE
      ICRD=5
      IPRT=3
      PI=3.14159
C
5101  READ(ICRD,11,END=5102) TITLE
      READ(ICRD,10)  NVANES,NROTOR,NKID,NCAM,NAMGAS
      READ(ICRD,30)  T4,P4,P6,RPM,P4END,DELP4,VTHROW
      READ(ICRD,35)  RMAJ,RMIN,RROT,VWIDTH,VHGT,VTHICK,TROTOR
      READ(ICRD,35)  ETAT,THETAC,LKS,TKS,RKS,TCS,RCS,ROSPLN
      READ(ICRD,20)  BVT,BVS,BRS,BKS,BCS,LVT,BKHP
      READ(ICRD,50) (PINVT(J),J=1,NVANES),(POUTVT(J),J=1,NVANES)
      WRITE(IPRT,12) TITLE
11    FORMAT(20A4)
12    FORMAT(1H1,20A4)
      IF(RKS.EQ.0.0) RKS=(RROT+ROSPLN)/2.0
      P5=P4
      P7=P4
      P8=P4
      P9=P4
      PINPT1=P4
      PINPT2=P6
      VOLD=2.0*PI*(RMAJ*RMAJ-RMIN*RMIN)*TROTOR
      VOLC=2.0*THETAC*PI*(RMIN*RMIN-RROT*RROT)*TROTOR
      TVT=VWIDTH
      TVS=VTHROW
       TRS=RROT-(RKS+0.5*TKS)
      LVS=VTHICK
      LRS=(2.0*PI*RROT)/NVANES
      LCS=PI*(RMAJ+RMIN)/4.0
      RVT=(RMAJ+RMIN)/2.0
      RVS=0.5*(RMAJ+RMIN)-0.5*VTHROW
      RRS=RROT-0.5*TRS
      R11=RKS-0.5*TKS
      RM=(ROSPLN+R11)/2.0
      LM=R11-ROSPLN
      IF(NAMGAS.EQ.1) GO TO 1
      IF(NAMGAS.EQ.2) GO TO 2
1     CALL O2
      RCM=.4325
      WRITE(IPRT,5)
      GO TO 8
2     CALL PH2
      RCM=.03143
      WRITE(IPRT,6)
8     CONTINUE
C
C *** IF SOME VALUE OF B SHOULD BE ZERO THE PROGRAM WILL MAKE IT
C     NON-ZERO AND SET THE CORRESPONDING T VALUES EQUAL TO ZERO.
C     THIS WILL AVOID MEANINGLESS QDOT AND WDOT EQUATIONS.
      IF(BVT.NE.(0.0)) GO TO 40
```

```
      BVT=0.1
      TVT=0.0
40    IF(BRS.NE.(0.0)) GO TO 42
      BRS=0.1
      TVS=0.0
42    IF(BKS.NE.(0.0)) GO TO 45
      BKS=0.1
      TKS=0.0
45    IF(BCS.NE.0.0) GO TO 47
      BCS=0.1
      TCS=0.0
47    CONTINUE
      GO TO 52
5000  CONTINUE
      DO 5005 J=1,NVANES
      IF(PINVT(J).EQ.P4) PINVT(J)=P4+DELP4
      IF(POUTVT(J).EQ.P4) POUTVT(J)=P4+DELP4
5005  CONTINUE
      P4=P4+DELP4
      WRITE(IPRT,12)  TITLE
      P5=P4
      P7=P4
      P8=P4
      P9=P4
      PINPT1=P4
52    CONTINUE
      WRITE(IPRT,60)NVANES,NROTOR,NKID,NCAM,RMAJ,RMIN,VWIDTH,VHGT,
     1              VTHICK,RHOT,TROTOR,ETAT,THETAC,ROSPLN,RPM
      WRITE(IPRT,6006) VOLC,VOLD,VTHROW
      WRITE(IPRT,61) BKHP,LM,RKS,R11
C
C ***SET VALUE OF J FOR VARIABLES
C
      DO 70 J=1,NVANES
      PIN(J)=PINVT(J)
      PIN(J+20)=PINVT(J)
      PIN(J+40)=PINVT(J)
      POUT(J)=POUTVT(J)
      POUT(J+20)=POUTVT(J)
      POUT(J+40)=POUTVT(J)
70    CONTINUE
      DO 80 J=1,NROTOR,2
      JJ=J+1
      PIN(JJ+60)=PINPT2
      PIN(J+60)=PINPT1
      POUT(J+60)=PINPT2
      POUT(JJ+60)=PINPT1
80    CONTINUE
      DO 90 J=1,NKID,2
      JJ=J+1
      PIN(J+70)=PINPT1
      PIN(JJ+70)=PINPT2
      POUT(J+70)=PINPT2
      POUT(JJ+70)=PINPT1
90    CONTINUE
      DO 95 J=1,NCAM
      JJ=J+80
      PIN(JJ)=P6
      POUT(JJ)=P4
95    CONTINUE
C
C
C     THE NUMBERING SCHEME FOR VARIABLES WITH SUBSCRIPT J IS AS FOLLOWS
C             VS=VANE SIDE  RS=ROTOR SIDE  KS=KIDNEY SIDE  VT=VANE TIP
C     NVANES=NUMBER OF VANES,MAX. NUMBER OF VANES IS 20
C     NROTOR=NUMBER OF ROTOR SIDE LEAKAGE  MAX IS 10
C     NKID=NUMBER OF KIDNEY SIDE LEAKAGE PATHS MAX IS 10
C     J=1,2,3,.....NVANES   FOR VT
C     J=21,22,.......(20+NVANES) FOR VS SIDE1
C     J=41,42,.......(40+NVANES) FOR VS SIDE2
C     J=61,62,.....   (60+NROTOR) FOR ROTOR SIDES
C     J=71,72,.......(70+NKID)    FOR KIDNEY SIDE
C     J=81,82,.......(80+NCAM)    FOR CAM SIDE
C
      DO 100  J=1,NVANES
      L(J)=LVT
      R(J)=RVT
```

```
      B(J)=BVT
      T(J)=TVT
100   CONTINUE
      DO 130  I=1,NVANES
      J=20+I
      L(J)=LVS
      R(J)=RVS
      B(J)=BVS
      T(J)=TVS
130   CONTINUE
      DO 140 I=1,NVANES
      J=40+I
      L(J)=LVS
      R(J)=RVS
      B(J)=BVS
      T(J)=TVS
140   CONTINUE
      DO 170 I=1,NROTOR
      J=I+60
      L(J)=LRS
      R(J)=RRS
      T(J)=TRS
      B(J)=BRS
170   CONTINUE
      DO 200 I=1,NKID
      J=70+I
160   L(J)=LKS
      R(J)=RKS
      T(J)=TKS
      B(J)=BKS
200   CONTINUE
      DO 180 I=1,NCAM
      J=I+80
      L(J)=LCS
      R(J)=RCS
      T(J)=TCS
      B(J)=BCS
180   CONTINUE
C
C
C
C CALCULATION OF PROPERTIES AT 4
C
      CALL CM(1,T4,OUT)
      TM=OUT
      CALL CM(2,P4,OUT)
      PM=OUT
      ENTRY=3
      NP=7
      CALL FLUID(TM,PM,D,PROPS,NP,ENTRY,VAPOR,ERROR)
      CALL CB(3,D,RHO4)
      CALL CB(4,PROPS(2),S4)
      CALL CB(5,PROPS(3),H4)
      CALL CB(6,PROPS(7),XMU4)
C
C
C ITERATION ON MDOT4 (ETAVIT
C
      ICON=1
C   INITIALIZE MDOT4
      XM4L=0.0
      XM4R=VOLD*RPM*RHO4/60.
220   CONTINUE
      MDOT4=(XM4L+XM4R)/2.0
C
C
C CALCULATION OF PROPERTIES AT 6 AND 8
C
      CALL  CM(2,P6,OUT)
      PM6=OUT
      PS6=S4
      CALL CM(4,S4,PS6M)
      PROPS(2)=PS6M
      NPROPS=7
      ENTRY=4
      CALL FLUID(TEMP,PM6,D,PROPS,NPROPS,ENTRY,VAPOR,ERROR)
      IF(ERROR.NE.0) WRITE(IPRT,555)ERROR
```

```
      PR6M=D
      CALL CB(1,TEMP,PT6)
      CALL CB(3,PR6M,PR6)
      CALL CB(5,PROPS(3),PH6)
      RHO46=(RHO4+PR6)/2.0
C
C ITERATION ON MDOT11
C
      XM11L=0.0
      XM11R=MDOT4
      ICOUNT=1
225   CONTINUE
      MDOT11=(XM11L+XM11R)/2.0
      MDOT6=MDOT4-MDOT11
      ETAV1=(MDOT6*60.0)/(RHO4*VOLD*RPM)
      ETAOVP=ETAT*ETAV1
      H6NEW=H4+(144.*(P6-P4))/(778.16*RHO46*ETAOVP)
      H6=H6NEW
      CALL CM(5,H6NEW,OUT)
      H6M=OUT
      PROPS(3)=H6M
      NPROPS=7
      ENTRY=5
      CALL FLUID(TEMP,PM6,D,PROPS,NPROPS,ENTRY,VAPOR,ERROR)
      IF(ERROR.NE.0) WRITE(IPRT,555)ERROR
      VP6=VAPOR
       CALL CB(1,TEMP,T6NEW)
      IF(VP6) GO TO 215
      CALL CB(3,D,RHO6)
      CALL CB(4,PROPS(2),S6)
      GO TO 216
215   CALL VAPR(1,XVAL6,S6,H6,RHO6,VOID6)
      NP=7
      CALL FLUIDL(PROPS,NP,ERROR)
216   CONTINUE
      CALL CB(6,PROPS(7),XMU6)
      T6=T6NEW
      ENTRY=2
      CALL FLUID(TEMP,PM6,REM,PROPS,NPROPS,ENTRY,VAPOR,ERROR)
      CALL CB(1,TEMP,T6SAT)
C
      CALL CM(2,P8,P8M)
      H8=H6
      CALL CM(5,H6,H8M)
      PROPS(3)=H8M
      ENTRY=5
      NPROPS=7
      CALL FLUID(TEMP,P8M,D,PROPS,NPROPS,ENTRY,VAPOR,ERROR)
      CALL CB(1,TEMP,T8)
      VP8=VAPOR
      IF(VAPOR) GO TO 690
      CALL CB(3,D,RHO8)
      CALL CB(4,PROPS(2),S8)
      GO TO 695
690   CALL VAPR(1,XVAL8,S8,H8,RHO8,VOID8)
      NP=7
      CALL FLUIDL(PROPS,NP,ERROR)
695   CONTINUE
      CALL CB(6,PROPS(7),XMU8)
      MU68=(XMU8+XMU6)/2.0
      RHO68=(RHO6+RHO8)/2.0
      XM11=((PI*RM*(BKHP**3)*RHO68)/(6.0*MU68*LM))*((144.0*
     1    32.174*(P6-P4))-(RHO68*((PI*RPM/60.0)**2)*LM*RM))
      XMDOT=(XM11*NKID)/4.0
      TOLR=0.01*XMDOT
      IF(ABS(MDOT11-XMDOT)-TOLR)235,235,230
230   ICOUNT=ICOUNT+1
      IF(ICOUNT.GT.100) GO TO 240
      IF(XMDOT-MDOT11)242,242,243
242   XM11R=MDOT11
      GO TO 225
243   XM11L=MDOT11
      GO TO 225
 240  WRITE(IPRT,72) ICOUNT
C
C END ITERATION MDOT11
C
```

```
C *** INITIALIZE FOR ITERATION ON T7
C
235   CONTINUE
      TOLER=.005
      HL=H6-10.0
      HR=H6+10.0
        JCOUNT=1
250   CONTINUE
310   H7=(HL+HR)/2.0
      CALL CM(2,P7,P7M)
      CALL CM(5,H7,H7M)
      PROPS(3)=H7M
      NPROPS=7
       ENTRY=5
      CALL FLUID(T7M,P7M,D,PROPS,NPROPS,ENTRY,VP7,ERROR)
      IF(ERROR.NE.0) WRITE(IPRT,555)ERROR
      CALL CB(1,T7M,T7)
      IF(VP7) GO TO 8000
      CALL CB(3,D,RHO7)
      CALL CB(4,PROPS(2),S7)
      X7=PROPS(7)
360   CONTINUE
      CALL CB(6,X7,XMU7)
      MU=0.5*(XMU6+XMU7)
      CALL MAGQ(QSIN,WIN67,0)
C
      MDOT7=((RHO6+RHO7)*QSIN)/2.0
      H7NEW=H6+(WIN67/(MDOT7*778.16))
      IF(ABS(H7NEW-H7)-TOLER)400,400,370
370   JCOUNT=JCOUNT+1
      IF(JCOUNT.GE.100) GO TO 700
      IF(H7NEW-H7)320,320,330
320   CONTINUE
      HR=H7
      GO TO 310
330   CONTINUE
      HL=H7
      GO TO 250
8000  CONTINUE
      CALL VAPR(1,XVAL7,S7,H7,RHO7,VOID7)
      NP=7
      CALL FLUIDL(PROPS,NP,ERROR)
      X7=PROPS(7)
      GO TO 360
700   WRITE(IPRT,72) JCOUNT
400   H7=H7NEW
C END ITERATION H7
C
C CALCULATION OF PROPERTIES AT 5
      CALL CM(2,P5,P5M)
      H5=H4+(((H6-H4)*MDOT7+WIN67/778.16)/(MDOT4+MDOT7))
      CALL CM(5,H5,H5M)
      PROPS(3)=H5M
      NPROPS=3
      ENTRY=5
      CALL FLUID(TEMP,P5M,D,PROPS,NPROPS,ENTRY,VAPOR,ERROR)
      IF(ERROR.NE.0) WRITE(IPRT,555)ERROR
      CALL CB(1,TEMP,T5)
      IF(VAPOR) GO TO 2000
      CALL CB(3,D,RHO5)
      CALL CB(4,PROPS(2),S5)
      GO TO 390
2000  CALL VAPR(1,XVAL,S5,H5,RHO5,VOID5)
 390    CONTINUE
C
C
      MDOT8=RHO6*VOLC*RPM/60.
      TOLER=0.01
      ICON=ICON+1
      IF(ICON .GT.50) WRITE(IPRT,72) ICON
      ETAV2=1-((VOLC/VOLD)*(RHO6/RHO5-1))-((MDOT7*60.0+MDOT11*60.0)/
     1  (RHO4*VOLD*RPM))
      IF(ABS(ETAV2-ETAV1)-TOLER)411,411,401
401   IF(ETAV2-ETAV1)402,402,403
402   CONTINUE
      XM4R=MDOT4
      GO TO 220
```

```
403    CONTINUE
       XM4L=MDOT4
        GO TO 220
C
C   END ITERATION ON MDOT4
C
411    CONTINUE
       CALL MAGQ(QSIN,WIN67,2)
       GPM=(MDOT4*448.83)/RHO4
       GPM6=(MDOT6*448.83)/RHO4
       GPM7=(MDOT7*448.83)/RHO4
       GPM8=(MDOT8*448.83)/RHO4
       GPM11=(MDOT11*448.83)/RHO4
       WRITE(IPRT,520) ETAV1,ETAT,ETAOVP,MU68,MU
       WRITE(IPRT,6200) MDOT4,GPM,MDOT6,GPM6,MDOT7,GPM7,
     1          MDOT8,GPM8,MDOT11,GPM11
       WRITE(IPRT,65) P4,T4,RHO4,H4,S4
       WRITE(IPRT,260) PT6,PR6,PH6,PS6
       IF(VP6)      WRITE(IPRT,6002) XVAL6,VOID6
       WRITE (IPRT,66) P6,T6,RHO6,H6,S6,T6SAT
       IF(VP7) WRITE(IPRT,6120) VP7,XVAL7,VOID7
       WRITE(IPRT,67) P7,T7,RHO7,H7,S7
       IF(VAPOR) WRITE(IPRT,6130) VAPOR
       IF(VAPOR) WRITE(IPRT,6002) XVAL, VOID5
       WRITE (IPRT,68) P5,T5,RHO5,H5,S5
       IF(VP8) WRITE(IPRT,6008) XVAL8,VOID8
       WRITE(IPRT,6180) P8,T8,RHO8,H8,S8
C
       TEST=144*MDOT4*(P6-P4)/(RHO46*WIN67)
       IF(TEST.LE.ETAOVP) WRITE(IPRT,77)
        WRITE(IPRT,670) TEST,ETAOVP
670    FORMAT(/,2X,'TEST= ',E12.5,5X,'ETA-OVP = ',E12.5)
C
C CALCULATION OF PROPERTIES AT 9
C
       CALL CM(2,P9,P9M)
       H9=H4+(((MDOT7+MDOT8)*(H6-H4)+WIN67/778.16)/(MDOT4+MDOT7+MDOT8))
       CALL CM(5,H9,H9M)
       NPROPS=3
       ENTRY=5
       PROPS(3)=H9M
       CALL FLUID(TEMP,P9M,D,PROPS,NPROPS,ENTRY,VAPOR,ERROR)
       IF(ERROR.NE.0) WRITE(IPRT,555)ERROR
       CALL CB(1,TEMP,T9)
       IF(VAPOR) GO TO 2050
       CALL CB(3,D,RHO9)
       CALL CB(4,PROPS(2),S9)
       GO TO 2030
2050   CALL VAPR(1,XVAL,S9,H9,RHO9,VOID9)
       WRITE(IPRT,6140) VAPOR
       WRITE(IPRT,6002) XVAL, VOID9
2030   CONTINUE
       ENTRY=2
       NPROPS=3
       CALL FLUID(TEMP,P9M,RCM,PROPS,NPROPS,ENTRY,VAPOR,ERROR)
       IF(ERROR.NE.0) WRITE(IPRT,555)ERROR
       CALL CB(1,TEMP,TSAT)
       WRITE (IPRT,69) P9,T9,RHO9,H9,S9,TSAT
C
C     INITIALIZE TO ITERATE ON P10
C CALCULATION OF PROPERTIES AT 10
C
       JCOUNT=1
       TOLER=0.005
       S10=S9
       V10=2*PI*RMAJ*RPM/60.0
       H10=H9-(V10**2)/(2.0*32.174*778.16)
        CALL CM(4,S10,S10M)
       P10L=0.0
       P10R=P9+10.0
405    CONTINUE
       P10 = 0.5*(P10L + P10R)
       CALL CM(2,P10,P10M)
       PROPS(2)=S10M
       NP=3
       ENTRY=4
       CALL FLUID(TM,P10M,D,PROPS,NP,ENTRY,VAPOR,ERROR)
```

```
      IF(ERROR.NE.0) WRITE(IPRT,555)ERROR
      CALL CB(1,TM,T10)
      IF(VAPOR) GO TO 9000
      CALL CB(3,D,RHO10)
       H10M=PROPS(3)
      CALL CB(5,H10M,H10NEW)
9010   CONTINUE
       DIFF=H10-H10NEW
      JCOUNT=JCOUNT+1
      IF(JCOUNT.GE.100) GO TO 721
       IF(ABS(DIFF)-TOLER)450,450,410
410   IF(DIFF)415,415,420
  415 P10R=P10
      GO TO 405
  420 P10L=P10
      GO TO 405
9000   CONTINUE
      CALL VAPR(2,XVAL,S10,H10NEW,RHO10,VOID10)
      GO TO 9010
721   WRITE(IPRT,72) JCOUNT
450   CONTINUE
      WRITE(IPRT,6150) VAPOR,H10NEW
      IF(VAPOR) WRITE(IPRT,6002) XVAL,VOID10
      NP=3
      ENTRY=2
      CALL FLUID(TEMP,P10M,RCM,PROPS,NP,ENTRY,VAPOR,ERROR)
      CALL CB(1,TEMP,T10SAT)
      WRITE(IPRT,680) P10,T10,RHO10,H10,S10,T10SAT
      GO TO 910
1000  WRITE(IPRT,75)
      GO TO 910
900   WRITE(IPRT,77)
910   CONTINUE
      IF(P4.LT.P4END) GO TO 5000
5     FORMAT(//,30X,'VANE PUMP ANALYSIS FOR OXYGEN',//)
6     FORMAT(//,30X,'VANE PUMP ANALYSIS FOR PARA-HYDROGEN',//)
10    FORMAT(8I10)
20    FORMAT(8E10.4)
30     FORMAT(8F10.4)
35    FORMAT(8F10.5)
36    FORMAT(5X,'RMAJ=',F10.6,2X,'FT',5X,'RMIN=',F10.6,2X,'FT',5X,'RROT
     1 = ',F10.6,2X,'FT',/,5X,'VANE WIDTH=',F10.6,2X,'FT',5X,'VANE HEIGH
     2T=',F10.6,2X,'FT',5X,'VANE THICKNESS=',F10.6,2X,'FT',5X,'TROT=',
     3F10.6,2X,'FT',/)
50     FORMAT(8F10.4)
60     FORMAT(/,T5,'NUMBER OF VANES =',I3,T45,'NUMBER OF ROTOR SIDE LEAKA
     1GE PATHS =',I3,T90,'NUMBER OF KIDNEY SIDE LEAKAGE PATHS =',I3,/,T5
     2,'NUMBER OF PRES PLATE LEAKAGE PATHS =',I3,T45,'RMAJ =',E12.5,1X,
     3'FT',T90,'RMIN =',E12.5,1X,'FT',/,T5,'VANE WIDTH =',E12.5,1X,'FT',
     4T45,'VANE HEIGHT =',E12.5,1X,'FT',T90,'VANE THICKNESS =',E12.5,1X,
     5'FT',/,T5,'ROTOR RADIUS =',E12.5,1X,'FT',T45,'ROTOR WIDTH =',E12.5
     6,1X,'FT',T90,'TORQUE EFF (ETA-T) =',E12.5,/,T5,'THETA-C =',E12.5,
     7T45,'OUTER SPLINE RADIUS =',E12.5,1X,'FT',T90,'RPM =',E12.5)
61     FORMAT(//,5X,'SPLINE LEAKAGE DATA',//5X,'MDOT11 LEAKAGE CLEARANCE
     1=',E12.5,1X,'FT',T60,'MDOT11 LEAKAGE LENGTH =',E12.5,1X,'FT'/5X,
     2'RADIUS OF KIDNEY LOCATION =',E12.5,1X,'FT',T60,'RADIUS TO KIDNEY
     3EDGE =',E12.5,1X,'FT')
65     FORMAT(/,5X,'PRESSURE P4 = ',F10.4,' PSIA',5X,'TEMPERATURE T4 =',
     1F10.4,' DEG. R',5X,'DENSITY RHO4 = ',F10.4,' LBM/FT**3',/,5X,'ENTH
     2ALPY H4 =',F10.4,' BTU/LBM',5X,'ENTROPY S4 = ',F10.4,' BTU/LBM-R')
66     FORMAT(/,5X,'PRESSURE P6 = ',F10.4,'PSIA',5X,'TEMPERATURE T6 =',
     1F10.4,' DEG. R',5X,'DENSITY RHO6= ',F10.4,' LBM/FT**3',/,5X,'ENTHA
     2LPY H6 = ',F10.4,' BTU/LBM',5X,'ENTROPY S6 = ',F10.4,' BTU/LBM-R',
     35X,'T6SAT = ',F10.4)
67     FORMAT(/,5X,'PRESSURE P7 = ',F10.4,' PSIA',5X,'TEMPERATURE T7 =',
     1F10.4,' DEG. R',5X,'DENSITY RHO7 = ',F10.4,' LBM/FT**3',/,5X,'ENTH
     2ALPY H7 =',F10.4,' BTU/LBM',5X,'ENTROPY S7 = ',F10.4,' BTU/LBM-R')
68     FORMAT(/,5X,'PRESSURE P5 = ',F10.4,' PSIA',5X,'TEMPERATURE T5 =',
     1F10.4,' DEG. R',5X,'DENSITY RHO5 = ',F10.4,' LBM/FT**3',/,5X,'ENTH
     2ALPY H5 =',F10.4,' BTU/LBM',5X,'ENTROPY S7 = ',F10.4,' BTU/LBM-R')
69     FORMAT(/,5X,'PRESSURE P9 = ',F10.4,' PSIA',5X,'TEMPERATURE T9 =',
     1F10.4,' DEG. R',5X,'DENSITY RHO9 = ',F10.4,' LBM/FT**3',/,5X,'ENTH
     2ALPY H9 =',F10.4,' BTU/LBM',5X,'ENTROPY S9 = ',F10.4,' BTU/LBM-R',
     3/,5X,'SATURATION TEMPERATURE T9 = ',F10.4,2X,'DEG R')
72     FORMAT(/,5X,'SOLUTION FAILED TO CONVERGE IN ',I3,' TRIES')
75     FORMAT(5X,'****ERROR****',//,5X,'FAILED TO CONVERGE IN 50 TRIES')
77     FORMAT(5X,'TEST FAILED FOR ETAOVP')
```

```
500    FORMAT(/5X,'T4=',F10.4,2X,'DEG R',5X,'P4=',F10.4,2X,'PSIA',5X,'P5=
     1       ',F10.4,2X,'PSIA',5X,'P6=',F10.4,2X,'PSIA',/,5X,'P7=',F10.4,
     2  2X,'PSIA',5X,'P9=',F10.4,2X,'PSIA',5X,'MDOT4=',F10.4,2X,'LBM/SEC
     3 ',5X,'RPM=',F10.4,/)
 260   FORMAT(//,5X,'PSUEDO VALUES OF  T6, RHO6, H6,S6 : ',8E12.5)
510    FORMAT(/,5X,'ETA-T =',F10.4,5X,'THETA-C =',F9.4,5X,'ROSPLN=',F10.
     16,2X,'FT',5X,'LKS =',F10.5,2X,'FT',/,5X,'TKS =',F10.5,2X,'FT',5X,
     2       'TCS =',F10.5,2X,'FT',5X,'RCS =',F10.5,2X,'FT')
555    FORMAT(1X,'ERROR = ',I10)
600    FORMAT(//,5X,'VAPOR REGION   ENTRY= ',I2)
680    FORMAT(/,5X,'PRESSURE P10= ',F10.4,' PSIA',5X,'TEMPERATURE T10=',
     1F10.4,' DEG. R',5X,'DENSITY RHO10= ',F10.4,' LBM/FT**3',/,5X,'ENTH
     2ALPY H10=',F10.4,' BTU/LBM',5X,'ENTROPY S10= ',F10.4,' BTU/LBM-R',
     3/,5X,'SATURATION TEMPERATURE T10= ',F10.4,2X,'DEG R')
6002   FORMAT(/,2X,'XVAL = ',F10.4,5X,'VOID = ',F10.4)
6004     FORMAT(/,5X,'MDOT7 = ',E10.4,5X,'MDOT8 = ',E10.4)
6006     FORMAT(T5,'VOL-C =',E10.4,1X,'FT**3',T45,'VOL-D =',E10.4,
     1     1X,'FT**3',T90,'VANE THROW =',E10.4,1X,'FT',/)
6008   FORMAT(/,1X,'VAP = T   CALC FROM P8 AND H8',5X,'XVAL8 =',F10.4,5X,
     1             'VOID =',F10.4)
6120   FORMAT(/,2X,'VAP =',L2,2X,'CALC FROM P7 AND H7',         5X,'XVAL =
     1 ',F10.4,5X,'VOID = ',F10.4)
6130   FORMAT(/,2X,'VAP =',L2,2X,'CALC FROM P5 AND H5')
6140   FORMAT(/,2X,'VAP =',L2,2X,'CALC FROM P9 AND H9')
6150   FORMAT(/,2X,'VAP =',L2,2X,'CALC FROM S10 = S9 AND P10',5X,
     1             'H10NEW = ',F12.4)
6180   FORMAT(/,5X,'PRESSURE P8 = ',F10.4,' PSIA',5X,'TEMPERATURE T8 =',
     1F10.4,' DEG. R',5X,'DENSITY RHO8 = ',F10.4,' LBM/FT**3',/,5X,'ENTH
     2ALPY H8 =',F10.4,' BTU/LBM',5X,'ENTROPY S8 = ',F10.4,' BTU/LBM-R')
6200   FORMAT(/,5X,30(1H*),'FLOW RATES',35(1H*),//,5X,'FLOW',T35,'LBM/SE
     1C',T65,'GPM',/,5X,'----',T30,15(1H-),T60,15(1H-),//,5X,'MDOT4',
     2T30,E12.5,T60,E12.5,/,5X,'MDOT6',T30,E12.5,T60,E12.5,/,5X,'MDOT7',
     3T30,E12.5,T60,E12.5,/,5X,'MDOT8',T30,E12.5,T60,E12.5,/,5X,'MDOT11'
     4,T30,E12.5,T60,E12.5,//,5X,75(1H*),/)
520    FORMAT(/,5X,'VOLUMETRIC EFFICIENCY =',E10.4,/5X,'TORQUE EFFICIENCY
     1=',E10.4,/,5X,'TOTAL EFFICIENCY =',E10.4,//,5X,'MU68 =',E12.5,5X,
     2'MU67 =',E12.5,/)
5100   CONTINUE
       GO TO 5101
5102   STOP
       END
       SUBROUTINE CM(N,BIN,OUT)
C
C      CONVERT TO METRIC UNITS
C      N=1 FOR TEMP, N=2 FOR PRES   N=3 FOR DENSITY
C      N=4 FOR ENTROPY    N=5 FOR ENTHALPY    N=6 FOR VISCOSITY
C
       DIMENSION VAL(10)
       VAL(1)=0.55556
       VAL(2)=0.0068948
       VAL(3)=.01602
       VAL(4)=4.186
       VAL(5)=2.326
       VAL(6)=14.87
       OUT=VAL(N)*BIN
       RETURN
       END
       SUBROUTINE CB(N,CIN,BOUT)
C
C      CONVERT TO BRITISH  ENG. UNITS
C      N=1 FOR TEMP, N=2 FOR PRES   N=3 FOR DENSITY
C      N=4 FOR ENTROPY    N=5 FOR ENTHALPY    N=6 FOR VISCOSITY
C
       DIMENSION VAL(10)
       VAL(1)=1.8
       VAL(2)=1./.0068948
       VAL(3)=1./0.01602
       VAL(4)=1./4.186
       VAL(5)=1./2.326
       VAL(6)=1./14.87
       BOUT=VAL(N)*CIN
       RETURN
       END
       SUBROUTINE VAPR(N,XVAL,S,H,RHO,VOID)
C
C SUBROUTINE FOR TWO PHASE FLUID
C CALCULATES MASS FRACTION XVAL AND VOLUME FRACTION VOID
```

```
C  CALCULATES DENSITY OF THE MIXTURE
      COMMON/FLUIDC/GAMMA,WL,WG,DENSL,DENSG,ENTL,ENTG,ENTHL,ENTHG
      DL=DENSL/.01602
      DG=DENSG/.01602
      SG=ENTG/4.186
      SL=ENTL/4.186
      HL=ENTHL/2.326
      HG=ENTHG/2.326
      IF(N.EQ.2) GO TO 50
      XVAL=(H-HL)/(HG-HL)
      S= XVAL*SG+(1.0-XVAL)*SL
      GO TO 60
50    CONTINUE
      XVAL=(S-SL)/(SG-SL)
      H=XVAL*HG+(1.0-XVAL)*HL
60    RHO=(DL*DG)/(DL*XVAL+(1-XVAL)*DG)
      VOID=(XVAL*RHO)/DG
      RETURN
      END
      SUBROUTINE MAGQ(QSIN,WIN67,IFLAG)
C
C
      REAL MU,L,MQDOT,MALPHA
      DIMENSION WDOT(220),MALPHA(200)
      DIMENSION ALPHA(200),QDOT(200),MQDOT(200)
      COMMON L(200),B(200),T(200),R(200),PIN(200),POUT(200),P4,P6,PI,
     1     RPM,MU,NVANES,NROTOR,NKID,NCAM
      IPRT=3
      IF(IFLAG.EQ.1) WRITE(IPRT,80)
      QSIN=0.0
      WIN67=0.0
      DO 50 I=1,90
      IF((I.GE.1).AND.(I.LE.NVANES)) GO TO 10
      IF((I.GE.21).AND.(I.LE.(NVANES+20))) GO TO 10
      IF((I.GE.41).AND.(I.LE.(NVANES+40))) GO TO 10
      IF((I.GE.61).AND.(I.LE.(NROTOR+60))) GO TO 10
      IF((I.GE.71).AND.(I.LE.(NKID+70)))  GO TO 10
      IF((I.GE.81).AND.(I.LE.(NCAM+80))) GO TO 10
      GO TO 50
10    J=I
      QDOT(J)=(PI*RPM*R(J)*B(J)*T(J))/60.+(144.*B(J)**3*T(J)*(PIN(J)-
     1          POUT(J))*(32.174))/(12.*MU*L(J))
      IF((PIN(J).EQ.P6).AND.(POUT(J).EQ.P4))ALPHA(J)=1.0
      IF((PIN(J).EQ.P6).AND.(POUT(J).EQ.P6)) ALPHA(J)=0.0
      IF((PIN(J).EQ.P4).AND.(POUT(J).EQ.P4)) ALPHA(J)=0.0
      IF((PIN(J).EQ.P4).AND.(POUT(J).EQ.P6).AND.(QDOT(J).GT.0.))ALPHA(J)
     1   =0.0
      IF((PIN(J).EQ.P4).AND.(POUT(J).EQ.P6).AND.(QDOT(J).LT.0.))ALPHA(J)
     1   =-1.0
      MQDOT(J)=ALPHA(J)*QDOT(J)
      QSIN=QSIN+MQDOT(J)
      MALPHA(J)=ABS(ALPHA(J))
      WDOT(J)=(MALPHA(J)*2.0*PI*RPM/60.0)*((2.0*PI*MU*RPM*L(J)*T(J)*R(J)
     1  *R(J))/(60.0*32.174*B(J))+(144.0*B(J)*R(J)*T(J)*(POUT(J)-
     2   PIN(J)))/2.0)
      WIN67=WIN67+WDOT(J)
      IF(IFLAG.NE.1) GO TO 50
      IF(J.EQ.1) WRITE(IPRT,90)
      IF(J.EQ.21)WRITE(IPRT,100)
      IF(J.EQ.41)WRITE(IPRT,110)
      IF(J.EQ.61)WRITE(IPRT,120)
      IF(J.EQ.71)WRITE(IPRT,130)
      IF(J.EQ.81)WRITE(IPRT,140)
      WRITE(IPRT,60) J, L(J),B(J),T(J),R(J),PIN(J),POUT(J),ALPHA(J),
     1      QDOT(J),WDOT(J)
50    CONTINUE
      IF(IFLAG.EQ.1) WRITE(IPRT,70) WIN67,QSIN
60    FORMAT(5X,I10,9E13.5)
70    FORMAT(5X,'WIN67 = ',F10.5,1X,'FT*LBF/SEC',5X,'QSIN = ',F10.5,1X,
     1      'FT**3/SEC')
80    FORMAT(//,14X,'J',7X,'L(J)',9X,'B(J)',9X,'T(J)',9X,'R(J)',8X,'PIN(
     1J)',6X,'POUT(J)',6X,'ALPHA(J)',6X,'QDOT(J)',5X,'WDOT(J)',/)
90    FORMAT(/,1X,'VANE TIP')
100   FORMAT(/,1X,'VANE SIDE 1')
110   FORMAT(/,1X,'VANE SIDE 2')
120   FORMAT(/,1X,'ROTOR SIDE')
130   FORMAT(/,1X,'KIDNEY SIDE')
```

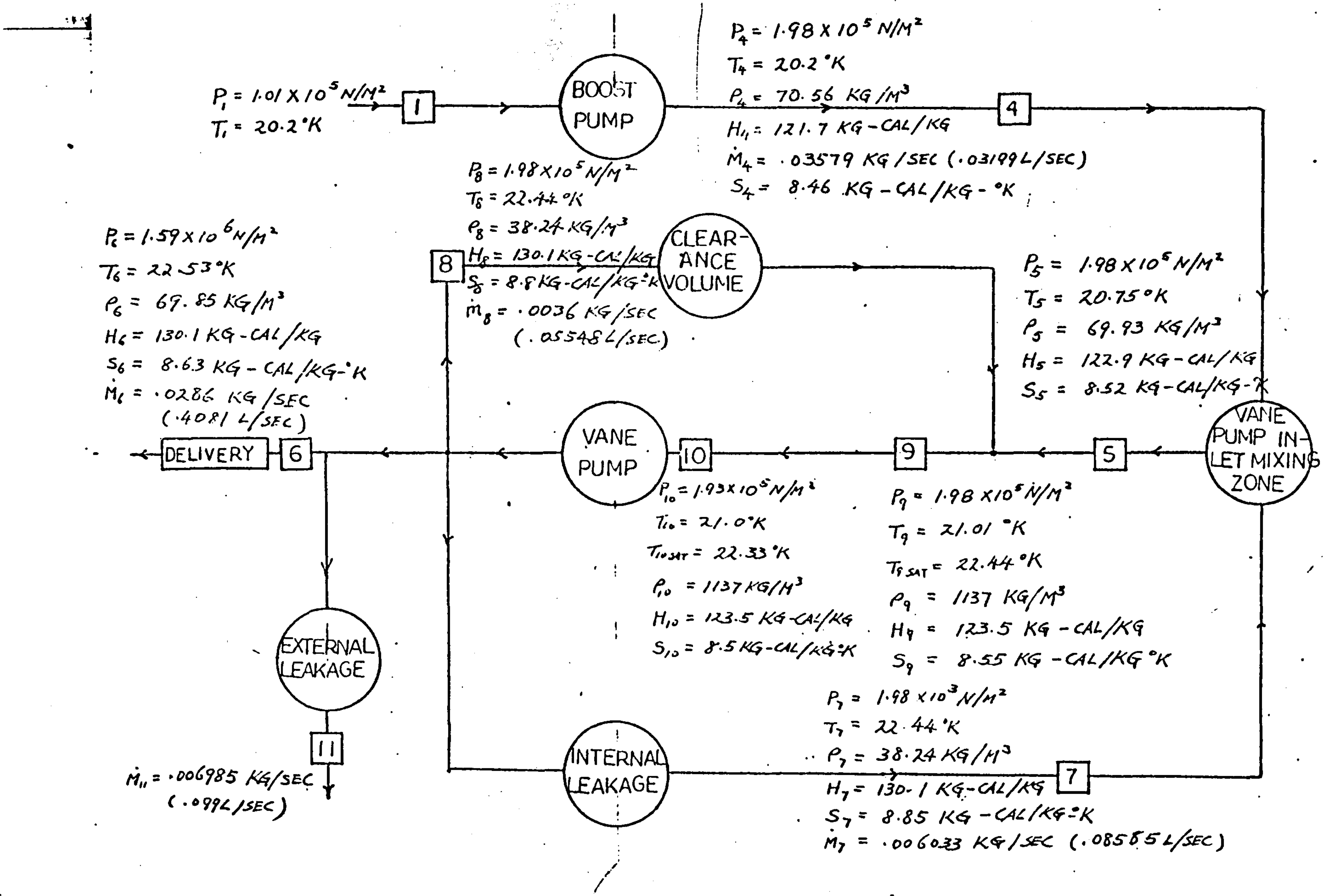

Fig.5.3-FLUID PROPERTIES OF LIQUID HYDROGEN ESTIMATED IN EACH FLOW PATH

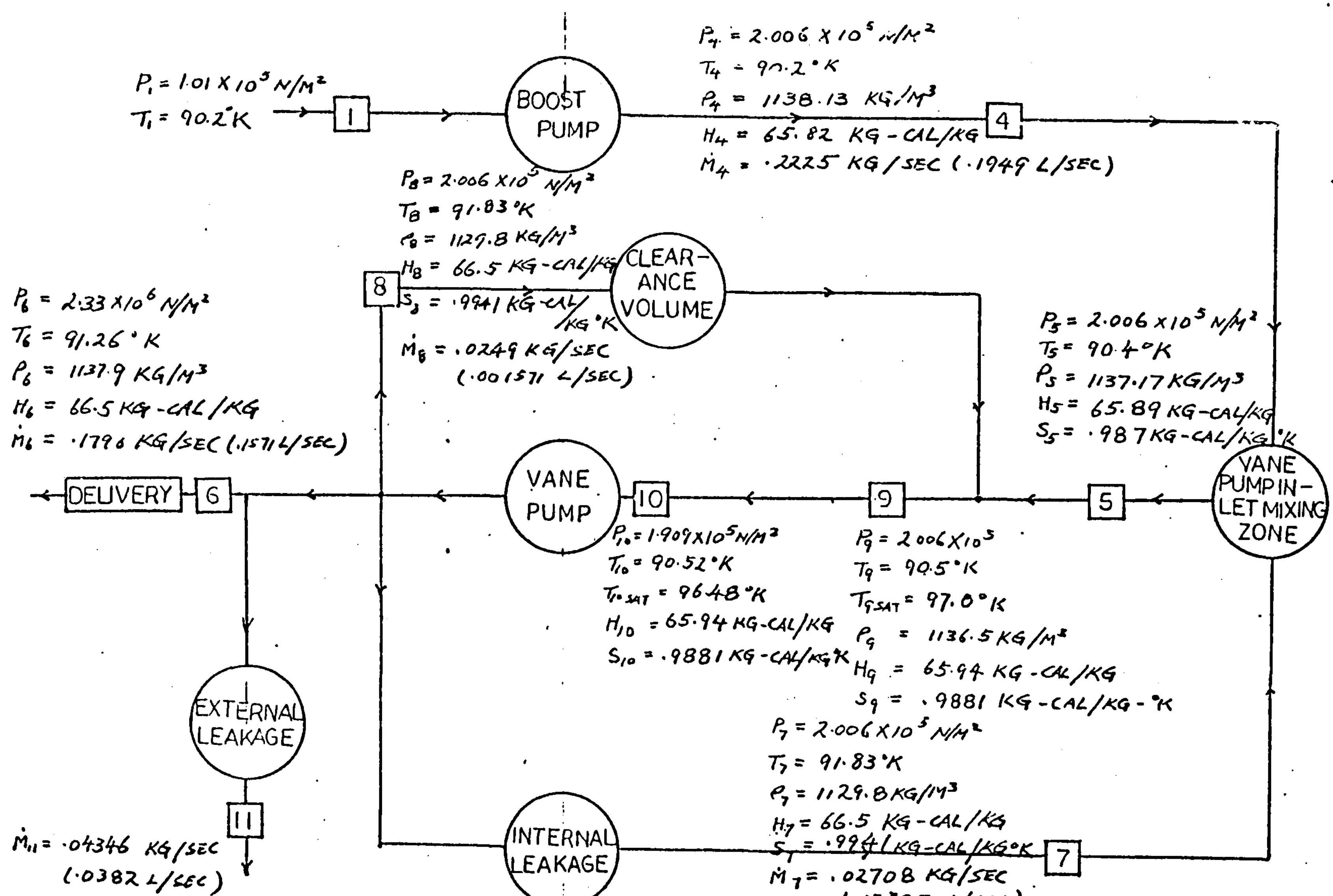

Fig. 5.4 - FLUID PROPERTIES OF LIQUID OXYGEN ESTIMATED IN EACH FLOW PATH

6. VANE STAGE DESIGN

VANE PUMP DESIGN

6.1 GENERAL MECHANICAL FEATURES

A vane pump generally consists of a rotor, shaft, vanes, a liner, 2 port plates, bearings and housing. Pumping is accomplished both by the undervane and the overvane swept volume pumping action.

The rotor can either be keyed to the shaft or driven by splines.

The vanes are rounded at both ends with a tip radius less than the minimum radius of curvature of the liner cam profile.

A cam profile is machined on to the liner or cam ring.

Flow paths for undervane kidneys, main inlet and discharge ports are on the port plates.

Bearings are placed as close to the rotor as possible in order to minimize the amplitude of shaft whirl at critical speeds. Tighter clearances can be held if the displacement amplitude is small.

Housings have a thermal expansion coefficient similar to that of the liner in order to reduce the sealing problem. Same thing holds for the shaft and rotor for limiting the leakage and stress.

6.2 SIZING

The total displacement of the vane pump is calculated by the following equation;

$$\text{Displacement} = 2\pi L\,(R^2 - r^2)$$

where L = width of the vane

R = major radius of the cam ring

r = minor radius of the cam ring

The value of R is limited by the maximum allowable surface rubbing speed of the vane tips. In the case of LH_2, this is 14.3 m/sec , LOX, it is 6.1 m/sec. The other dimensions of the pump are governed by such aspect ratios as rotor length/diameter, vane height/width, max. vane throw/height. The allowable ranges of these ratios are based on the previous experience in vane fuel pump design (Fig. 6.2.2). The basic information of the vane pump designed is shown in Fig. 6.2.3.

The cam contour is generated by two computer programs - 7th degree Polynomial and Trapezoidal. The acceleration curve of the Trapezoidal design consists of a constant and a sinusoidal acceleration curve. Both the 7th degree polynomial and the trapezoidal can be matched with a dwell depending on the circumstances. A trade-off between the two profiles was made and the 7th degree polynomial was chosen. The cam profile is selected on the basis of low "jerk*", minimum and maximum radial accelerations of the cam.

*jerk - rate of change of acceleration ($m./sec^3$)

Generally we try to hold the jerk below 10^7 m/sec^3, maximum acceleration, no higher than 16764 m/sec^2 and minimum acceleration no lower than 6705 m/sec^2 (at 15000 rpm). A smooth contour will give a low jerk value. The minimum acceleration determines the lowest limit that a vane can ramain in contact with the liner. The maximum acceleration dictates the boundary where wear and stress failure may occur.

The original design goals for the LH_2 pump set the operating speed at 12,000 rpm, and LO_2 pump at 4,000 rpm. As a result of the restrictions listed above, the optimum speed for LH_2 has to be 8000 rpm. If the same cam profile is to be used for LO_2, the width of the pump has to be reduced to obtain the target displacement per minute, but this will place the design outside the conservative design limit set by the aspect ratios, and at 4000 RPM the rubbing speed will be at the boundary value of 6.1 m/sec. The operating speed of LO_2 Pump is then chosen to be at 3000 rpm to avoid these problems. Plots for the displacement, velocity, acceleration, jerk and the cam contour are shown in Figures 6.2.4 to 6.2.8. The computer print out is shown in Fig. 6.2.9.

The next step in evaluating the cam design is to study the vane dynamics. A computer program is available for this purpose. The program takes into consideration:-

- the pressure forces on the vane,
- centrifugal force on vane,
- centrifugal force on the undervane fluid,
- friction force in the vane guide slot due to the Coriolis component of acceleration,
- the friction force in the vane guide slot due to the tip friction load on the vane,
- the friction force in the vane guide slot due to pressure side load,

and calculates the vane/liner reaction force. This vane/liner reaction force is used to evaluate the cam design. A zero or very small value dictates that the vane may leave the cam surface at that location. The maximum value of the force is used to calculate the Hertz contact stress between the vane and the liner. For fuel pumps, good experience falls below 8.27×10^8 N/m^2. Our design is only 1.79×10^8 N/m^2 for the LH_2 Pump. A plot showing the magnitude of forces listed above through a complete rise & fall cycle is shown in Fig. 6.2.10.

6.3 LEAKAGE AND CARRYOVER VOLUME

The performance of a vane pump is greatly dependent on its volumetric efficiency which in turn is affected by the following factors:

I. Leakages through the clearances at

A. Vane Tips (minimized by hydraulic force balance and centrifugal force on vanes).

B. Vane Sides (controlled by clearance between vane and port plate).

C. Rotor Side (controlled by clearances between rotor and port plates).

D. High pressure undervane kidney slot leakage (controlled by rotor/port plate clearance).

1. To inlet kidney slot.

2. To the center of the pump in to spline area.

E. Clearance between vane slot and vane
The leakage paths are shown in Figure 6.3.1.

II. Carryover volume

A. At the bottom of vane slot when the vane is at its minimum rise.

B. Between the rotor O.D. and liner minor radius.

Some designs have a circular cross-hole at the bottom of the slot, but in this design, since the fuel is going to be contamination free, the cross-hole is eliminated to provide a minimum carryover volume.

When the fluid is incompressible, carryover volume at the cross-hole is insignificant, but it has a very adverse effect on the volumetric efficiency when the fluid is as compressible as LH_2.

In order to reduce the leakage, 16 vanes are used so there will always be at least 2 vanes sealing the low pressure side from the high pressure side. In other words, at any instant, the leakages across the vane tip have to leak around two obstacles before they can see low pressure. The leakages controlled by the liner/port plate interface are minimized by a liner pressure plate. This approach is to spring load the plate against the pump liner. The critical operating temperature and operating clearances are selected. This allows the pump to be basically designed to have zero clearance between the rotor/port plate interface and the port plate/liner interface at a pre-selected condition. When the rotor width is less than the liner width caused by thermal, manufacturing or design constraints a clearance exists between the rotor and port plate. As the rotor increases in width from operational or thermal considerations, the rotor clearance with the port plate decreases until rubbing contact and zero clearance is achieved. Should the rotor continue to expand during operation, it will lift the pressure plate off of the liner interface at a pre-determined load consistent with the pump speed, differential pressure, material bearing compatibility and other design considerations. This design thus allows a very close fixed clearance operating condition.

6.4 VANE STAGE PERFORMANCE PREDICTION & BOOST STAGE MATCHING

The major leakage of the vane pump is contributed by the undervane discharge kidney to the shaft key area. This leakage decreases as the length of the leakage path increases. This dimension is restricted by the rotor diameter and the height of the vane. All the parameters involved have to weigh against one another with the aid of the cam contour, vane dynamics and thermal leakage program. Using the thermal leakage program, plots of volume flow rate ($\dot{Q}$), volumetric efficiency (N_v), amount of subcooling from saturation temperature (ΔT) at the vane pump entry point vs. inlet pressure (P_4) were generated over a range of side clearances for the purpose of optimizing the design. This was done on both fluids (Figure 6.4.1 to 6.4.6). These plots are the tools with which the operating point, performance and inlet pressure requirement are determined. The procedure for selecting the operating condition is as follows:

First, the amount of subcooling desired to enter the vane stage was estimated. From Fig. 6.4.3 (ΔT vs. P in) clearances and inlet pressure were found and plotted on the flow vs. inlet pressure curve Figure 7, and also plotted on the efficiency curve Figure 6.4.1. With the desired flow rate known, the clearance and inlet pressure were fixed. These parameters were used to obtain the volumetric efficiency of the pump.

For liquid hydrogen, an inlet pressure of 75838 to 89627 n/m^2 is sufficient to enable the vane pump to operate with a low percentage of vapor in the leakage path and with all liquid at the entry point of the vane pump. A two-stage boost pump is required to achieve this pressure rise. At this design point the LH_2 pump will operate with a wide margin of subcooling while maintaining a reasonable volumetric efficiency. For LH_2 fluid, it is possible to tolerate a small percentage of vapor in the system without creating major problems. This avoids using a higher number of boost stages and sacrificing volumetric effieiency. With a single boost stage using the same impeller at 3000 rpm, a pressure rise of 782733 n/m^2 will be generated for LOX. This will provide 100% liquid throughout the entire pump package. This design feature is important because only oxygen in vapor phase can support combustion. Without O_2 vapor in the system, no fire can occur unless there is a sudden localized temperature rise occuring somewhere along the rubbing surface and the liquid gains enough energy to flash into vapor to support ignition.

6.5 PORT TIMING

The main inlet and discharge ports on the cam ring are situated at the middle of the cam rise and fall. In order to improve sealing, a 45° arc is left between the inlet and discharge main ports. This configuration insures two vanes sealing at any instant. The undervane kidneys on the port plates perform two functions:

1. They provide flow passages for the undervane inlet and discharge.

2. They pressurize the vane from underneath . This reduces leakage across the vane tips.

Where the over-vane pressure is low, the undervane pressure is designed to be low. This keeps the contact stress between the vane tip and the liner to a low value. The extend of the discharge undervane kidney is designed so that the vane sees high pressure underneath 1° before it sees high pressure over-vane, and the high undervane pressure is also maintained until the vane is 1° past the end of the high pressure zone. This assures good sealing between vane tip and liner.

MODEL #	3	4	8	9	10	12	13	14	15	16	17	19	20	21	22	23	23A	19A	19B
Stroke (cm)	0.127	0.127	0.127	0.102	.076	0.127	.127	0.102	0.076	0.102	.076	.127	.102	.078	.102	.102	.102	.127	.127
Angular Displacement (degrees)	45°	90°	70°	90°	90°	90°	90°	90°	90°	70°	70°	90°	90°	90°	90°	90°	90°	90°	90°
Base Radius (cm)	1.02	1.02	1.02	1.02	1.02	1.02	1.31	1.31	1.31	1.31	1.31	1.34	1.34	1.34	1.33	1.33	1.33	1.34	1.34
Rotational Speed (rpm)	12000	12000	12000	12000	12000	8000	12000	12000	12000	12000	12000	8000	8000	8000	12000	12000	12000	3000	8000
Cam Width L (cm)	1.52	1.52	1.52	2.15	1.52	1.52	1.34	1.69	2.27	1.69	2.27	1.96	2.47	3.33	1.98	1.52	1.57	1.96	1.96
L/D or L/2R	.748	.748	.748	1.058	1.427	.748	.511	.645	.868	.645	.868	.7296	.921	1.239	.743	.571	.591	.378	.378
Max. Cam Rad. Vel (m/sec)	4.45	2.22	2.86	1.77	1.33	1.48	2.22	1.78	1.33	2.28	1.71	1.48	1.18	0.89	1.77	1.77	1.77	0.55	1.4807
Max. Cam Rad Acc (m/sec^2)	24,412	6,104	10095	4864	3664	2713	6106	4885	3664	8075	6056	2714	2171	1628	4885	4885	4885	382	2,714
Max Comp.Rad Acc. (m/sec^2)	42,255	23,131	27,945	22,356	20,799	10,653	26,581	26,419	25,411	30,183	27,048	12,942	12,942	11,533	27,397	27,397	27,397	1,819	12,936
Min. Comp. Rad Acc. (m/sec^2)	326	10,125	6,147	11,311	12,483	4,500	14,742	15,924	17,107	12,737	14,716	6,791	7,316	7,842	16,325	16,325	16,325	955	6790
Max Comp. Jerk ($m/sec.^3 \times 10^6$)	273	34	72	27	20	10	34	27	20	46	43	10	8	6	27	27	27	0.533	10.1

Fig. 6.2.1 (A) Vane Stage Cam Profile Design - Metric

MODEL #	3	4	6	9	10	12	13	14	15	16	17	19	2	2	22	23	23A	19A	198
STROKE (in.)	.08	.05	.05	.04	.03	.05	.05	.04	.03	.04	.03	.05	.04	.03	.04	.04	.04	.05	.05
ANGULAR DISPLACEMENT (degrees)	45°	90°	70°	90°	90°	90°	90°	90°	90°	70°	70°	90°	90°	90°	90°	90°	90°	90°	90°
BASE RADIUS R (in.)	.4	.4	.4	.4	.4	.4	.515	.515	.515	.515	.515	.5284	.5284	.5284	.525	.525	.525	.5284	.5284
ROTATIONAL SPEED (rpm)	12000	12000	12000	12000	12000	8000	12000	12000	12000	12000	12000	8000	8000	8000	12000	12000	12000	3000	8000
CAM WIDTH L (in.)	.5987	.5987	.5987	.8464	1.1422	.5987	.5267	.6645	.8944	.6645	.8944	.771	.9733	1.3097	.78	.600	.62	.771	.771
L/D or L/2R	.748	.748	.748	1.058	1.427	.748	.511	.645	.868	.645	.868	.7296	.921	1.239	.743	.571	.591	.378	.378
MAX. CAM VELOSITY (ft./sec)	14.6	7.29	9.37	5.8	4.37	4.86	7.29	5.83	4.37	7.49	5.62	4.85	3.89	2.91	5.8	5.8	5.8	1.82	4.858
MAX. CAM ACC. (ft./sec^2)	80,093	20,027	33,119	15,957	12,020	8,902	20,034	16,028	12,021	26,493	19,869	8,904	7.123	5.343	16.028	16.028	16.028	1.252	8,904
MAX. COMPOSITE ACC. (ft./sec^2)	138,633	75,889	91,684	73,347	68,237	34,950	93,770	86,678	83,370	99,025	88,741	42,459	40,140	37,837	89,886	89,886	89,886	5,968	42,440
MIN. COMPOSITE ACC. (ft./sec^2)	1,070	33,219	20,168	37,110	40,955	14,767	48,367	82,246	56,125	41,789	48,281	22,280	24,004	25,728	53,561	53,561	53,561	3,135	22,279
MAX. COMPOSITE JERK ($ft/sec^3 x 10^6$)	895	112	238	89	67	33	111	89	67	150	142	33	26	19	89	89	89	1.75	33.2

Fig. 6.2.1 (B) Stage Cam Profile Design - English Units

VANE	EXPERIENCE	LH_2/LO_2 PUMP #19A&B
Max. Rubbing Velocity (ft/sec), (m/sec)	LH_2 : 47, 14.3	40.7, 12.4
	LOX : 20, 6.1	15.1, 4.6
Max. Total Radial Vane Acceleration (ft/sec^2), (m/sec^2)	200,000, 60,960	LH_2 : 42,459, 12941
		LOX : 5,968, 1819
Max/Mean Total Vane Acceleration	1.5 Max	1.3
Min/Mean Total Vane Acceleration	.45 Min	.69
Width/Throw	7.5 - 15	15.4
Vane Height/Width	.2 - .5	.26
Max Vane Throw/Height	.33	.25
ROTOR		
L/D	.35 - .9	.74
Throw/D Maj.	.015 - .06	.043
Throw/D Rot	.04 - .07	.048
Width/Height	2.25 - 3.75	4.0
Minor Ext/ In Rotor	.015 - .065	.026
Major Ext/ In Rotor	.30 - .65	.38

Fig. 6.2.2 Vane Stage Design Constraints & Aspect Ratios

VANE STAGE PARAMETERS

	LH_2		LOX	
Rotor Radius, in.	.523	1.33 cm	.523	
Cam Major Radius, in.	.578	1.47 cm	.578	
Cam Minor Radius, in.	.528	1.34 cm	.528	
Shaft Radius, in.	.160	0.41 cm	.160	
Rotor Width, in.	.771	1.96 cm	.771	
Throw, in.	.050	0.127 cm	.050	
Vane Height, in.	.200	0.51 cm	.200	
Vane Thickness, in.	.040	0.10 cm	.040	
Vane Crown Radius, in.	.040	0.10 cm	.040	
Number of Vanes	16		16	
Speed, RPM	8000		3000	
Max. Tip Speed, FPS	40.4	12.31m/sec	15.1	4.6m/sec.
Rotor Side Clearance, in.	.0003	0.00076 cm	.0005	.00127 cm
Inlet Pressure, psia	27.7	190975N/m^2	26.7	184080N/m^2
Flow, GPM	7.80	29.51/min	2.67	10.11/min
N_v, %	82.2		75.8	
N_m, %	80.0		90.0	

FIGURE 6.2.3

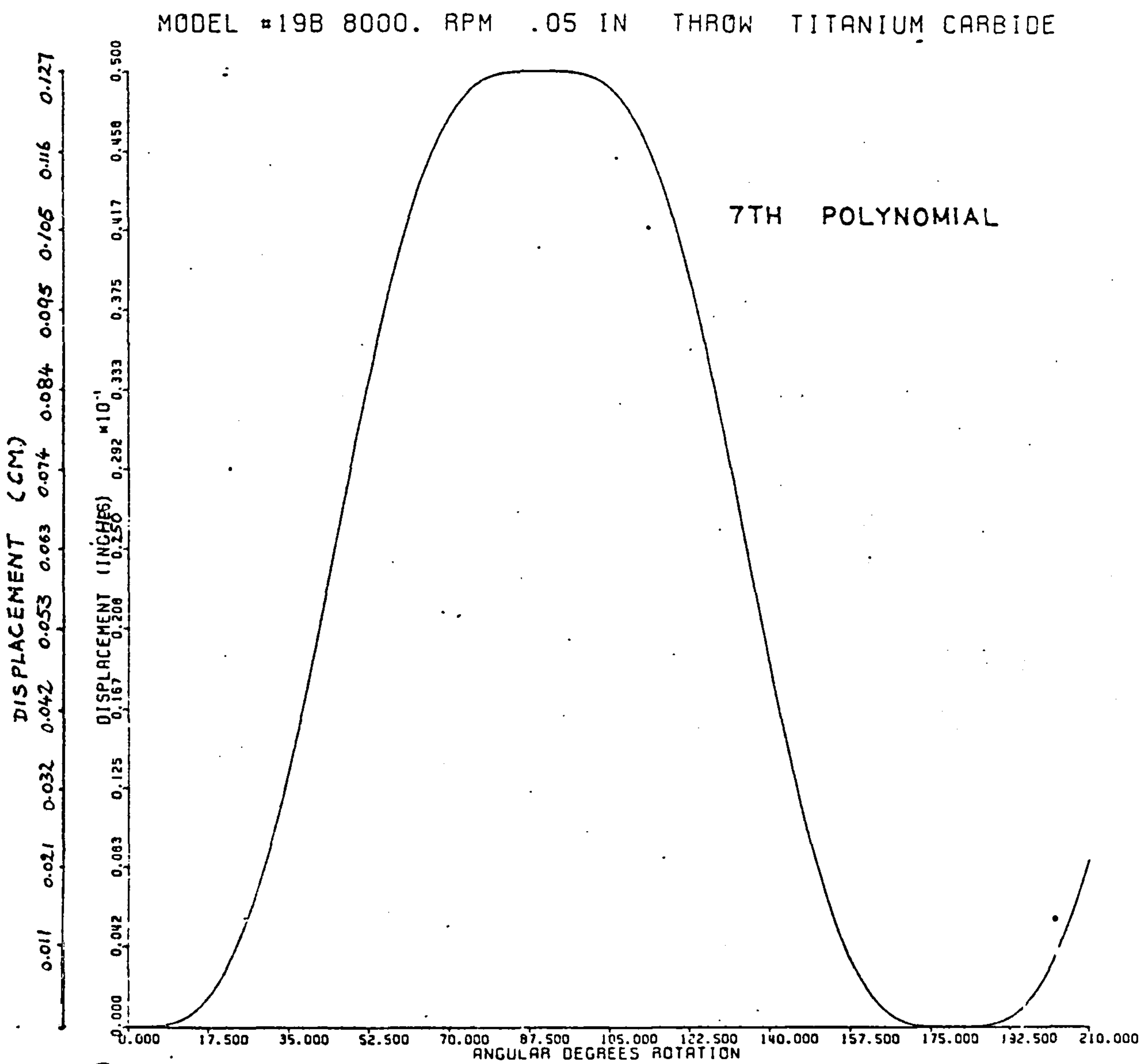

Fig. 6.2.4 Cam Contour Design - Cam Rise vs. angular rotation

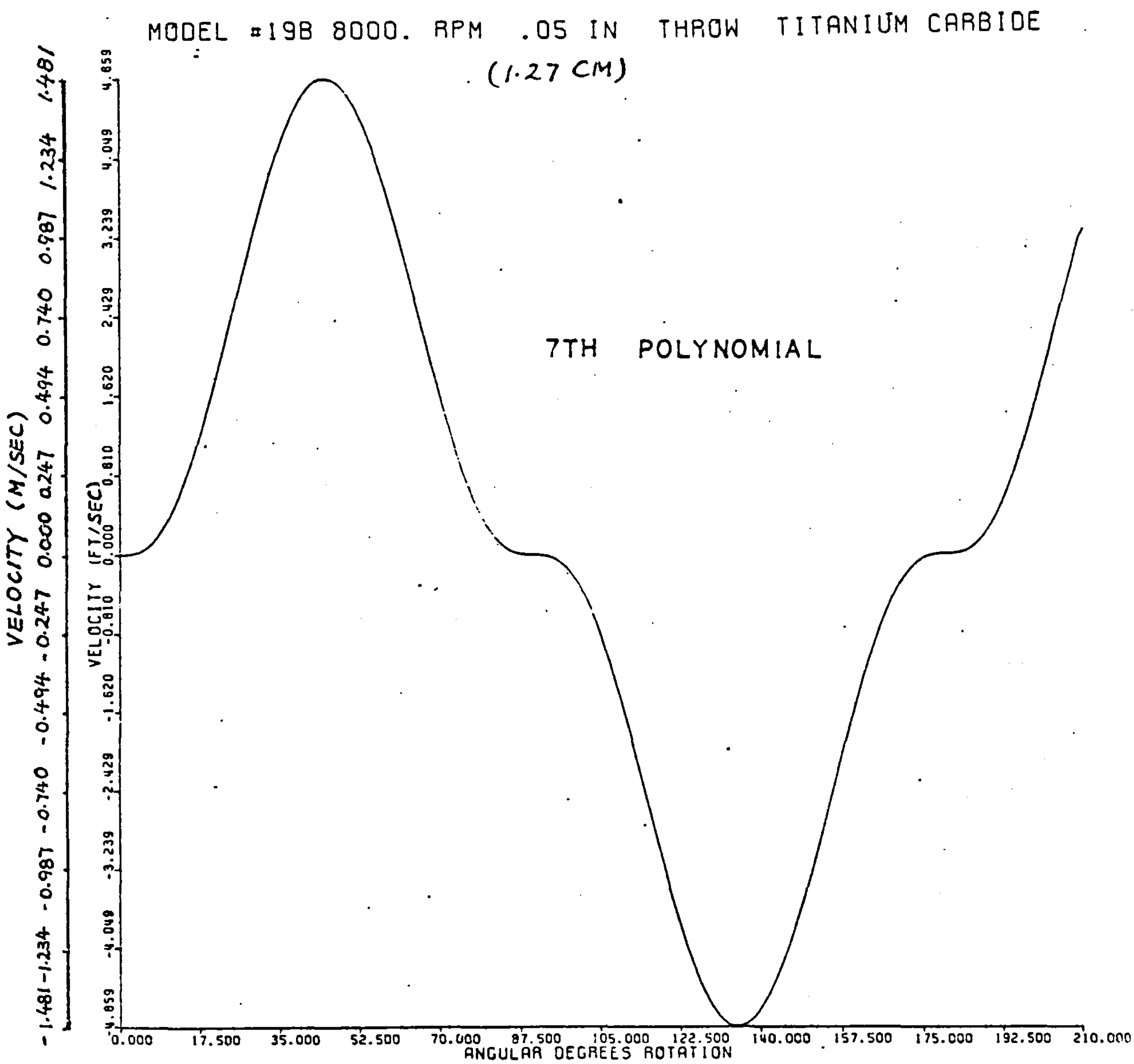

2

Fig. 6.2.5 Cam Contour Design - Cam Radial Velocity vs. Angular Rotation

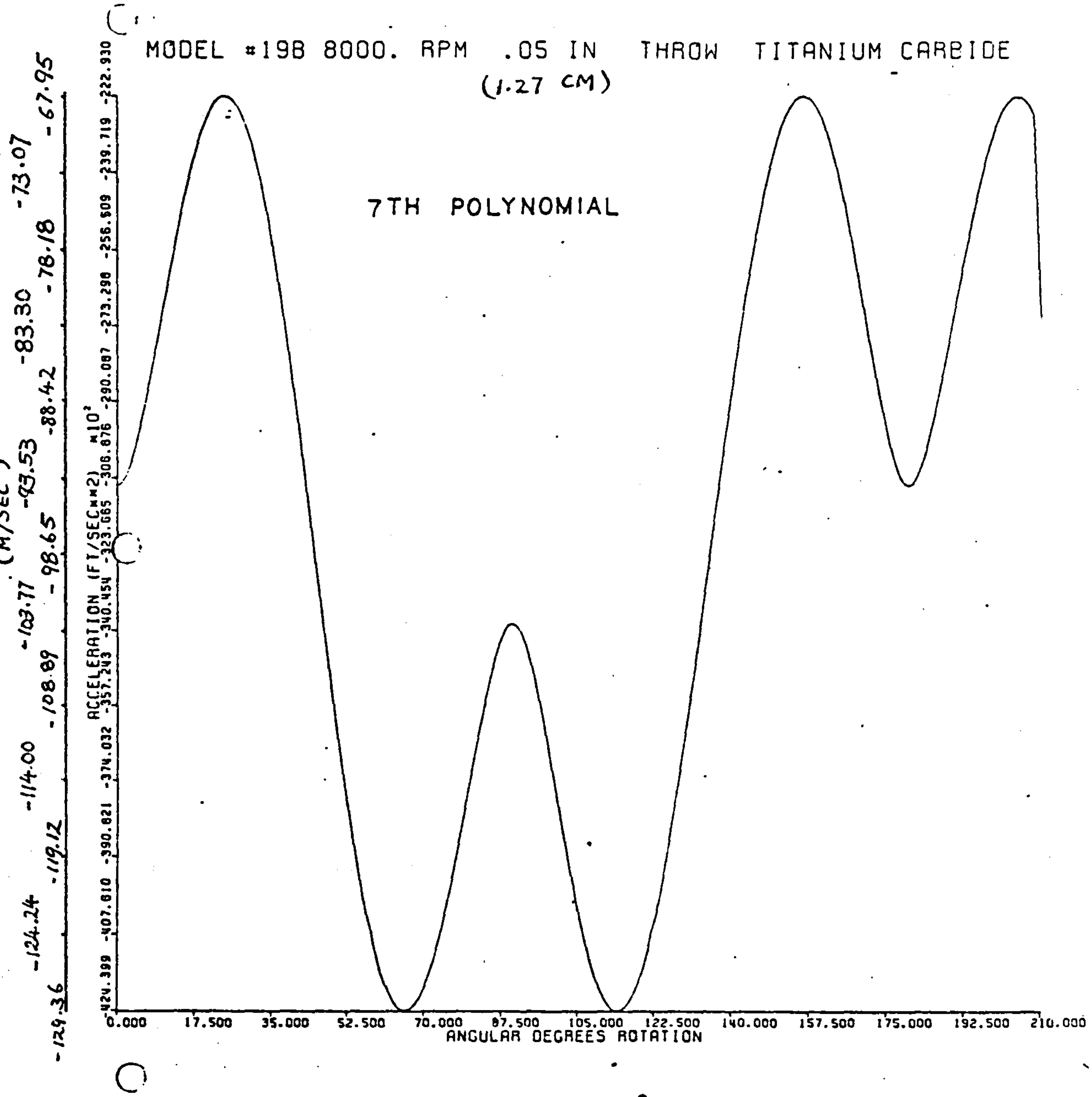

Fig. 6.2.6 Cam Contour Design - Cam Radial Acceleration vs. Angular Rotation

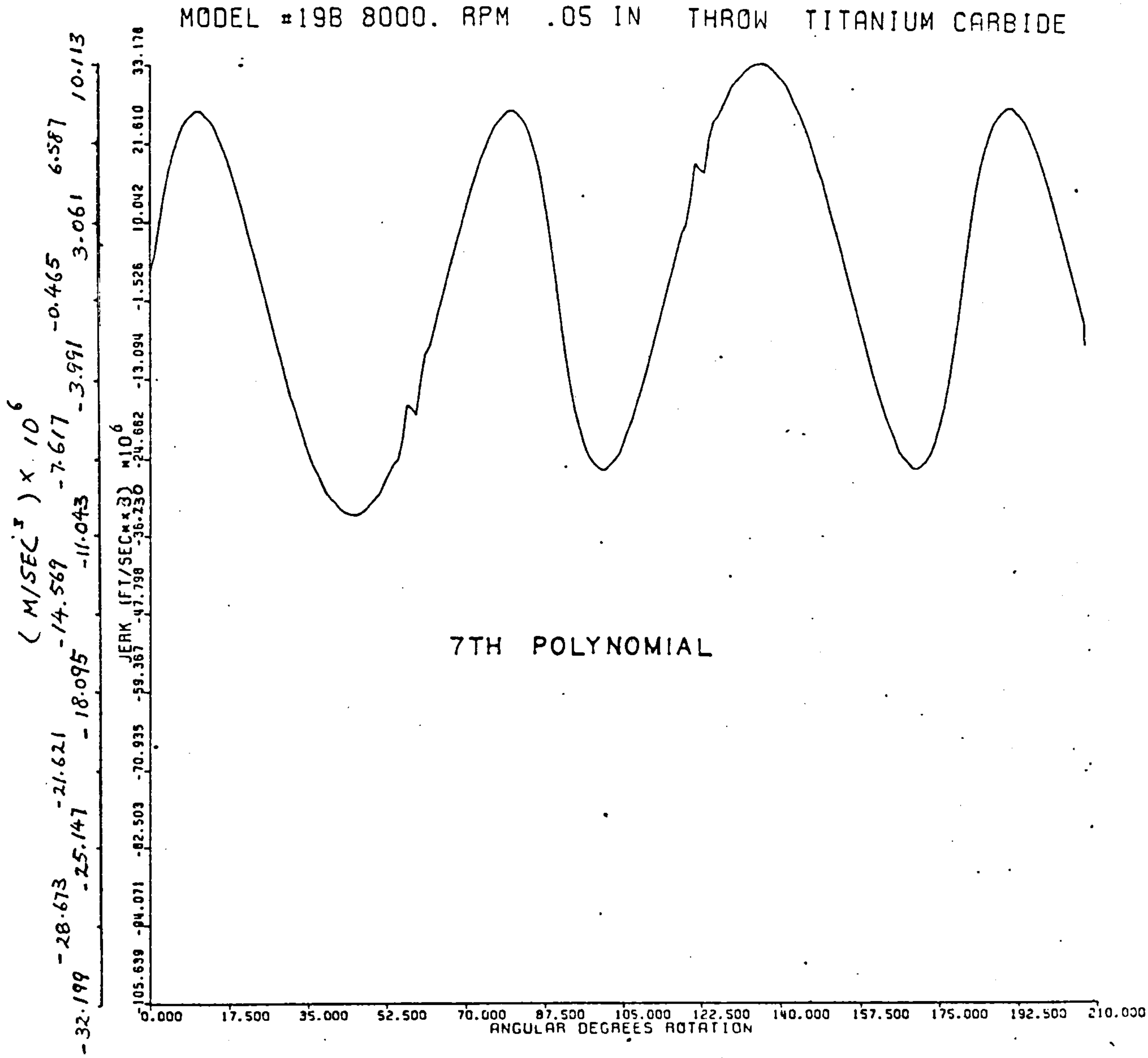

Fig. 6.2.7 Cam Contour Design - Cam Jerk vs. Angular Rotation

6.2.8 Intentionally left blank.

LEWIS LOEW ... CAM ... DESIGN ... DEGREES ... 1 1111

TOTAL ANGULAR DISPLACEMENT	TOTAL INCREMENTS	BASE RADIUS		CURVE SPACING FACTOR	SPACING
0.65000 01	0.65000 01	5.2000D-01	[illegible] 01	3.0	0.0

CAM FOLLOWER TIP RADIUS = [illegible]D-01

ANGULAR DISPLACEMENT (DEGREES)	THEORETICAL INCREMENTAL DISPLACEMENT	RAD. OF ROT. TO K.E. CONTACT PT.	CAM VELOCITY	CAM ACCELERATION	CENTRIPETAL ACCELERATION		
0	0	[illegible]	0	[illegible]	[illegible]	[illegible]	[illegible]
[illegible]	[illegible]	[illegible]	[illegible]	[illegible]	[illegible]	[illegible]	[illegible]
5.0000000 01	3.[illegible]01930-02	5.5940170-01	4.[illegible]43380	[illegible]	[illegible]	[illegible]	[illegible]
5.1000000 01	3.2167610-02	5.6056740-01	4.6476470 00	[illegible]	[illegible]	[illegible]	[illegible]
5.2000000 01	[illegible]	5.6170410-01	4.5674090 00	[illegible]	[illegible]	[illegible]	[illegible]
5.3000000 01	[illegible]	[illegible]	4.4661120 00	[illegible]	[illegible]	[illegible]	[illegible]
5.4000000 01	[illegible]	[illegible]	[illegible]	[illegible]	[illegible]	[illegible]	[illegible]
5.5000000 01	3.6570210-02	5.6697020-01	4.2146750 00	[illegible]	[illegible]	[illegible]	[illegible]
5.6000000 01	3.7597500-02	5.6549750-01	4.1019090	[illegible]	[illegible]	[illegible]	[illegible]
5.7000000 01	3.8589790-02	[illegible]	3.9684300	[illegible]	[illegible]	[illegible]	[illegible]
5.8000000 01	3.9546820-02	[illegible]	3.8063720	[illegible]	[illegible]	[illegible]	[illegible]
5.9000000 01	4.0460540-02	5.6886050-01	3.6453380 00	[illegible]	[illegible]	[illegible]	[illegible]
6.0000000 01	4.1335180-02	5.6973570-01	3.6760940	[illegible]	[illegible]	[illegible]	[illegible]
6.1000000 01	4.2167130-02	5.7156710-01	3.3070650	[illegible]	[illegible]	[illegible]	[illegible]
6.2000000 01	4.2955150-02	5.7135510-01	3.1218730 00	[illegible]	[illegible]	[illegible]	[illegible]
6.3300000 01	[illegible]	[illegible]	[illegible]	[illegible]	[illegible]	[illegible]	[illegible]
[illegible]	[illegible]	[illegible]	[illegible]	[illegible]	[illegible]	[illegible]	[illegible]

... HAS BEEN CORRECTED FOR ROTATION ... DUE TO ... FOLLOWER ...

Fig 6.2.9 Cam Contour Computer Printout

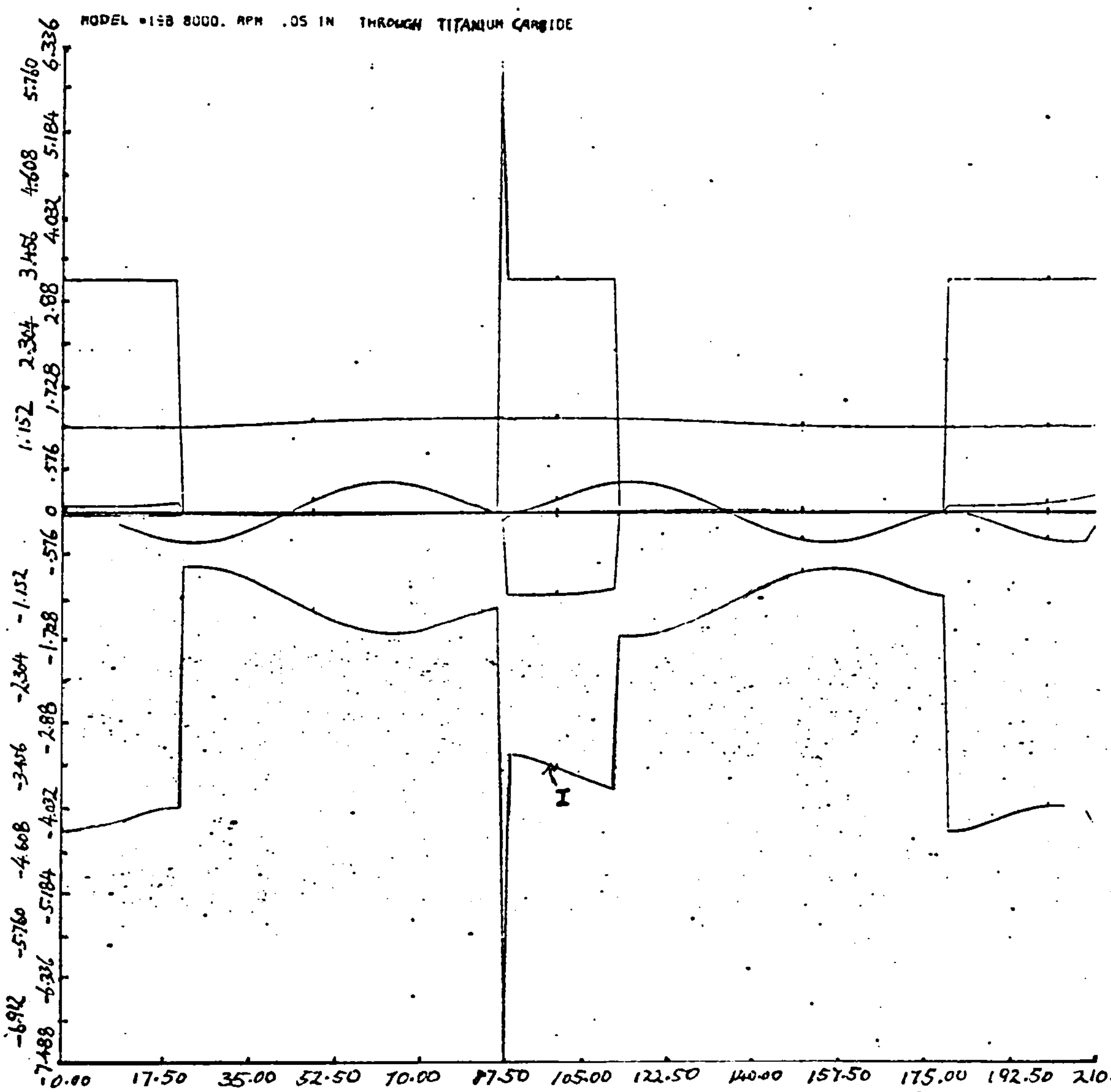

Fig. 6.2.10 Vane/Liner Reaction (Force I)

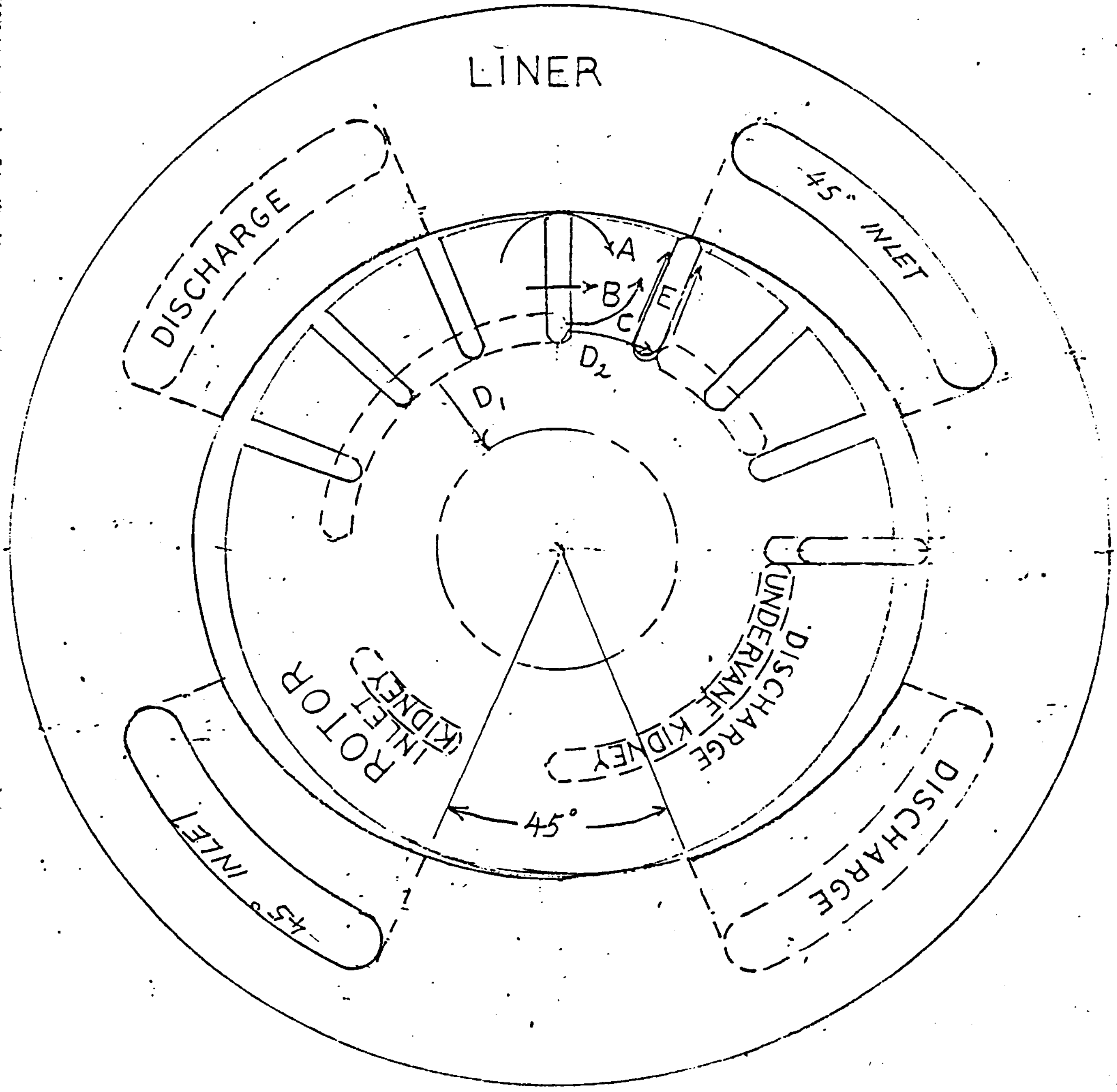

Fig. 6.3.1 Leakage Paths in Vane Stage

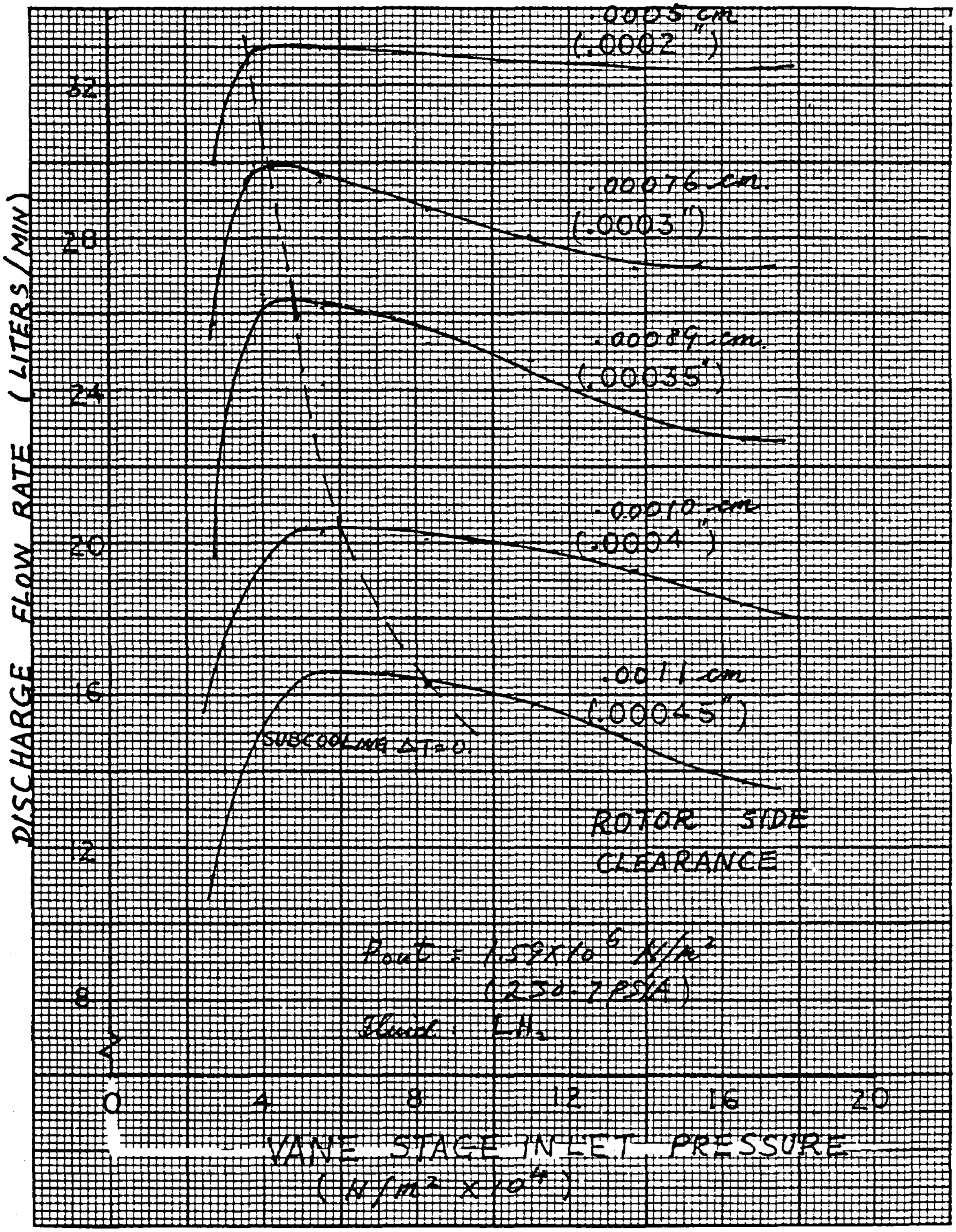

Fig. 6.4.1 VANE STAGE PERFORMANCE (LH_2) - EFFECT OF INLET PRESSURE ON DISCHARGE FLOW

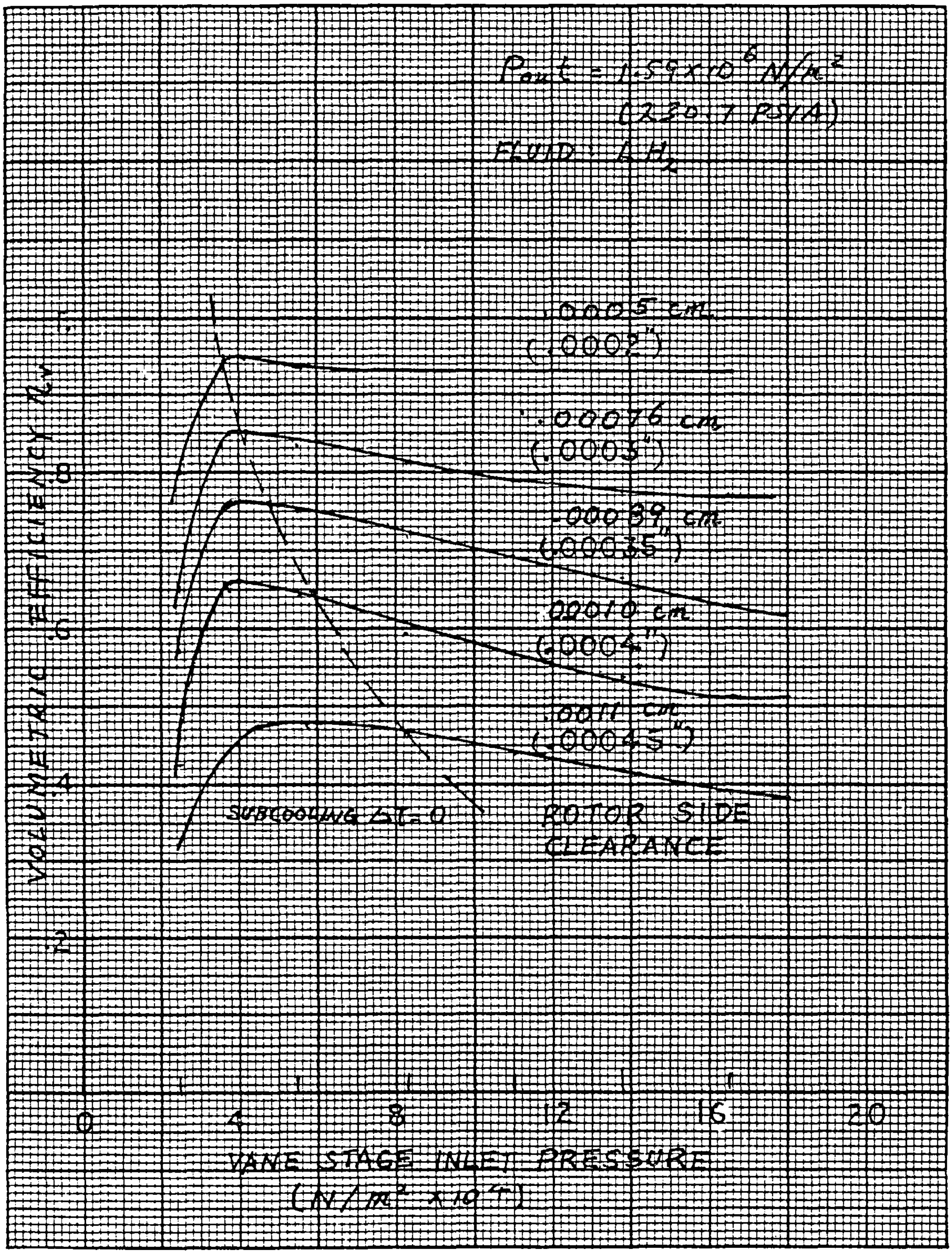

Fig. 6.4.2 VANE STAGE PERFORMANCE (LH_2)

EFFECT OF INLET PRESSURE ON PUMP VOLUMETRIC EFFICIENCY

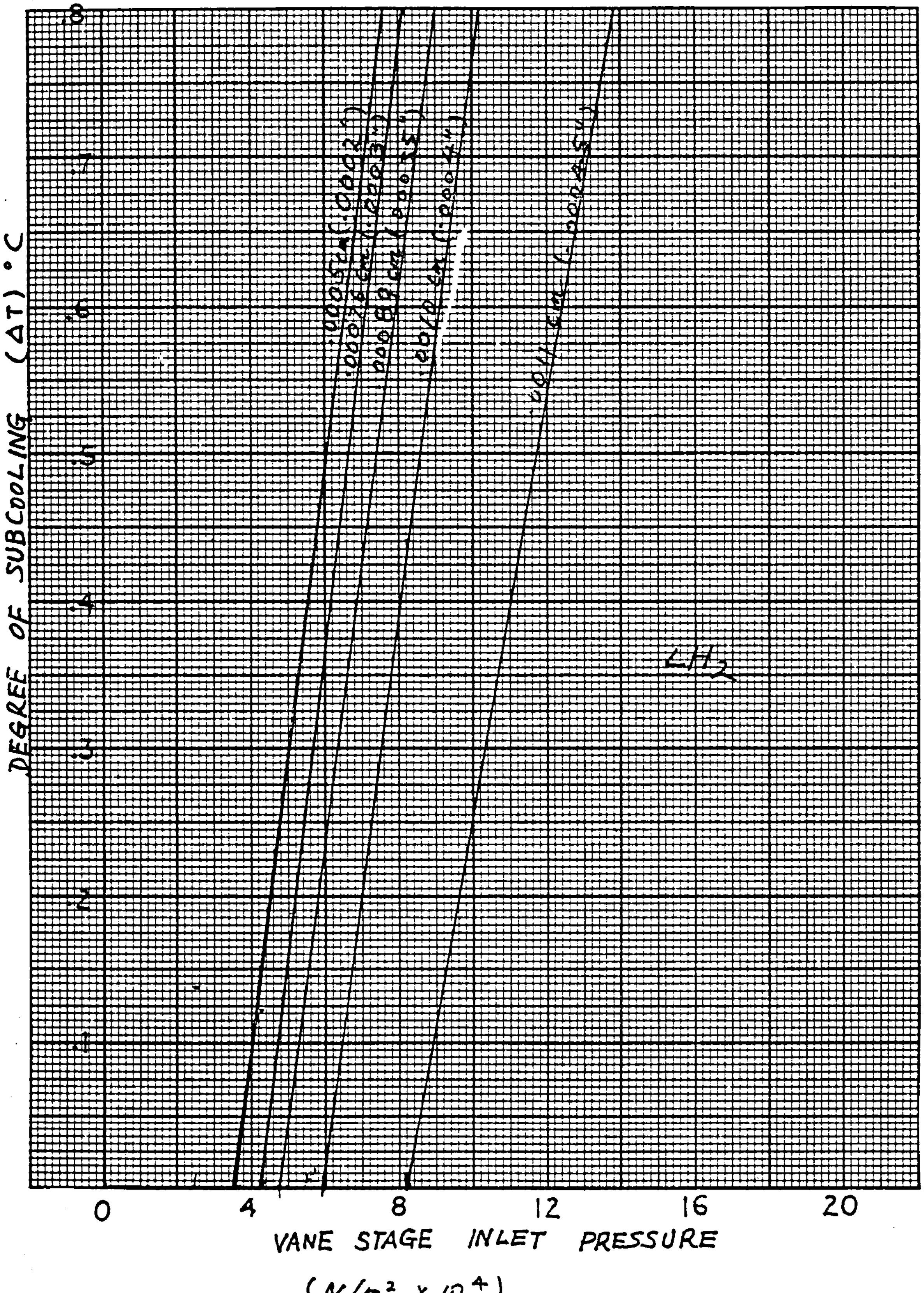

Fig. 6.4.3 VANE STAGE PERFORMANCE (LH_2)

SUBCOOLING EFFECT OF INLET PRESSURE ON LH_2

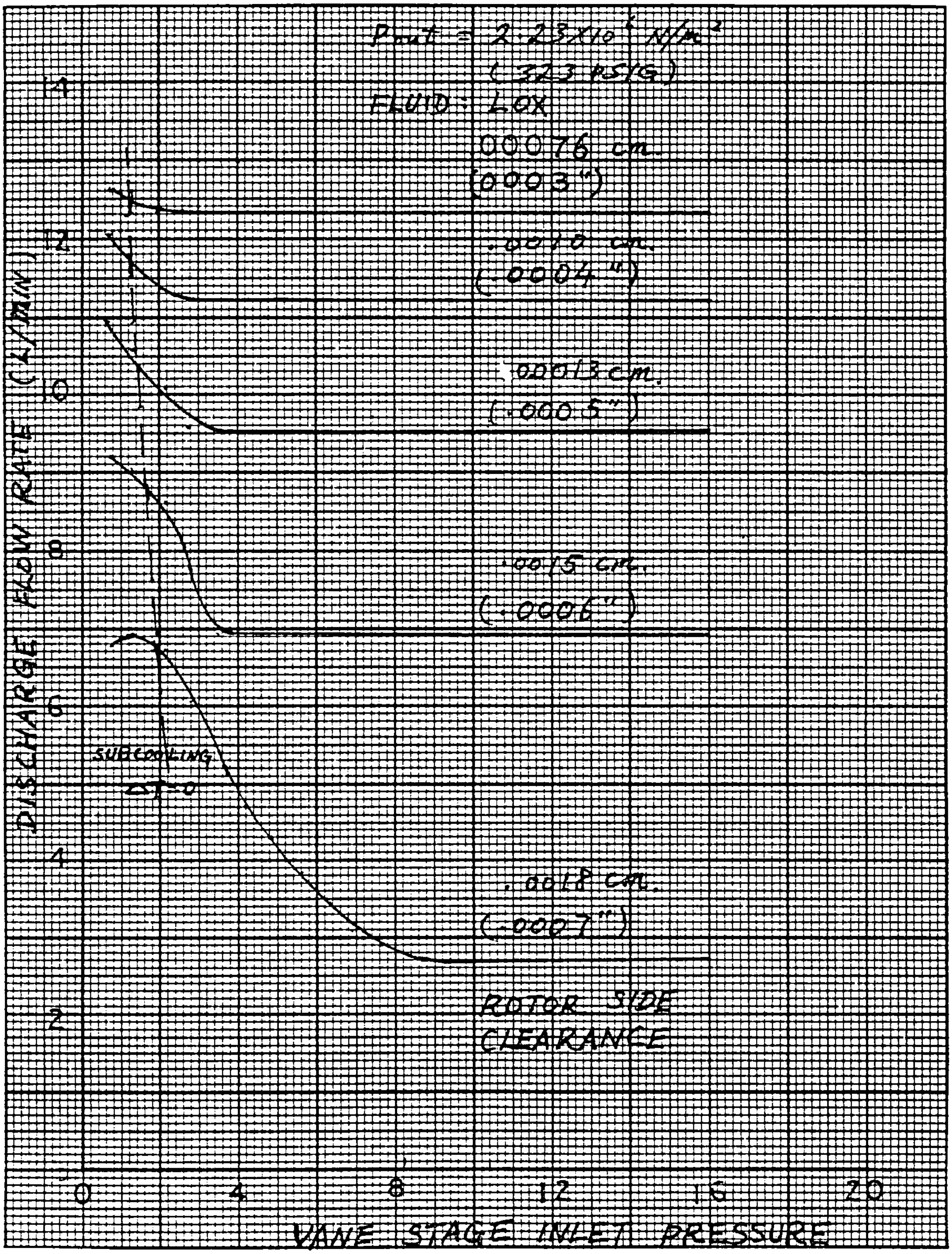

($N/m^2 \times 10^4$)

Fig. 6.4.4 VANE STAGE PERFORMANCE (LOX)
- EFFECT OF INLET PRESSURE ON DISCHARGE FLOW

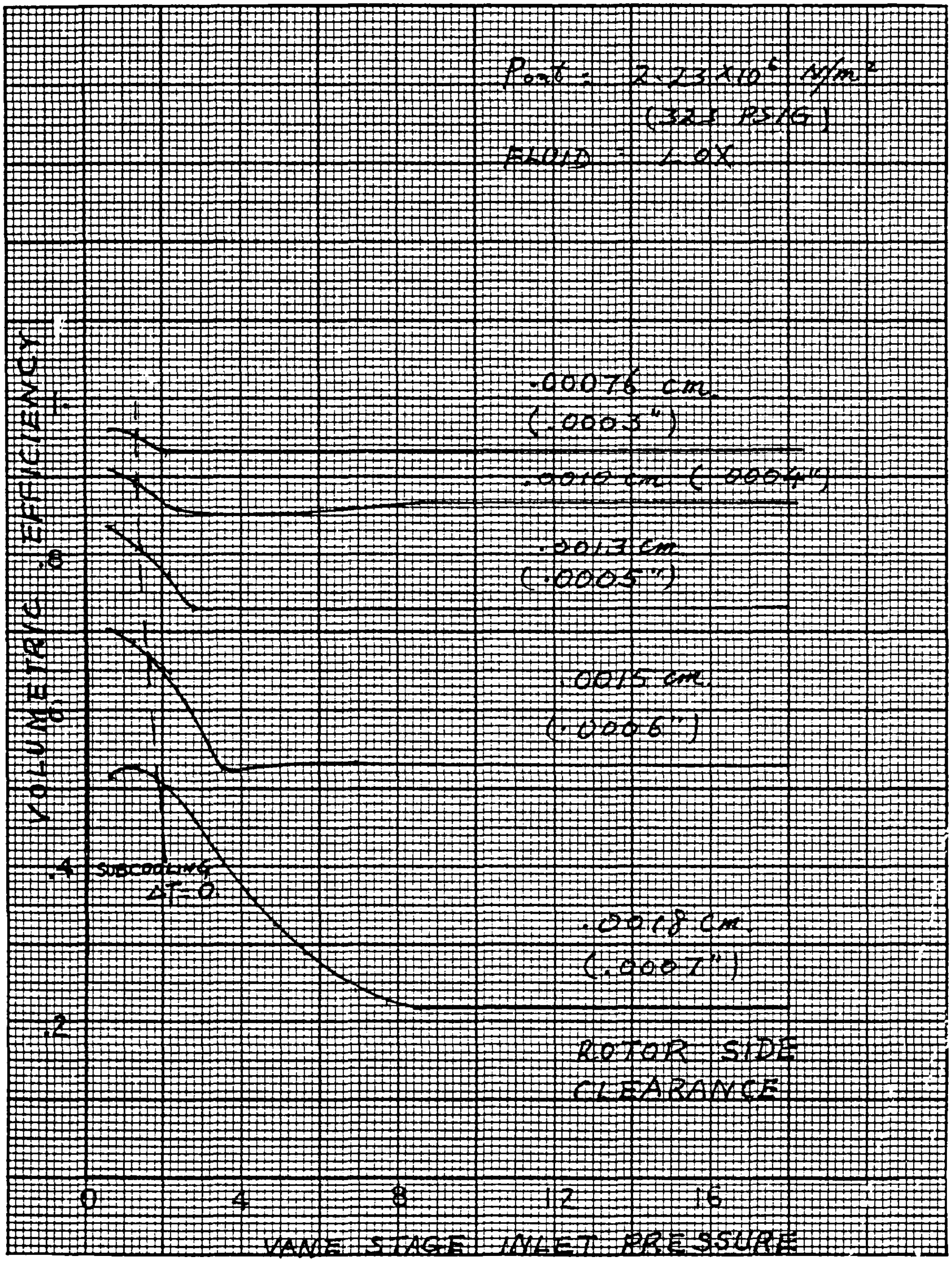

($N/m^2 \times 10^4$)

Fig. 6.4.5 VANE STAGE PERFORMANCE (LOX) - EFFECT OF INLET PRESSURE ON PUMP VOLUMETRIC EFFICIENCY

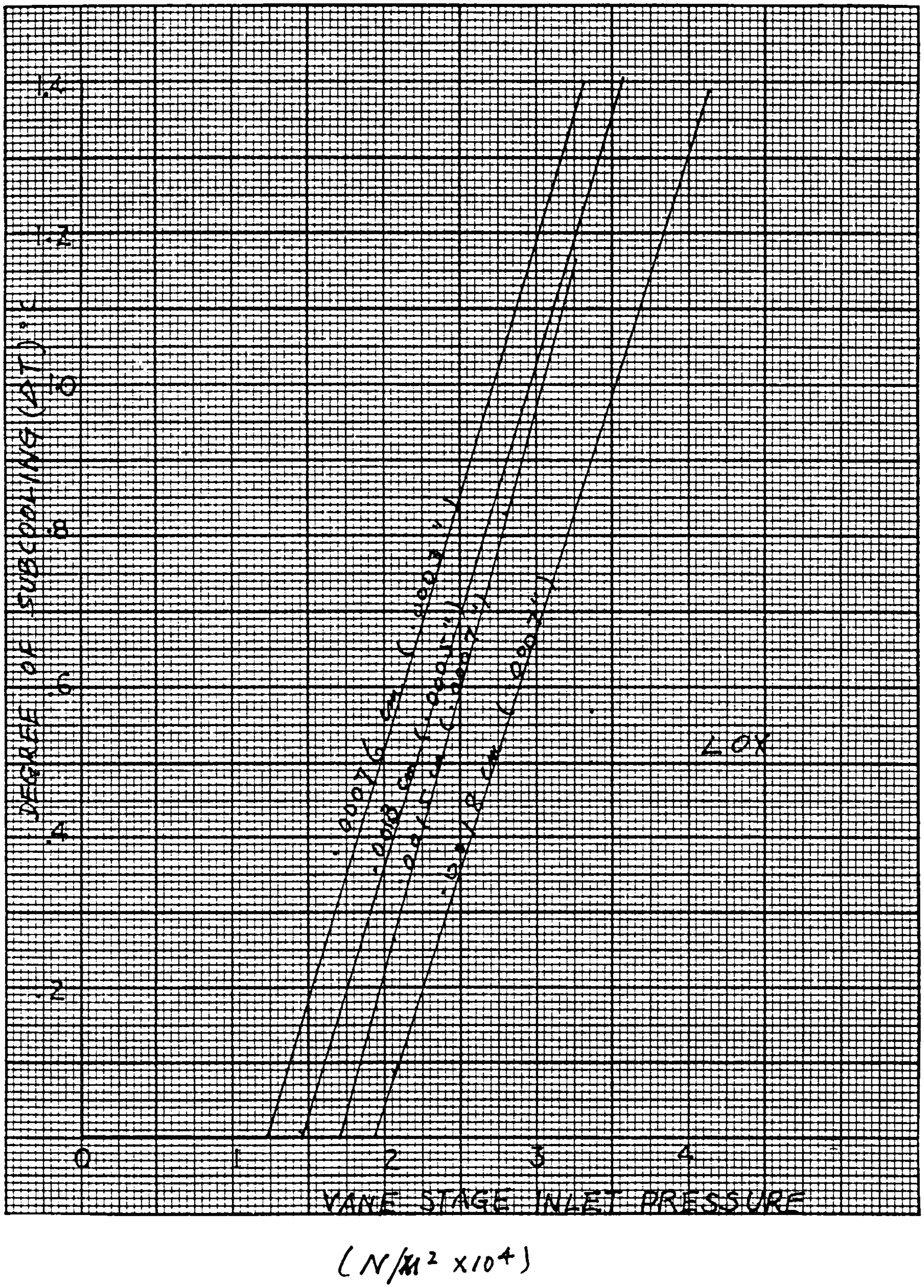

VANE STAGE PERFORMANCE (LOX) -

Fig. 6.4.6 SUBCOOLING EFFECT OF INLET PRESSURE ON LOX

7. BOOST STAGE DESIGN

FLUID DYNAMIC DESIGN OF THE TWO-STAGE LIQUID HYDROGEN CENTRIFUGAL PUMP

7.1 Design Specification

The fluid dynamic design of the two-stage centrifugal pump for boiling liquid hydrogen is based on the following design specification:

Volume flow rate	7.5 gpm (28.39 l/min)
Rotational speed	8000 rpm
Pump pressure rise	13.0 psi (89.627 N/M^2)
Liquid temperature	37.0 deg R (20.2 ^oK)
Pump efficiency	0.35 to .040

7.2 Characteristic Calculations

In the above specification, the pump pressure rise is equally divided between the two stages, and the hydrogen at 37 deg R is saturated liquid with 10 percent vapor (by volume) upstream from the pump inlet. The pump efficiency includes recirculation and disk friction losses. The density of the liquid hydrogen has been assumed constant at 4.404 lb/ft^3 (692 N/m^3) so that the stage head H becomes

$$H = \frac{144 \Delta p}{2 \rho_\ell} = 212.5 \text{ ft.} = 64.77 \text{ m}$$

For the above design specification values, the stage specific speed Ns becomes

$$N_s = \frac{N\ (rpm)\quad Q\ (gpm)^{\frac{1}{2}}}{H\ (ft)^{\ 3/4}} = 393.6$$

$$N_s = \frac{W(sec^{-1})\quad Q\ (ft^3/sec)^{\frac{1}{2}}}{g(ft/sec^2)\quad H(ft)^{\ 3/4}} = 1.116$$

This low value for N_s is responsible for the relatively small specified values of pump ifficiency, and has been a major factor determining the final pump geometry, particularly the relatively large impeller diameters and the highly backward curved impeller blades.

Sundstrand Aviation Operations
unit of Sundstrand Corporation

4747 HARRISON AVENUE, ROCKFORD, IL 61101 • PHONE 815 226-6000 • TWX 910 631-4255 • TELEX 25-7440

September 24, 1979
775-L-794080

NASA, Lewis Research Center
21000 Brookpart Road
Cleveland, Ohio 44135

Attention: Mr. L. E. Light
Head, Space Systems Section
MS500-213

Subject: Final Engineering Report No. CR159648
Liquid Oxygen/Liquid Hydrogen Boost/
Vane Pump for the Advanced Orbit Transfer Vehicle Auxiliary Propulsion System

Reference: Contract No. NAS3-20401

Gentlemen:

Please find enclosed a copy of the subject report. Distribution has been made in accordance to the instructions contained in your letter no. 1434(1868:IS) dated 8-16-79.

Sincerely,

SUNDSTRAND AVIATION OPERATIONS
Advanced Technology Group
Sundstrand Corporation

Richard Alms

Richard Alms
Data Administrator

For: S. Tamborello
Contract Administrator

ST/RA:aj
Enclosures

7.2.1 Friction Losses

For the above low value of specific speed, friction losses are a dominant factor affecting pump efficiency, both internally and in terms of disk friction. Fortunately, the kinematic viscosity of liquid hydrogen at 20.2 K is about 2.03×10^{-7} m^2/sec (reference 1), compared with about 9.29×10^{-7} m^2/sec for water at 23.9°C. Thus, for comparable velocities and sizes of pump, the Reynolds number is five times larger for liquid hydrogen than for water. This difference in Reynolds number ameliorates the adverse effects of friction at low specific speeds and permits, for example, larger impeller tip diameters and larger l/d ratios for the channel between impeller blades than might otherwise be used.

7.2.2 V/L Ingestion

A second problem area having a major impact on the pump geometry is the 10 percent vapor (by volume) upstream from the pump inlet. Normal design procedure at low NPSH calls for a separate axial-flow inducer to increase the impeller inlet head so that the suction specific speed of the impeller is reduced below about 7500. For this liquid hydrogen pump with 10 percent vapor at inlet, sufficient inducer head must be developed to: (1) condense the vapor, and (2) raise the impeller NPSH. Here the head required to condense the vapor was three times larger than that required to raise the NPSH. To achieve the inducer head required under the above conditions, it was necessary to use a mixed-flow inducer geometry.

7.2.3 Dynamic Head at Impeller Discharge

The third problem area having a major impact on the pump geometry is the high absolute velocity (kinetic energy) of the liquid hydrogen at the impeller discharge. This high absolute velocity v occurs in spite of highly backward curved blades (large β), because the relative velocities w in the impeller have been kept low to minimize internal friction losses. Thus,

It is clear that special care must be taken to convert this kinetic energy to static pressure rise, and so the diffuser design consists in a multiplicity of optimum conical diffusers.

7.3 Boost Stage Design

7.3.1 First stage inducer- The inducer inlet area was sized conservatively to handle the liquid hydrogen plus twice the 10 percent volume occupied by the vapor. For a hub-tip radius ratio ξ_H of 0.5, and an inlet relative flow angle $\beta_{I,T}$ at the leading-edge tip of 86.00 degs, simple continuity gives

$$\xi_H = 0.5$$

$$\beta_{I,T} = 86.00 \text{ degs}$$

$$r_{I,T} = 0.6307 \text{ ins} = 1.6 \text{ cm}$$

$$r_{I,H} = 0.3154 \text{ ins.} = .8 \text{ cm}$$

The blade angle $\beta^*_{I,T}$ at the leading edge tip was set at 82.92 degs, thus providing an incidence angle $i_{I,T}$ of 3.08 degs to accomodate the vapor cavity, which is attached to the leading edge and lies along the suction surface, and to accomodate to a much lesser degree the blade blockage of the relatively sharp leading edges. Thus,

$$\beta^*_{I,T} = 82.92 \text{ degs}$$

$$i_{I,T} = \beta_{I,T} - \beta^*_{I,T} = 3.08 \text{ degs}$$

The leading-edge profile has a 5-deg wedge angle, with all material removed from the suction surface, and a nominal nose radius of .0025 cm ins; otherwise, the inducer blades have a constant thickness of .51 cm along the shroud and .076 cm along the hub.

The inducer head required to condense the 10 percent vapor (by volume) was estimated from the velocity head required to generate 10 percent vapor when generated from saturated liquid hydrogen at static conditions, as given in reference 2. This head $H_{I,1}$ is 4.83 m The additional inducer head $H_{I,2}$, required to obtain a suction specific speed of 6000 for the first-stage impeller, is 1.71 m Thus, the required inducer head H_I becomes

$$H_I = H_{I,1} + H_{I,2} = 15.87 + 5.62 = 21.49 \text{ ft.} = 6.55\text{m}$$

A design value of 25 feet was used, and it was assumed that the hydraulic efficiency $\eta_{I,HYD}$ to produce this head is 50 percent. The resulting work input cannot, as discussed earlier, be achieved in this pump by an axial-flow inducer. However, for a mixed-flow configuration (where the average exit radius r_{EX} from the inducer can be larger), based on continuity and assuming a slip factor μ_I of 0.75, the required work input is achieved at r_{EX} equal to 2.235cm with an exit vane height h_{EX} of .51cm when the product of the exit flow coefficient $c_{FL,EX}$ and the blade blockage factor δ_{EX} is 0.871, and when the exit blade angle β^*_{EX} is equal to the leading-edge tip angle $\beta^*_{I,T}$.

Thus, $H_I = 25.00 \text{ ft.} = 7.62\text{m}$

$$\eta_{I,Hyd} = 0.50$$

$$\mu_I = 0.75$$

$$r_{EX} = 0.880 \text{ ins.} = 2.235\text{cm}$$

$$h_{EX} = 0.202 \text{ ins.} = .51\text{cm}$$

$$(c_{FL,EX})\ (\delta_{EX}) = 0.871$$

$$\beta^*_{EX} = \beta^*_{I,T} = 82.92 \text{ degs}$$

The meridional configuration of the inducer is shown in figure 7.3.1.1 or 7.3.1.2 . The hub radius of curvature r_H and the shroud radius of curvature r_S are 2.706 and 2.667 cm respectively. The blade angle β_I^* is a constant 82.92 degs along the shroud, and the mean blade surface is generated by straight line elements lying in meridional planes (constant θ) and extending from shroud to hub at equal percentages of shroud and hub lengths.

For this configuration, the relative velocity ratio $W_{EX}/W_{I,T}$ across the inducer is 0.800, and the dwell time t_D of the liquid hydrogen in the inducer is 0.0253 sec. The values of both parameters are excellent; the first, because deceleration of the flow is moderate so that separation should not occur on the suction surface; and the second, because sufficient time is available to achieve condensation of the hydrogen vapor before leaving the inducer.

A computerized quasi-three- dimensional analysis was made to determine the velocity distributions on the blade surfaces along the hub and shroud lines. The results for the 3-bladed inducer *are shown in figure 7.3.1.3 (See NOTE on next page) It is noted that the velocity distribution along the suction surfaces at both hub and shroud are relatively constant or steadily increasing. Their types of velocity distribution are considered to be excellent because flow separation from the suction surface is precluded.

Along the pressure surface at the hub, the velocity becomes negative,

* A 2 bladed inducer will be used.

thus indicating a small reverse flow for a portion of that surface. Although negative velocities on the pressure surface are not desirable, neither are they especially harmful and in the actual pump may not in fact exist.

NOTE: A 3 bladed inducer was proposed at the time when this section was written. But it was later modified to a 2 bladed configuration. The hardware will conform to the 2 bladed structure.

For two blades, the solidity σ_I based on the wrap angle of 533 degrees is 2.96. Thus,

Z_I^* = number of blades = 2

σ_I = blade solidity = 2.96

In conclusion, it should be noted that the relative velocities will be higher than shown in the figure, at least for the first half of inducer length, due to the presence of the vapor and vapor cavity. This vapor has been partially accounted for by specifying flow coefficients that increase linearly with station number from 0.833 at the leading-edge (station 1) to 0.925 at the inducer exit (station 16). However, the one-dimensional design value for the average inlet relative velocity at the inducer tip is 13.4m/sec The inducer dimensions are tabulated in Fig. 7.3.1.

7.3.2 First Stage Impeller. The leading-edge of the first-stage impeller is nearly contiguous with the exit from the inducer. Thus, the mean leading-edge radius and annulus height are essentially the same. The impeller has 6 blades and the inlet blade angle $\beta^*_{I,LE}$ is 84.00 degrees (vs 82.92 degrees for the inducer exit angle). Thus,

Z_I^* = number of blades = 6

$\beta^*_{I,LE}$ = 84.00 degs

A recirculation flow rate of 4 percent was assumed for both the first and second stage impellers.

To achieve the stage head H of 64.7m as given in the design specification, assuming a stage hydraulic efficiency η_{HYD} of 52 percent, and with an exit blade angle B_T^* of 78.29 degrees, continuity and the required work input give a tip radius r_T of 4.62cm and a tip blade height h_T of .429 cm The slip factor μ_T, based on the method of Wiesner (ref. 5), is 0.871 and the impeller-tip flow-coefficient $C_{FL,T}$ is 0.925. Thus,

$$H = 212.5 \text{ ft.} = 64.77\text{m}$$

$$\eta_{HYD} = 0.52$$

$$\beta_T^* = 78.29 \text{ degs.}$$

$$r_T = 1.822 \text{ ins.} = 4.63\text{cm}$$

$$h_T = 0.169 \text{ ins.} = .429\text{cm}$$

$$\mu_T = 0.871$$

$$C_{FL,T} = 0.925$$

The blade angle β^* varies linearly from 84.00 degrees at the leading edge to 78.29 degrees at the tip. The blade thickness t_I is constant at .0508cm and the meridional profile is shown in figure 7.3.1.1 (supplied by Sundstrand) or 7.3.1.2.

For this design, the stage head coefficient ψ is 0.423 and the relative velocity ratio W_{ex}/W_{TI} across the impeller is 0.825. Based on the method of Daily and Nece (ref. 4), the stage disk-friction power is 15 watts. Also, the useful hydraulic output power is 20.88 watts and the hydraulic input power HP_{IN} is 0.0571, giving an estimated stage efficiency η_p of 36.6 percent. Thus,

ψ = 0.423

W_{EX}/W_{TI} = 0.825

HP_D = 0.0205

HP_{HYD} = 0.0284

HP_{IN} = 0.0571

η_p = 0.366

Dimensions are tabulated in fig. 7.3.2

7.3.3 Second-Stage Impeller

For reasons to be discussed, the second stage impeller is assumed to have the same hydraulic efficiency (0.52) as the first-stage inducer and impeller combined. Thus, for the same tip radius r_T, blade height h_t and blade exit angle β^*_T, the flow conditions out of the second-stage impeller are the same as those of the first stage impeller. (Thus, the vaned diffuser design is the same for both stages.)

The second stage impeller does not require a separate inducer, thus, the impeller can have a radial inlet and a constant blade height .429cm) between parallel plates, as shown in figure 7.3.1.1 or 7.3.1.2 . The leading-edge radius $r_{2,LE}$ is 1.651 cm. the blade angle $\beta^*_{2,LE}$ is 81.36 degrees, the inlet flow angle $\beta_{2,LE}$ (including the effects of blade blockage and a flow coefficient $C_{2,FL-LE}$ of 0.875) is 83.36 degrees. Thus, the effective incidence angle $i_{2,LE}$ is 2.00 degrees. This positive incidence is considered desirable, because of the relatively sharp turning upstream from the leading-edge in the meridional plane (see fig. 7.3.1.1) (Sundstrand). Thus,

$h_{2,LE}$ = 0.169 ins. =.429cm

$r_{2,LE}$ = 0.650 ins. = 1.651 cm

$\beta^*_{2,LE}$ = 81.36 degs

$\beta_{2,LE}$ = 83.36 degs.

$i_{2,LE}$ = 2.00 degs

$\tau_{2,FL-LE}$ = 0.875

Dimensions are tabulated in fig. 7.3.3.

The relative velocity ratio $W_{2,T}/W_{2,LE}$ across the impeller is 0.519, which value is considered marginally safe, and, for this reason, the hydraulic efficiency η_{HYD} is assumed to be equal (0.52) for both stages.

Computerized quasi-three-dimensional analyses to determine the relative velocity distributions on the blade surfaces along the hub and shroud lines were made for both the 1st and 2nd stage impellers. As for the 1st. stage inducer (fig. 7.3.1.3) the velocity distributions were found to be satisfactory.

Fianlly, it should be noted that the relatively large blade angles β^* used in from the second stage is not designed to create a static pressure rise, but merely to collect the flow at low velocity in order not to lose static pressure.

The performance curves for the boost stage (s) in liquid oxygen and liquid hydrogen are shown in Figures 7.4 and 7.5.

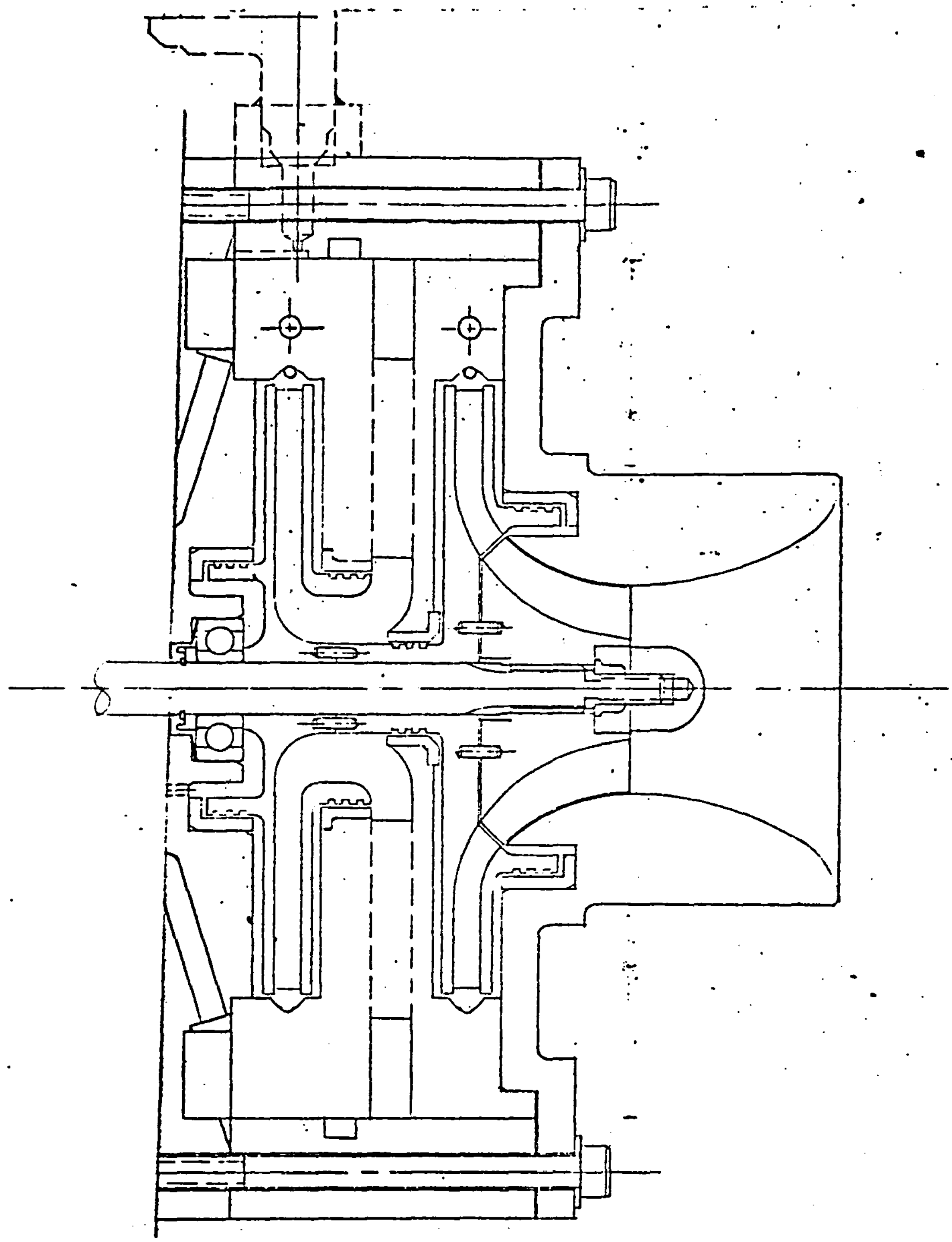

Fig. 7.3.1.1 - Meridional View of the LH_2 Boost Stages

FIRST STAGE INDUCER

Type: Mixed - flow, 2 blades

Inlet flow angle $B_{I,T}$ = 86.0^{o}

Inlet blade angle $B_{I,T}^{*}$ = 82.92^{o}

Incidence angle $_{I,T}$ = 3.08^{o}

Leading-edge profile wedge angle = 5^{o}

Nose radius	= 0.001 in. = .00254cm
Blade thickness	= 0.02 in. along shroud = .0508cm
	= 0.03 in. at hub = .0762cm
Exit Radius	= 0.88 in = 2.2352cm
Exit vane height	= 0.202 in = .513
Exit blade angle	= $B_{I,T}^{*}$ = 82.92^{o}

Fig. 7.3.1 Inducer Dimensions

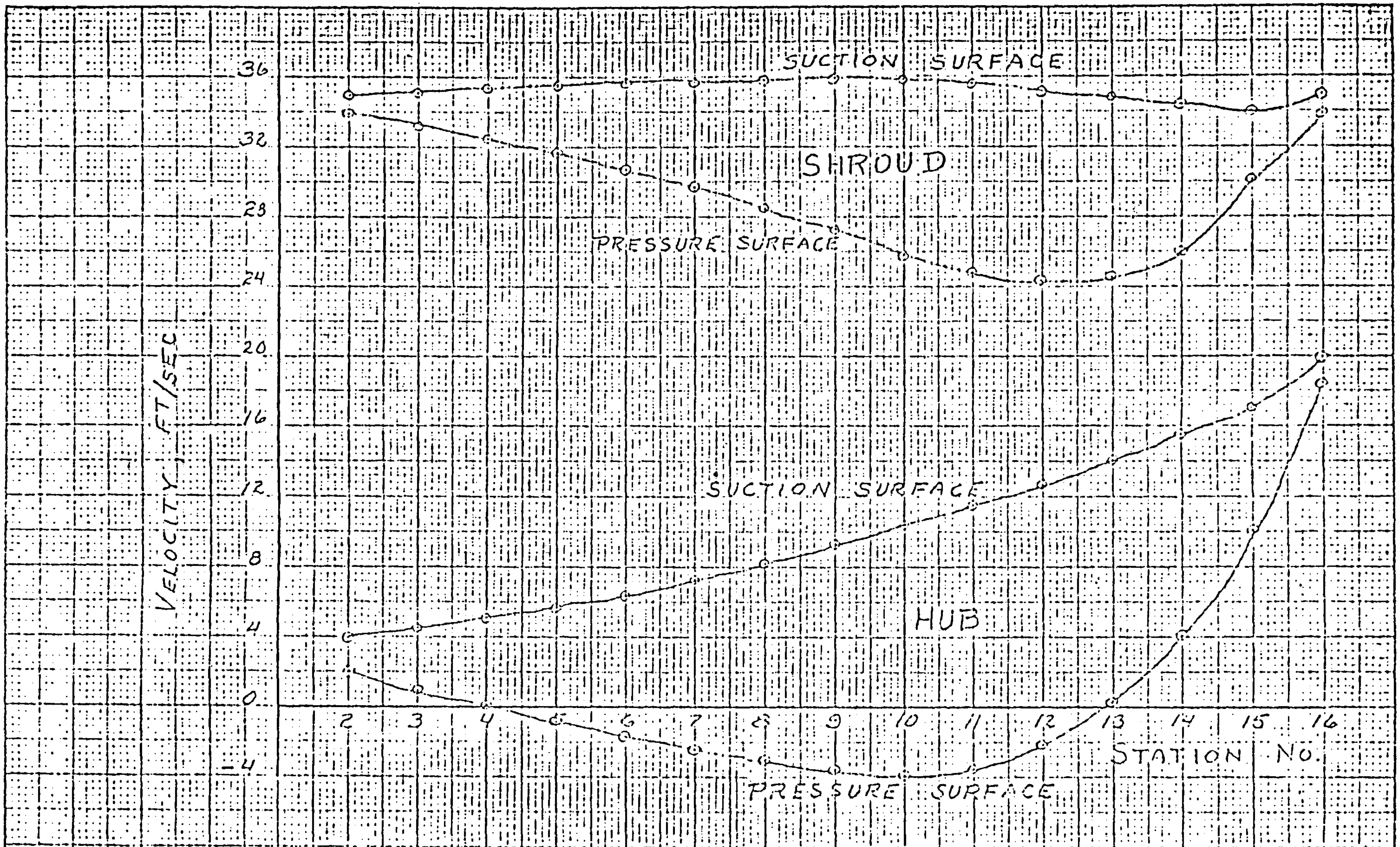

FIG. 7.3.13 VELOCITY DISTRIBUTION ON BLADE SURFACES OF FIRST-STAGE INDUCER AT EQUI-DISTANT STATIONS ALONG HUB AND SHROUD.
(STATIONARY)

FIRST STAGE IMPELLER

Number of blade	6	
Leading edge mean radius	0.88 in	(2.2352cm)
Inlet blade angle $B_{1,LE}$	84^o	
Exit blade angle B_T	78.29^o	
Tip Radius T_T	1.822 in	(4.628cm)
Tip Blade height h_T	0.169 in	(.429cm)
Blade Thickness t_I		

Fig. 7.3.2 *1ST STAGE IMPELLER DIMENSION*

SECOND STAGE IMPELLER

Number of blade	6	
Heady edge mean radius $T_{2,LE}$:	0.65"	(1.651cm)
Inlet blade angle $B_{2,LE}$ *:	81.36^o	
Inlet flow angle $B_{2,LE}$	83.36"	
Effective incidence angle $i_{2,LE}$:	2^o	
Exit Blade angle B_T^*	78.29^o	
Tip radius T	1.822 in	(4.628cm)
Tip blade height h_T	0.169 in.	(.429cm)
Blade thickness t	.02 in.	(.0508cm)

Fig. 7.3.3 *2ND STAGE IMPELLER DIMENSION*

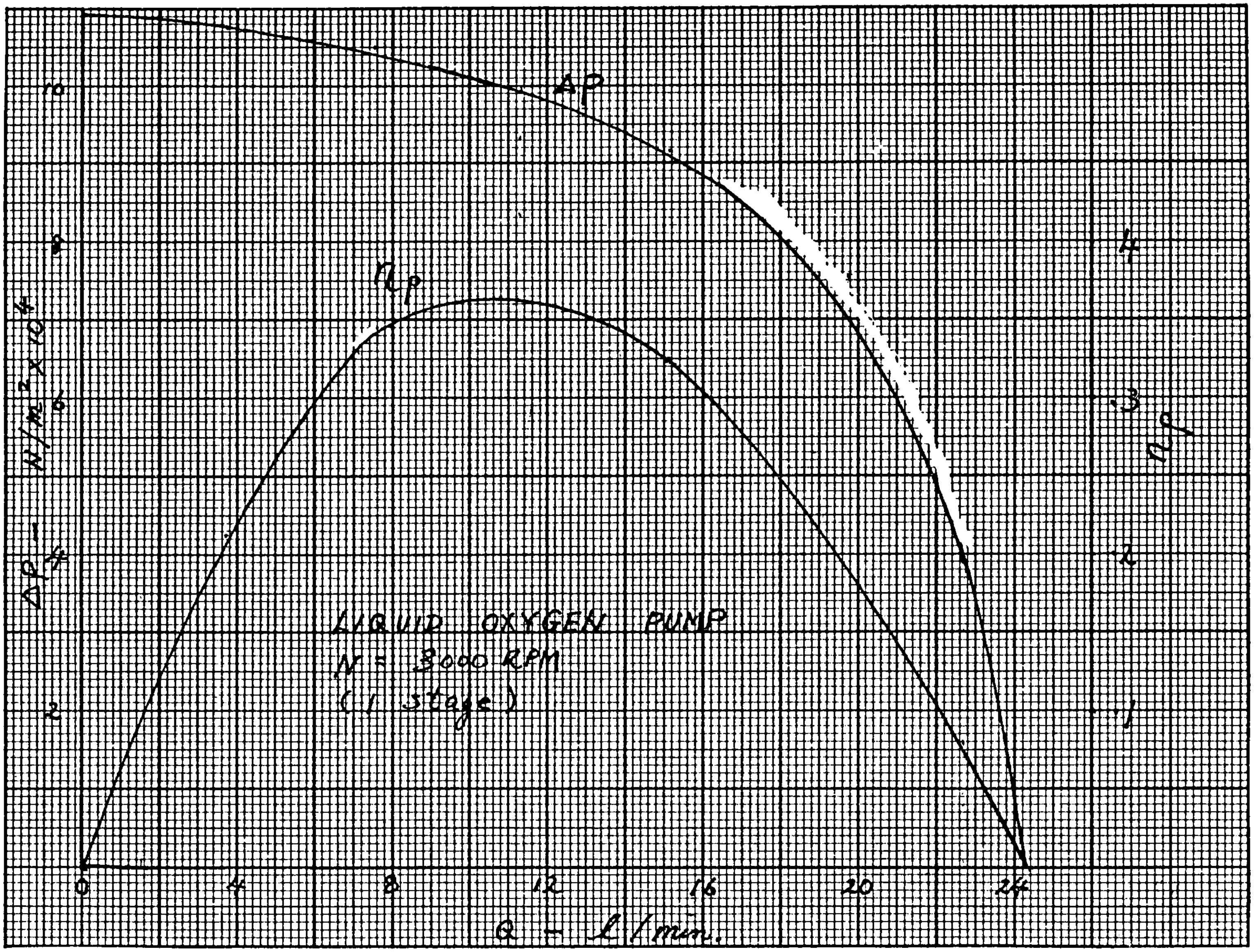

Figure 7.4 - LOX Boost Stage Performance Curves

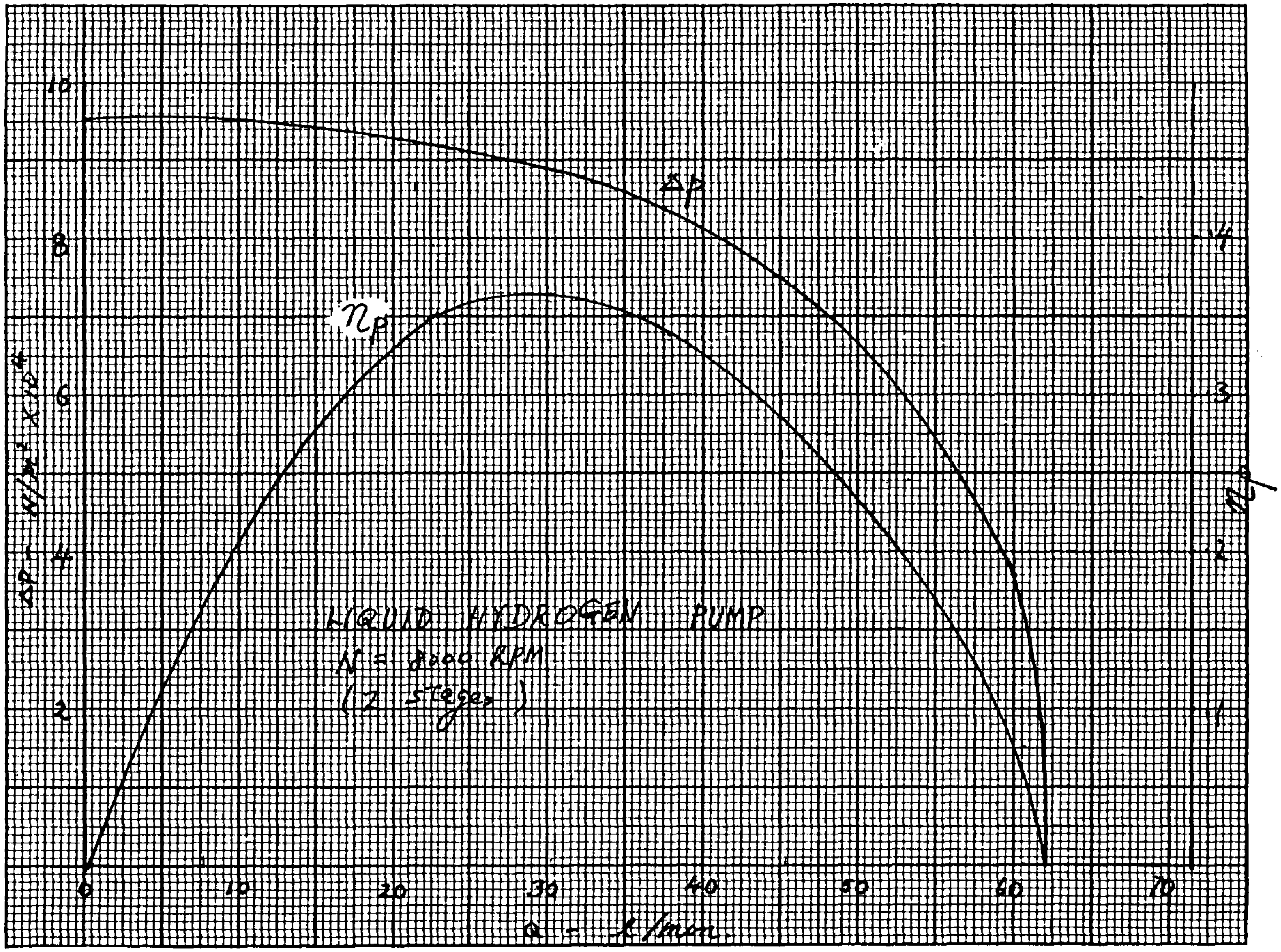

Figure 7.5 - LH_2 Boost Stages Performance Curves

8. BOOST/VANE PUMP

PERFORMANCE PREDICTION

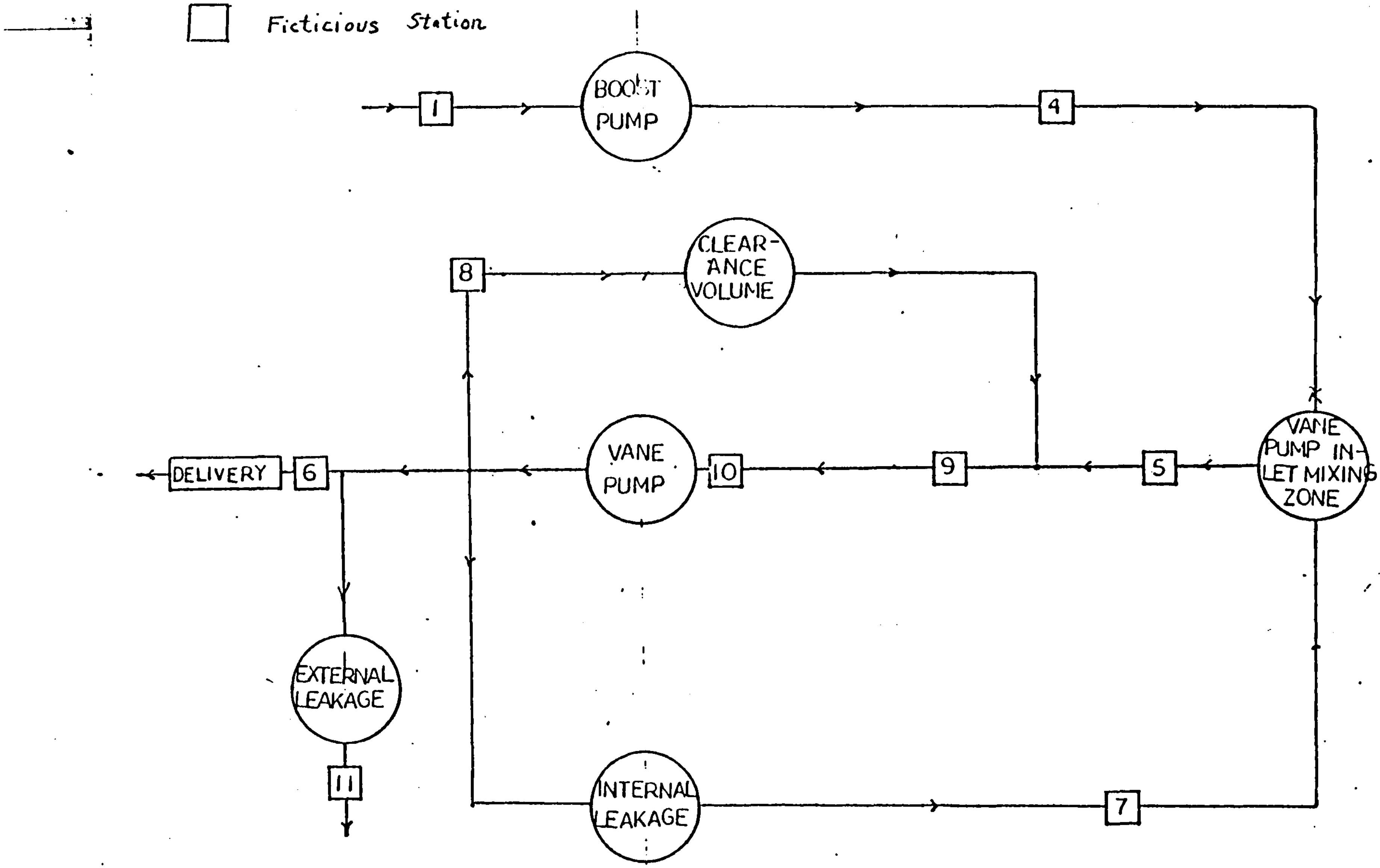

HYDRAULIC SCHEMATIC

The Performance curves of the individual vane stage (LH_2) and boost stage (LH_2) are shown in figures 6.4.1, 6.4.2, 7.5. In order to estimate the performance of the integrated unit, $\dot{Q}$ discharge vs. P_4 of the vane stage at various discharge pressures P_6 were generated and plotted on the same graph with the performance curve (ΔP vs. $\dot{Q}$) of the boost stage (Figure 8.1). The performance curve (ΔP vs. $\dot{Q}$) of the integrated boost/vane pump was then read off from the intersections of these two families of curves. The resulting LH_2 pump performance curve is shown in Figure 8.2 together with the H_p and η_p curves. The LOX pump's is shown in Figure 8.4.

LH_2

Boost Pump

GPM	$\eta_{cent.}$	$PSI_{cent.}$	$P_{cent/vane}$ (PSIG)	$\eta'_{cent.}$
5.5	.34	13.4	315	.014
6	.35	13.3	275	.0169
7	.365	13.0	152.5	.0311
8	.365	12.8	90	.0519
9	.367	12.5	35	.12

Vane Pump

GPM	η_{vane}	PSI_{vane}	$P_{boost/vane}$	η'_{vane}	$\eta'_{(boost\ \&\ vane)}$
5.5	.472	301.6	315	.4519	.4659
6	.504	201.7	275	.4796	.6137
7	.612	139.5	152.5	.5598	.6448
8	.691	77.2	90	.5929	.5909
9	.768	22.5	35	.4937	.4965

LOX

Boost Pump

GPM	$\eta_{cent.}$	$P_{cent.}$ (PSIG)	$P_{cent./vane}$ (PSIG)	$\eta'_{cent.}$
3.17	.36	14.5	95.3	.055
2.14	.36	14.75	265.3	.02
2.11	.345	15.25	435.3	.012

Vane Pump

GPM	η_{vane}	P_{vane} (PSIG)	$P_{boost/vane}$ (PSIG)	η'_{vane}	$\eta'_{(boost\ \&\ vane)}$
3.17	.828	80.8	95.3	.748	.803
2.64	.694	250.55	265.3	.655	.675
2.11	.545	420.05	435.3	.526	.538

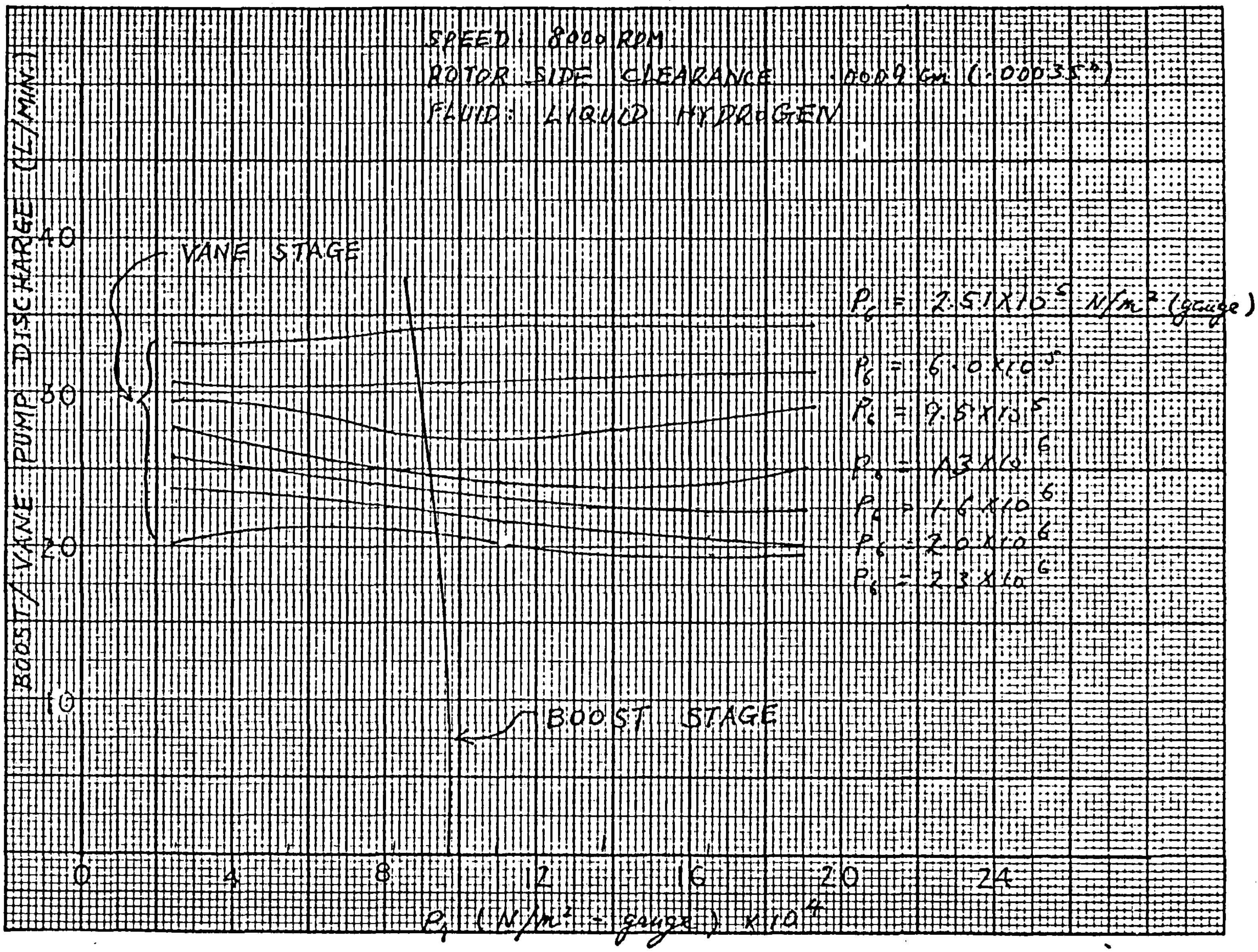

Fig. 8.1 - LH_2 Vane/Boost Stages Matching

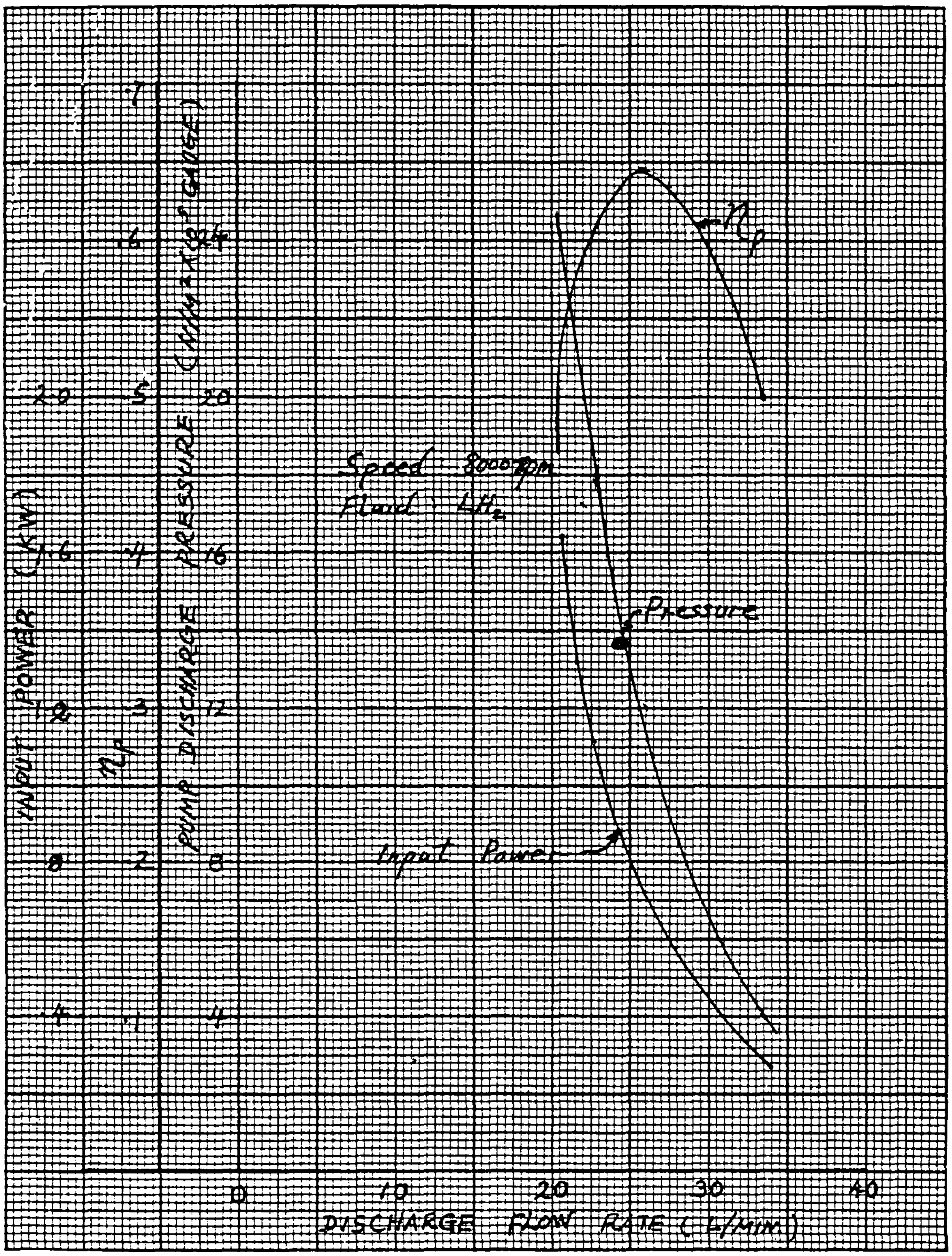

Fig. 8.2 - LH_2 Pump Performance

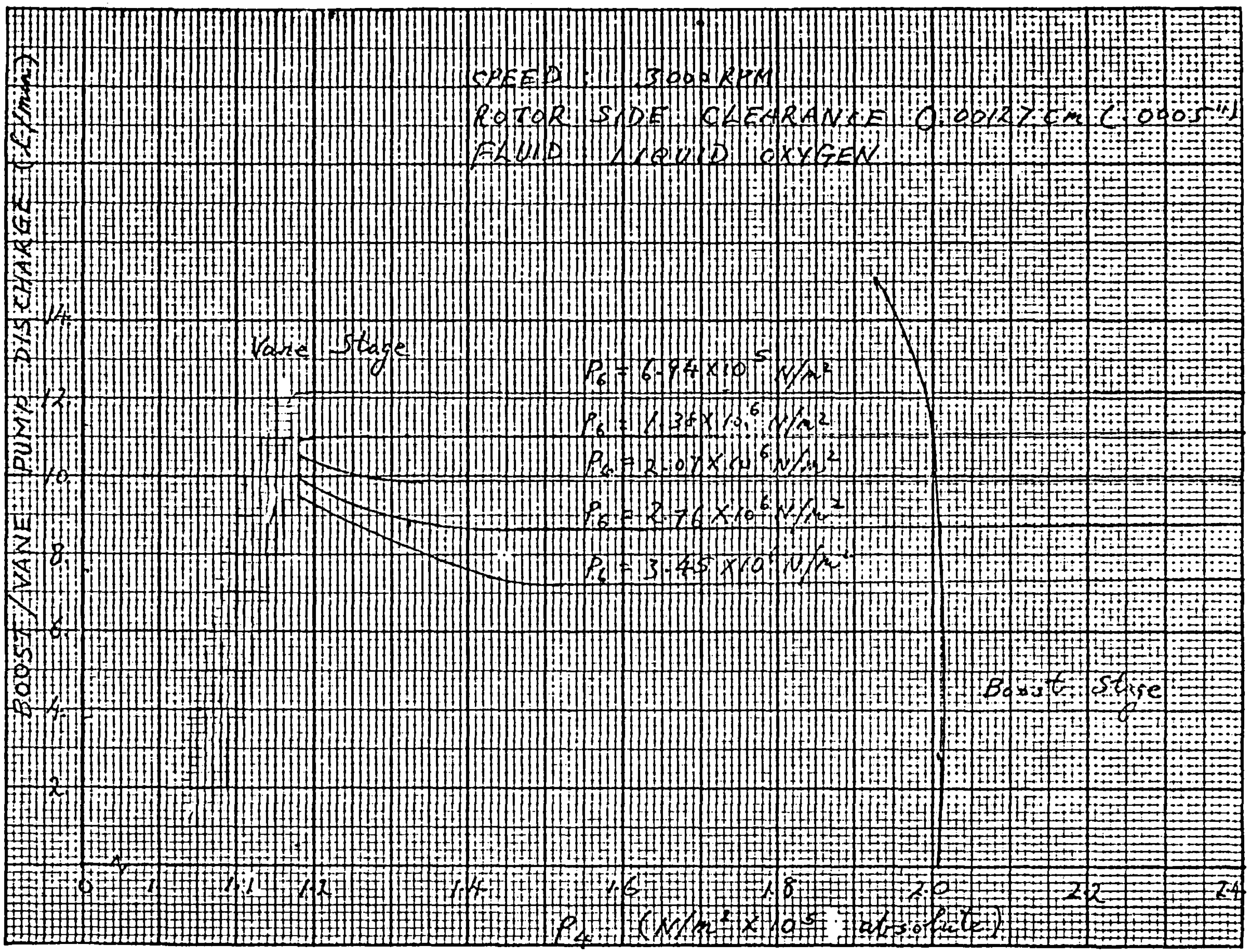

Fig. 8.3 - LOX Vane/Boost Stages Matching

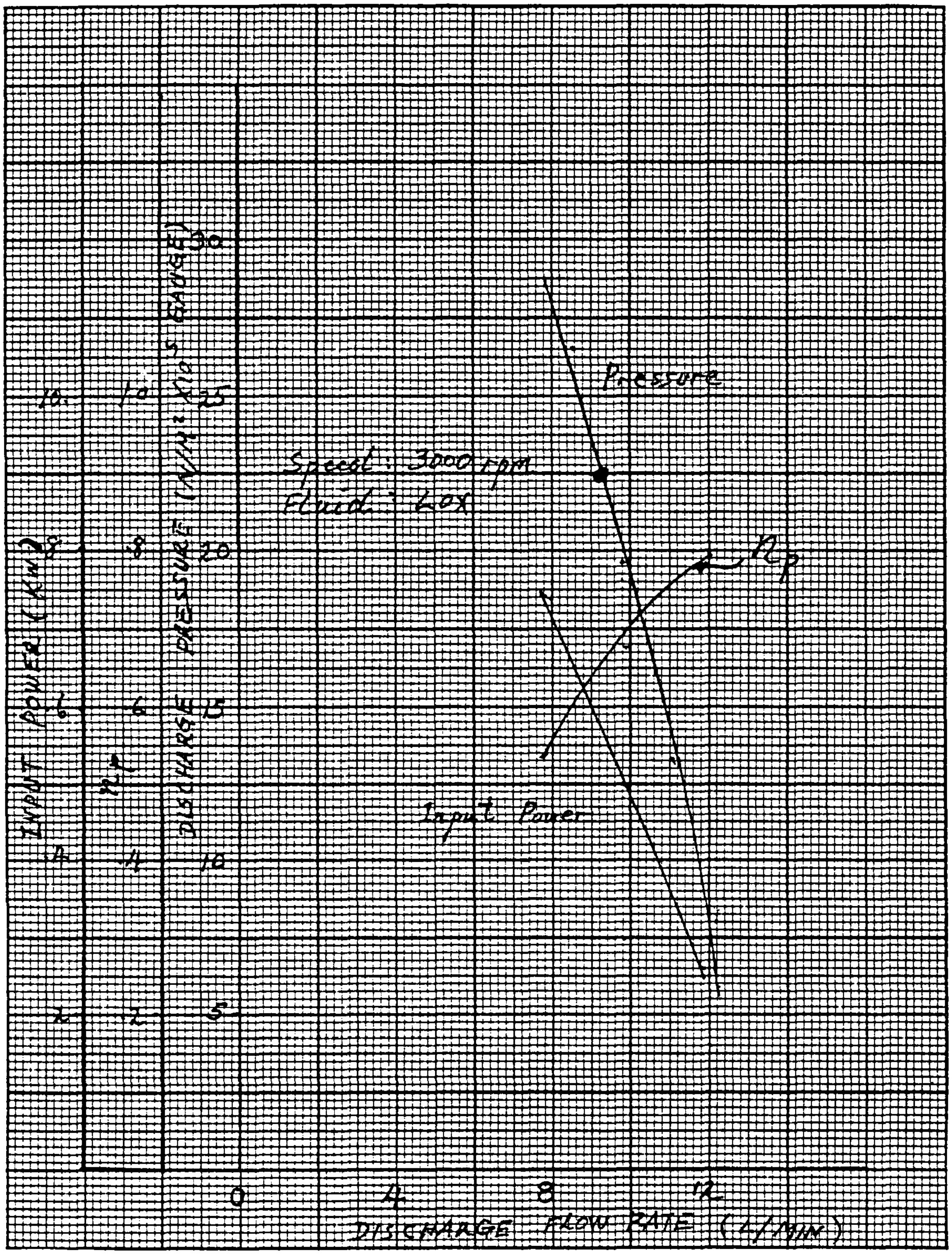

Fig. 8.4 - LOX Pump Performance

9. MECHANICAL DESIGN

9.1 Stress on Vane Stage
9.2 Thrust Load on Impellers
9.3 Bearing Life & Seal Selection
9.4 Liner Pressure Plate

JOB NASA-Lewis LOx/LH_2 Pump
EWR #09449

PAGE 6.0
DATE 6-10-77
REV. A 11-11-77

DESIGN PARAMETER LIMITATIONS

1. Adequate material properties at 20.2° K (A)
2. Surface speeds less than 6.096m/s for LOX pump
3. Zero NPSH operation
4. Eliminate vortex action at boost pump inlet
5. Gas inside the pump is to be avoided
6. Isolation of seal package from cryogenic temperatures
7. Material compatability with liquid O_2, design for safety. (A)
8. Material compatability with Liquid H_2, design for wear. (A)
9. Reprime capability
10. Same vane pump design to be used on both hydrogen and oxygen, only materials change. (A)
11. Pressure plate on vane pump to eliminate catastrophic failures due to rotor or vane growth. (A)

9.1 STRESSES

9.1 STRESSES ON VANE STAGE

BOOSTED VANE PUMPS

ROTOR KEY SIZE

HP @ 40% , HP = 2.25 (LH_2) = 2.28

= 1.47 (LOX) = 1.49

$$T = \frac{63025\ HP}{N}$$

N = 8000 rpm (LH_2)

= 3000 rpm (LOX)

$$T = \frac{63025\ (2.25)}{8000} = 17.73 \text{ in.lb. } (LH_2) = 20.4 \text{ cm. kg.}$$

$$= \frac{(63025)\ (1.47}{3000} = 30.88 \text{ in.lb. (LOX)} = 35.6 \text{ cm. kg.}$$

Shaft Dia. D = .3.25 in. = .7937 cm

For LOX:

Key shear,

$$= \frac{T}{.5blD} = \frac{T}{bl\tau}$$

b = key width
L - Key length

Material,

for A1S1 4130 (40-50 HRC)

σ_u = 180,000 psi τ_y = 93,000 psi
= 1.24×10^9 N/m^2 = 6.41×10^8 N/m^2
σ_y = 163,000 psi σ_{cy} =173,000 psi
= 1.12×10^9 N/m^2 = 1.19×10^9 N/m^2

Let b = .125 in. = .3175 cm

M.S.= .5

n = factor of safety = M.S. + 1
= 1.5

$$L = \frac{T\ 1.5}{.5}$$

$$L = \frac{30.88\ (1.5)}{.5\ (.125)\ (.3125)\ (93000)} = .026 \text{ in.} = .066 \text{ cm}$$

Use 1/8 in min. available key. (.3175 cm key)

Compression,

$$\sigma_c = \frac{T}{.25tLD}$$

let L 1/4"

$$\sigma_c = \frac{30.88}{.25\,(.125)\,(.25)\,(.3125)} = 12{,}650 \text{ psi} = 8.72 \times 10^7 \text{ N/m}^2$$

M.S. $\longrightarrow$ large

Shaft

$$\tau = \frac{Tr}{J} = \frac{T\frac{D}{2}}{\frac{\pi D^4}{32}} = \frac{16\,T}{\pi D^3}$$

$$= \frac{16\,(30.88)}{\pi\,(.3125)^3} = 5153 \text{ psi} = 3.55 \times 10^7 \text{ N/m}^2$$

Stress concentration due to keyslot,

$t = 3.0$ (Ref. Peterson, 1974, Fig. 183)

Max. stress,

$\tau' = 5153\,(3) = \underline{15{,}460 \text{ psi}} = 1.06 \times 10^8 \text{ N/m}^2$

$\sigma' = 27{,}122$ psi M.S. $\longrightarrow$ LARGE

$= 1.87 \times 10^8 \text{ N/m}^2$

Vane

Material properties: $\sigma_u = 280$ ksi $= 1.93 \times 10^9 \text{ N/m}^2$

Material - FERRO-TIC

Vane dimensions,

$t = .040$ in. $= .102$ cm

$a = .05$ in (stroke) $= .128$ cm

$w = .771$ in. $= 1.98$ cm

$h = .2$ in $= .514$ cm

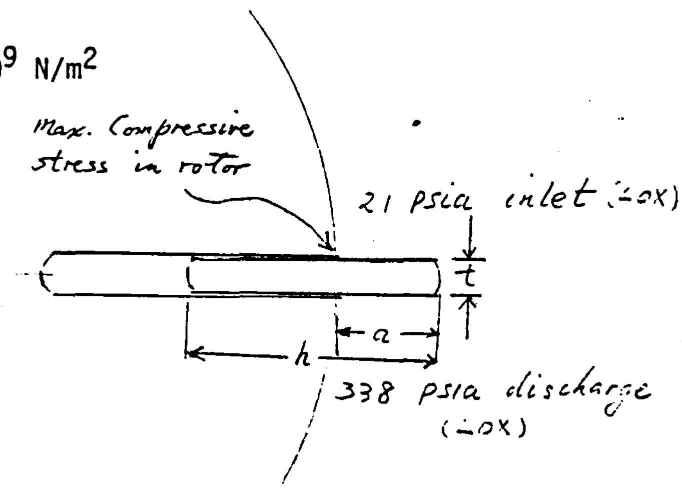

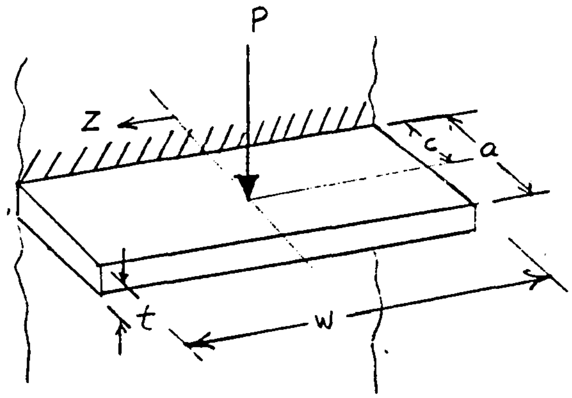

for a beam of relatively great width $\left(\frac{W}{a} > 4\right)$

bending stress, (reflecting the load due to friction between vane tip & liner)

$$\sigma_b = K_m \left(\frac{6P}{t^2}\right)$$

for $\frac{Z}{a} = 0 = \frac{c}{a} = .5$

$K_m = .370$ (see pg. 135 of Ref. Book 7)

$P = (\Delta\ PSI) \times (W) \times (a)$

$P = 317\ (.771)\ (.05) = 12.2$

$$\sigma_b = .37\ \frac{6\ (12.2)}{(.04)^2} = 16927 \text{ psi.} = 1.17 \times 10^8\ \text{N/m}^2$$

M.S. is LARGE

Compressive stress at edge of vane slot;

The vane/slot combination is similar to a pin in a solid body. The vane is assumed to be infinitely stiff and the rotor material linearly elastic.

The maximum pressure at the edge of the slot is,

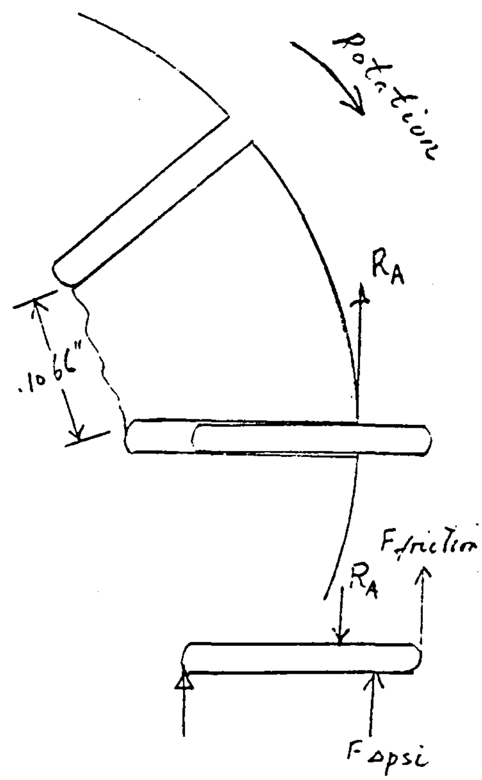

$$p\ max = \left[\frac{P}{h-a}\left(4 + \frac{6a}{h-a}\right)\right] \Big/ W$$

$$= \frac{13}{.15(.771)}\left[4 + \frac{6\ (.05)}{.15}\right]$$

$$= 674 \text{ psi} = 4.65 \times 10^6\ \text{N/m}^2$$

M.S. $\longrightarrow$ LARGE

Bending stress from vane load on the rotor

$$\sigma_b = K_m \left(\frac{6\,P}{t^2}\right) \qquad K_m = .51 \quad \text{for } \frac{C}{a} = 1$$

$P = R_A = 15.46$

$\sigma_b = \frac{.51\ (b)\ (15.46)}{(.1066)^2} = 4163$ psi $= 2.87 \times 10^7$ N/m^2

Stress concentration factor for bending

$K_t = 1.55 \quad \text{for } \frac{r}{d} = \frac{r}{t} = \frac{.020}{.1066} = .188$

$\frac{D}{d} = \frac{3t}{t} = 3$

(ref. Peterson, '74, fig. 73)

max. stress,

$\sigma_b' = 1.55\ (4163) = 6453$ psi $= 4.45 \times 10^7$ N/m^2

Ring section stress (neglecting vane load)

at bore, $\sigma_{eff} = 189$ psi (ref. E4 output)
$= 1.3 \times 10^6$ N/m^2

M.S. $\longrightarrow$ large.

Input and output are shown in Fig. 9.1.1 and 9.1.2

Rotor & Vane Material - Ferrotic

2 Pump Designs with same dimensions

Hydrogen - HT6

Oxygen - CN5

Rotor O.D. = 1.0468" = 2.66 cm

Rotor width = .771" = 1.96 cm

No. of Vanes = 16

Dual Lobe

Inlet and discharge ports 45^{o}

Vane Height	.200"	(0.508 cm)
Vane Thickness	.040"	(.1016 cm)
Shaft Diam.	.3125	(.7937 cm)

	LH_2	LOX
Inlet	28 PSIA 1.93×10^5 N/m^2	21 PSIA 1.45×10^5 N/m^2
Discharge	231 PSIA 1.59×10^6 N/m^2	338 PSIA 2.33×10^6 N/m^2
Flow,	7.0 GPM 26.49 l/min.	3.0 GPM 11.35 l/min.
Speed, RPM	8000	3000
Hp @ 40% N	2.25	1.47
Operating Temp.	37 ^{o}R 20^{o}K	163 ^{o}R 90.2^{o}K

9.1 VANE PORT SIZING BASED ON VANE CONTACT STRESS AND AREA PORTING

ENTERANCE PORTING AREA = .45 × .15 = .0675 in^2/PORT
= .4354 cm^2/port

FOR LH_2 PUMP 2 PORTS FOR 7.5 GPM (28.39 ℓ/min.)

$$\text{VELOCITY} = \frac{7.5 \times 231}{2 \times .0675} \times \frac{1}{720} = 17.8 \text{ FT/SEC}$$
$$= 5.425 \text{ m/sec}$$

PORTING ARC OF 45°

MEAN RADIUS OF PORTING ARC =
$$\tfrac{1}{2}(r_{MAJ} + r_{MINOR}) = \tfrac{1}{2}\left(\frac{1.056}{2} + \frac{1.156}{2}\right)$$
$$= .553''$$
$$= 1.404 \text{ cm}$$

VANE THICKNESS = .040" = .1016 cm
VANE RADIUS TIP = .040" = .1016 cm
VANE HEIGHT = 0.200" = .508 cm
VANE LENGTH = 0.771" = 1.958 cm
CNS (LOX) ρ = 11.8 gr/cc = .4263 LB/IN^3
HT6 (LH_2) ρ = 6.60 gr/cc = .2384 LB/IN^3
VANE MASS (LOX) = .04 × .771 × .2 × .4263 = 2.629×10^{-3} LB
= 1.235 gm
VANE MASS (LH_2) = .04 × .771 × .2 × .2384 = 1.470×10^{-3} LB
= .69 gm.

RADIUS OF VANE ROTATION = .553 − .20/2
= .453"
= 1.151

CENTRIFUGAL FORCE $F_c = MR\omega^2$

PRESSURE FORCE $F_p = \frac{1}{2}\Delta P \times \text{Area} = \frac{.04}{2} \times .771 \times \Delta P$
$= .03084\ \Delta P/2$
$= .01542\ \Delta P$

	LOX	LH_2
SPEED	3000	8000
ω, rad/sec	314.2	837.8
M, lb-sec²/FT	8.171×10^{-5} (1.235 gm)	4.569×10^{-5} (.69 gm)
r, FT	.03775 (.096 cm)	.03775 (.096 cm)
centri. force F_c, LB	.3045 (1.35 N)	1.2107 (5.385)
ΔP, psi	323 (2.23×10^6 N/m²)	216 (1.48×10^6 N/m²)
pressure force F_p, LB	4.981 (22.1 N)	3.331 (14.82 N)
F_{TOT}, LB	5.286 (23.45 N)	4.542 (20.21 N)
F_{TOT} +20%	6.343 (28.14 N)	5.450 (24.25 N)

USE MAX LOAD OF LOX PUMP FOR SIZING

P_o = 6.343 LB = 28.21 N
L = .771 IN = 1.958 cm.
r_a = .040 IN = .1016 cm D_a = .080 = .2032 cm.
r_b = −.553 IN = 1.40 cm D_b = 1.106 = 2.8 cm
E = 33×10^6 psi = 2.27×10^{11} N/m²
δ = .3
b = WIDTH OF RECTANGULAR CONTACT AREA
P = 6.343/.771 = 8.227 LB/IN = 14.25 N/cm

$$b = 1.6\sqrt{\frac{P\,(D_a D_b)}{(D_b - D_a)}\left[\frac{1-\delta^2}{E_1} + \frac{1-\delta^2}{E_2}\right]}$$

$$b = 1.6\sqrt{\frac{8.227(.080)(1.106)}{(1.106-.080)}\,2\left[\frac{1-.3^2}{33\times10^6}\right]}$$

$b = 3.165\times10^{-4}$ IN
$= 8.13\times10^{-4}$ cm.

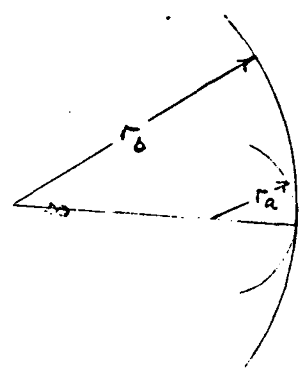

JOB NASA-Lewis LOX/LH_2 Vane Pump
EWR #09449

PAGE 7.6.2
DATE 11-11-77
REV.

MAX CONTACT STRESS

$$S_c = 0.798\sqrt{\frac{P\left[\frac{D_b - D_a}{D_b D_a}\right]}{2\left[\frac{1-\delta^2}{E}\right]}}$$

$$S_c = 0.798\sqrt{\frac{8.227\ \frac{(1.106 - .070)}{1.106(.070)}}{2\left[\frac{1-.3^2}{33\times10^6}\right]}}$$

$S_{c_{MAX}} = 33,189$ psi $\therefore$ LOAD $= (33189)(.771)(3.165\times10^{-4})$
$= 2.29\times10^8\ N/m^2$ $= 8.099^{\#} = 36.02\ N$

PORT ARC LENGTH $\theta = 45°$

$r\theta = .553 \times \pi/4 = .434'' = 1.102\ cm$

ENTERANCE AREA $= .0675\ IN^2 = .435\ cm^2$

PORT WIDTH $= \frac{.0675}{.434} = .1555'' = .3949\ cm$

USE PORT WIDTHS OF .086" FOR 2 PORTS

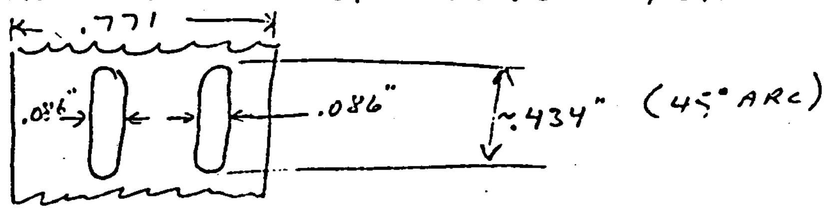

$l = .771 - 2(.086) = .599'' = 1.521$
$bl = 316.5\times10^{-6} \times .599 = 189.6\times10^{-6}\ IN^2 = 1.22\times10^{-3}\ cm^2$

$S_{c_{MAX}} = \frac{8.099}{189.6\times10^{-6}} = \underline{42,715\ psi} = 2.94\times10^8\ N/m^2$

9.2 Thrust Load

9.2 THRUST LOADS FROM BOOST PUMP
LH_2 — 7.5 GPM AT 8000 RPM, 6.5 psi/STAGE
1ST STAGE

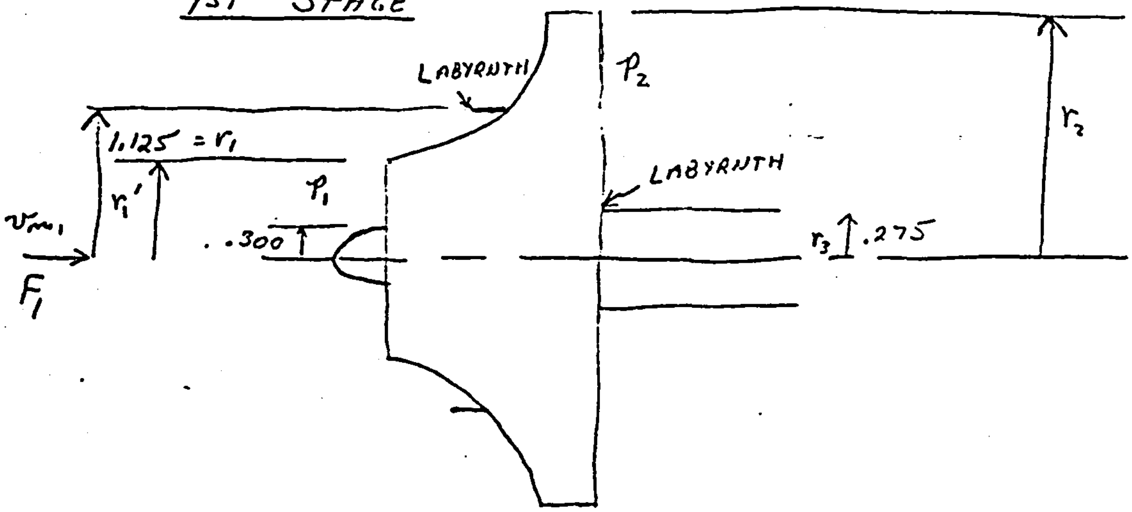

FROM PAUL HERMANN MEMO RE75/536

$$F = \frac{\pi}{3}(P_1 - P_2)(r_2^2 + r_1 r_2 + r_1^2) + \pi P_2 r_3^2 + \frac{\pi}{16}\frac{\rho_{av}}{144 g} u_T^2 \left[\frac{r_2^2 - r_3^2}{r_2}\right]^2 + \dot{m} v_{1m}$$

$r_1' = .625'' = 1.58$ cm
$r_2 = 1.822'' = 4.627$ cm
$r_3 = .275'' = .698$ cm
$P_1 = 14.7$ psia $= 1.01 \times 10^5$ N/m²
$P_2 = 21.2$ psia $= 1.46 \times 10^5$ N/m³

$\rho_{av} = 4.375$ lb/ft³ $= 687$ N/m³
$g = 32.174$ ft/sec² $= 9.8$ m/sec²
$u_2 = \frac{2\pi r_2 N}{720} = 127.2$ FT/SEC
$= 38.77$ m/sec

INLET AREA $= \pi(r_1^2 - .3^2) = .944$ IN² $= 6.09$ cm²

$$v_{m_1} = \frac{7.5\,(231)}{60 \times 12 \times .944} = 2.55 \text{ FT/SEC} = .777 \text{ m/sec}$$

$$\dot{m}_1 = \frac{7.5 \times 231 \times 4.375}{32.174 \times 60 \times 12^3} = 2.27 \times 10^{-3} \text{ LB-SEC}^2\text{/FT}$$
$$= 33.12 \text{ gm/sec}$$

$$F_1 = \frac{\pi}{3}(14.7-21.2)(1.822^2+1.822\times1.125+1.125^2)$$
$$+\ \pi(21.2)(.275)^2 + \frac{\pi}{16}\frac{4.375\times127.2^2}{\times144\times32.174}\left(\frac{1.822^2-.275^2}{1.822}\right)^2$$
$$+\ 2.27\times10^{-3}\times2.55$$

$$F_1 = -45.16 + 5.04 + 9.52 + .01$$
$$= \underline{-30.59\ \text{LBS.}} = -136.06\ N$$

2nd STAGE

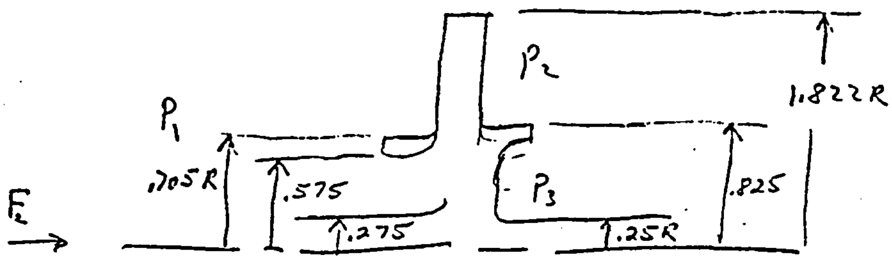

$r_1 = .705'' = 1.79$ cm $\qquad P_1 = 21.2$ psia $= 1.46\times10^5\ N/m^2$
$r_2 = 1.822'' = 4.63$ cm $\qquad P_2 = 27.7$ psia $= 1.91\times10^5\ N/m^2$
$r_3 = .825'' = 2.095$ cm $\qquad P_3 = 14.7$ psia $1.01\times10^5\ N/m^2$
$U_t = 127.2$ FT/SEC $= 38.8$ m/sec $\qquad \rho_{ov} = 4.375$ LB/FT^3 $= 68.7\ N/m^3$
$g = 32.174$ FT/SEC^2 $\qquad \dot{m} = 2.27\times10^{-3}$ LB-SEC/FT
$= 9.8$ m/sec^2 $\qquad = 33.12$ gm
INLET AREA $= \pi(.575^2 - .275^2) = .801$ IN^2
$= 5.17$ cm^2

$$v_{m_1} = \frac{7.5(231)}{720\times.801} = 3.00\ \text{FT/SEC}$$
$$= 0.774\ m/sec$$

JOB NASA-Lewis LOX/LH_2 Vane Pump
EWR #09449

BY

PAGE 7.2.2
DATE 11-11-77
REV.

$$F_2 = \pi/3\ (P_1 - P_2)(r_2^2 + r_1 r_2 + r_1^2) + \pi P_2 r_3^2$$
$$+ \frac{\pi}{16} \times \frac{\rho_{av}}{144 g}\ u_T^2 \left[\frac{r_2^2 - r_3^2}{r_2}\right]^2 + \dot{m}\, r_{m_1} - \pi P_3 (r_3^2 - .25^2)$$
$$- \pi P_1 (.275^2)$$

$$F_2 = \frac{\pi}{3}(21.2 - 27.7)(1.822^2 + 1.822 \times .705 + .705^2)$$
$$+ \frac{\pi}{16} \times \frac{4.375 \times 127.2^2}{144 \times 32.174}\left[\frac{1.822^2 - .225^2}{1.822}\right]^2 + \pi(27.7)(.225^2)$$
$$+ 2.27 \times 10^{-3} \times 3.00 - \pi \times 14.7(.618) - \pi(21.2)(.275^2)$$

$$F_2 = -34.72 + 6.29 + 59.23 + .01 - 28.54 - 5.04$$
$$= -2.77$$
$$= -12.32\ N$$

$$F_{TOTAL} = F_1 + F_2$$
$$= -30.59 + (-2.77)$$
$$= 33.36\ LBS.$$
$$= 148.4\ N$$

JOB NASA-Lewis LOX/LH_2 Vane Pump
EWR #09449

PAGE 7.2.3
DATE 11-11-77
REV.

THRUST LOADS FROM BOOST PUMP
LOX – 2.8 GPM AT 3000 RPM, 12 psi

$r_1' = .625'' = 1.58$ cm
$r_2 = 1.822'' = 4.63$ cm
$r_3 = .275'' = .698$ cm
$P_1 = 14.7$ psia $= 1.01 \times 10^5$ N/m^2
$P_2 = 26.7$ psia $= 1.84 \times 10^5$ N/m^2

$\rho_{av} = 71.0$ LB/FT^3 $= 1.12 \times 10^4$ N/m^3
$g = 32.174$ FT/SEC^2 $= 9.8$ m/sec^2
$u_r = 47.7$ FT/SEC $= 14.53$ m/sec

$$v_{m_1} = \frac{2.8\,(231)}{720 \times .944} = .952 \text{ FT/SEC} = .29 \text{ m/sec}$$

$$\dot{m} = \frac{2.8 \times 231 \times 71.0}{32.174 \times 60 \times 12^3} = .0138 = .2014 \text{ Kg}$$

$$F = \frac{\pi}{3}(14.7 - 26.7)(1.822^2 + 1.822 \times 1.125 + 1.125^2) + \pi(26.7)(.275)^2 + \frac{\pi}{16} \times \frac{71.0 \times 47.7^2}{144 \times 32.174}\left[\frac{1.822^2 - .275^2}{1.822}\right]^2 + .952 \times .0138$$

$$F = -83.38 + 6.34 + 21.70 + .01$$

$$F = 55.33 \text{ LBS} = 246.1 \text{ N}$$

Form G 7756

9.3 Bearings and Seals

9.3 BEARING CALCULATIONS

Bearing Selection:

Angular contact ball bearings were chosen having 440C stainless steel balls and races with rulon cages. Angular contact bearings were chosen over radials in order that one piece cages could be used. The radial contact bearings have rivetted cages. These 440C bearings have been run successfully at cryogenic temperatures and material compatability with hydrogen and oxygen is adequate. (A)

Only axial loads are assumed on the bearings. From the differential pressure balance on the boost pump and the two spring loads. MRC bearings were chosen. (A)

B_1 is an R_6 bearing on the hot end (outside the seal package). it is a deep groove radial ball bearing with a .9525 cm bore. This bearing is clamped axially to prevent seal damage, and will operate dry. (A)

B_2 is an R_8 bearing on the cold side that will take all of the thrust loading. It will operate in the flooded state at cryogenic temperatures. It is an angular contact ball bearing with a 1.27 cm bore. (A)

B_3 is a 38 bearing on the cold side closest to the boost pump. This is an angular contact ball bearing with a .8001 cm bore. It will operate in the flooded state at cryogenic temperatures. The only axial load on this bearing will be the thrust load from the wavy spring. (A)

PARAMETER BOOK

BEARING LIFE CALCULATIONS (MRC)

Wavy Spring Behind B3 Bearing - 5# Axial
Coil Spring At Spline - 2.85# Axial

3000 RPM LOX Pump

	B_1	B_2	B_3
Axial Load (T)	2.85	63.18	5.0
Thrust Load Index (K)	.171	.281	.171
T/K	16.7	225	29.2
Thrust Factor (Y)	3.25	2.1	2.98
Equivqlent Load (B)	9.26	132.7	14.9
Speed Rating	115	170	113
Speed Factor (.6934) (A)	79.7	117.9	78.4
Service Factor (A)/(B)	8.6	.888	5.3
Life Hrs.	9.5×10^5	1050	2.2×10^5
Derate to 20%, Hrs.	190,000	210	44,000

8000 RPM LH_2 Pump

	B_1	B_2	B_3
Axial Load (T)	2.85	41.21	5.0
Index (K)	.171	.281	.171
T/K	16.7	146.7	29.2
Thrust Factor (Y)	3.25	2.28	2.98
Equivalent Load (B)	9.26	94.0	14.9
Speed Rating	115	170	113
Speed Factor (.50) (A)	57.5	85	56.5
Service Factor (A/B)	6.21	.904	3.79
Life Hrs.	3.59×10^5	1108	$.816 \times 10^5$
Derate to 20%	71,800	222	16,300

JOB NASA-Lewis LOX/LH_2 Vane Pump
EWR #09449

PAGE 7.1
DATE 11-11-77
REV.

BEARINGS

THERMAL CONTRACTION (LH_2) 37°R

SHAFT IS MONEL 400 (K MONEL) $\alpha = 5.09 \times 10^{-6}$ IN/IN/°F
BEARING IS 440C STAINLESS $\alpha = 3.76 \times 10^{-6}$ IN/IN/°F
HOUSING IS MONEL 400 (K MONEL)

ABEC-5	R6	R8	-38
BEARING BORE	$.3750^{+.0000}_{-.0002}$	$.5000^{+.0000}_{-.0002}$	$.3150^{+.0000}_{-.0002}$
BORE AT (37°R)		.4991	.3144
SHAFT AT (37°R)		$.4993^{+.0000}_{-.0002}$	$.3146^{+.0000}_{-.0002}$
FIT (TIGHT)	0-4	0-4	0-4
SHAFT AT (68°F)	$.3752^{+.0000}_{-.0002}$	$.5005^{+.0000}_{-.0002}$	$.3154^{+.0000}_{-.0002}$
FIT (TIGHT)	0-4	3-7	2-6
INTERNAL CLEARANCE	.0003	.0006	.0005
BEARING O.D. (68°F)	$.8750^{+.0000}_{-.0002}$	$1.1250^{+.0000}_{-.0002}$	$.8661^{+.0000}_{-.0002}$
AT (37°R)		1.1229	.8645
FIT (LOOSE)	0-5	0-5	2-7
HOUSING (37°R)		$1.1229^{+.0003}_{-.0000}$	$.8647^{+.0003}_{-.0000}$
HOUSING (68°F)	$.8750^{+.0003}_{-.0000}$	$1.1257^{+.0003}_{-.0000}$	$.8669^{+.0003}_{-.0000}$
FIT (LOOSE)	0-5	7-12	8-13

INNER RACE

HOOP STRESS	25,700	33,500	42,000 PSI
RADIAL STRESS	6,800	7,400	13,000
MAX. EQUIV. YIELD	29,700	37,700	49,800
INTERNAL CLEARANCE REQUIRED, IN. (MIN. VALUE)	.0003	.0006	.0005

JOB NASA-Lewis LOX/LH_2 Vane Pump
EWR #09449

PAGE 7.1.1
DATE 11-11-77
REV.

THERMAL CONTRACTION (LOX) 163°R

SHAFT AND HOUSING MONEL 400 $\alpha = 6.24 \times 10^{-6}$ IN/IN/°F
BEARINGS 440C STAINLESS $\alpha = 4.71 \times 10^{-6}$ IN/IN/°F

ABEC-5	R6	R8	-38
BEARING BORE	.3750 $^{+.0000}_{-.0002}$	.5000 $^{+.0000}_{-.0002}$	.3150 $^{+.0000}_{-.0002}$
AT 163°R		.4991	.3145
FIT (TIGHT)	0-4	0-4	0-4
SHAFT (163°R)		.4993 $^{+.0000}_{-.0002}$	.3147 $^{+.0000}_{-.0002}$
AT (68°F)	.3752 $^{+.0000}_{-.0002}$	.5004 $^{+.0000}_{-.0002}$	.3154 $^{+.0000}_{-.0002}$
FIT (TIGHT)	0-4	2-6	2-6
BEARING O.D. (68°F)	.8750 $^{+.0000}_{-.0002}$	1.1250 $^{+.0000}_{-.0002}$	.8661 $^{+.0000}_{-.0002}$
AT (163°R)		1.1231	.8646
FIT (LOOSE)	0-5	0-5	2-7
HOUSING (163°R)		1.1231 $^{+.0003}_{-.0000}$	.8648 $^{+.0003}_{-.0000}$
AT (68°F)	.8750 $^{+.0003}_{-.0000}$	1.1257 $^{+.0003}_{-.0000}$	.8668 $^{+.0003}_{-.0000}$
FIT (LOOSE)	0-5	7-12	7-12

USE LH_2 SHAFT AND HOUSING DIMENSIONS FOR LOX PUMP

Form G 7756

9.3 SEAL ARRANGEMENT

Seal Selection:

For the oxygen pump a gas trap seal will be used since the pump will operate in the vertical position. The hydrogen pump will use a floating Gits radial seal acting as a labyrinth (controlled leakage) riding on the shaft. Both pumps will utilize back to back Sealol face seals operating at the warm end. Sundstrand experience has been to operate seals at room temperature isolated from the pump by a standoff pipe and insulation. Since Sundstrand has exhibited successful operation with warm seals this program will also use this concept.

Face Seals:

Sealol 800 Class

1.376" O.D. $^{+.002"}_{-.000"}$ (3.495 cm. O.D. $^{+.005\text{ cm}}_{-.000\text{ cm}}$)

.660" I.D. (1.676 cm I.D.)

.515" ± .020" operating length (1.308 cm ± .051 cm)

Face O.D. 1.014" ± .002" (2.57 cm ± .005)

I.D. .874" ± .002" (2.22 cm ± .005)

Metal Bellows - Inconel

Cup and Backplate - 347 Stainless

Carbon Face Clamped By Carpenter 42

Mating Ring 347 Stainless with chrome carbide spray

9.4 Liner Pressure Plate

JOB NASA-Lewis LOX/LH_2 Vane Pump
EWR #09449

PAGE 7.3.0
DATE 11-11-77
REV.

9.4 LINER PRESSURE PLATE

ROTOR SIDE

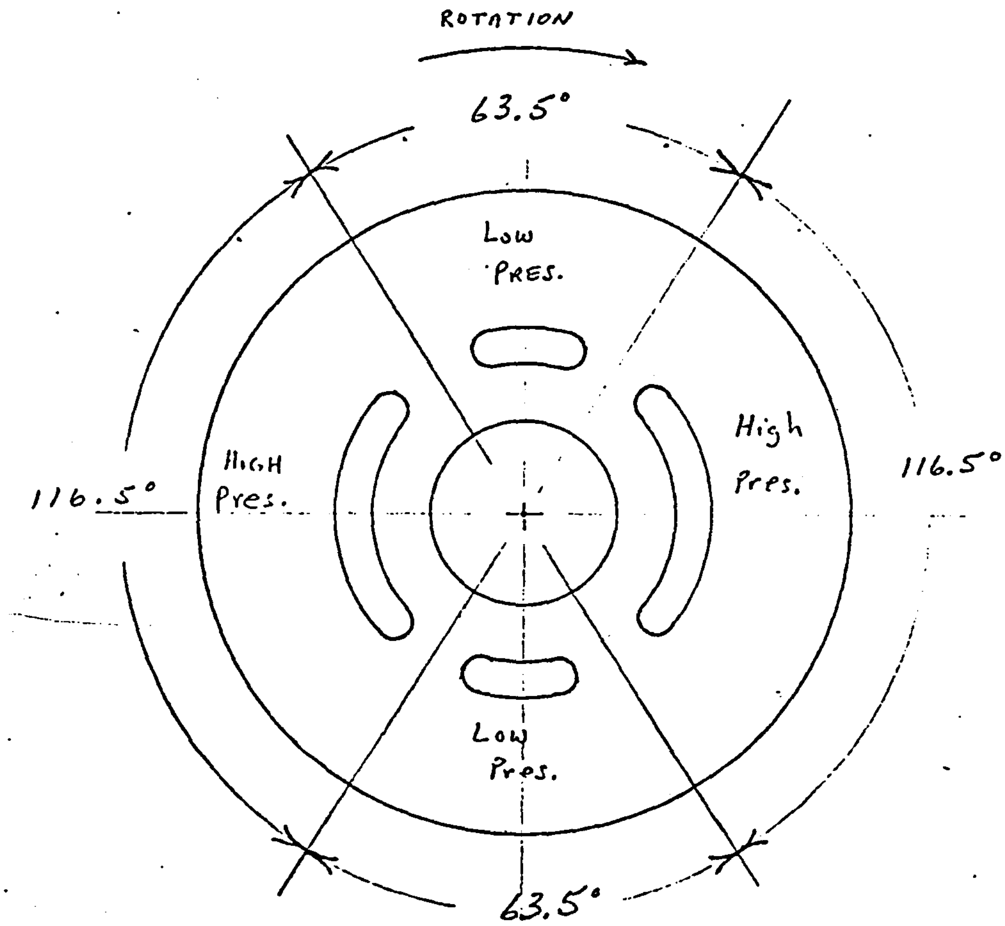

Low PRESSURE $\frac{63.5}{180} = 35.3\%$

High PRESSURE $\frac{116.5}{180} = 64.7\%$

PRESSURE PLATE O.D. = 1.308" = 3.32 cm
PRESSURE PLATE I.D. = .375" = .963 cm
AREA = $(1.308^2 - .375^2)\pi/4 = 1.233\ in^2 = 7.95\ cm^2$
SEAL O.D. = .824 = 2.09 in
HIGH PRES. AREA = $(1.308^2 - .824^2)\pi/4 = .8104\ in^2 = 5.23\ cm^2$
LOW PRES. AREA = $(.824^2 - .375^2)\pi/4 = .4228\ in^2 = 2.73\ cm^2$

JOB NASA-Lewis LOX/LH_2 Vane Pump
EWR #09449

PAGE 7.3.1
DATE 11-11-77
REV.

	LH_2	LOX
HIGH PRES.	230.7 psia (1.59×10^6 N/m²)	337.7 psia (2.33×10^6)
LOW PRES.	27.7 psia (1.91×10^5 N/m²)	27.7 psia (1.91×10^5)
PRESSURE LOADING ROTOR SIDE	196.1 lbs (872.25 N)	281.5 LBS (1252 N)
PRESSURE LOADING SEAL SIDE	198.7 lbs (883.8 N)	285.2 LBS (1268 N)
SPRING LOAD	33.0 lbs (146.78 N)	33.0 LBS (146.7 N)
SEAL PRES LOAD*	29.1 lbs (129.44 N)	42.6 LBS (189.48 N)
TOTAL HYDRAULIC CLAMPING	31.7 lbs. (141. N)	46.3 LBS (205.9 N)

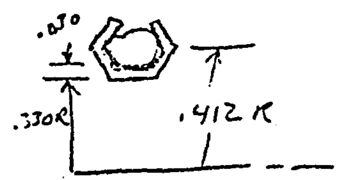

* $\text{LOAD} = (.412^2 - .360^2)\pi P = .126 P$

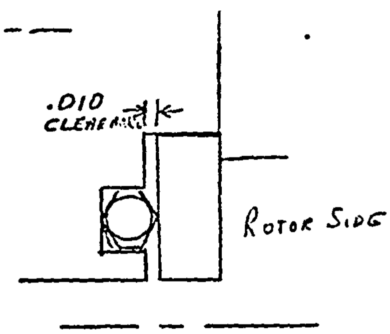

FLUOROCARBON OMNISEAL
AR 214 C 00.664 A1Q

Form G 7756

References

(1) Determination and Assessment of the State of the Art of High Pressure, Centrifugal Oxygen Compressors, Project 3528, Report XII SORI-EAS-76-320, Southern Research Institute, 1961.

(2) Schwartzberg, F. R.; Osgood, S. H.; Bryant, C.; and Knight, M.; Cryogenic Materials Data Handbook. Martin Marietta Corp., 1970.

Volume 1 - Sections A, B and C Revised AFML-TDR-64-280-Vol. I-Rev; AD-713619.

Volume 2 - Sections D, E, F, G, H and I, Revised. AFML-TDR-64-280-Vol. 2 - Rev.; AD 713620.

(3) NASA: Design of Liquid Propellant Rocket Engines. SP-125, 1971.

(4) URASEK, MENG AND CONNELLY: Investigation of Two-Phase Hydrogen Flow in Pump Inlet Line. NASA TN D-5258. July, 1969.

(5) WIESNER: A Review of Slip Factors for Centrifugal Impellers. ASME Paper No. 66-WA/FE-18.

(6) DAILY AND NECE: Chamber Dimension Effects on Induced Flow and Frictional Resistance of Enclosed Rotating Disks. ASME Jl. of Basic Engineering. March, 1960.

(7) RAYMOND J. ROARK, WARREN C. YOUNG: Formula for Stress and Strain, 4th Edition.

APPENDIX

A 4.0 Material

ΔH_f	Heat of oxidation	Kg. cal/100gms
α	Thermal diffusivity	$cm^2/sec.$
k	Thermal Conductivity	cal/sec. cm ^oK
ρ	Density	gm/cm^3
c	Specific Heat	cal/gm ^oK
$\frac{\Delta H_f}{\alpha}$	Burn factor	
V/O	Volume percentage	
WC	Tungsten Carbide	

A5.0 Thermal

$\dot{m}$	Mass Flow rate, kg/per sec.
$\dot{w}$	Work input rate, kcal/sec.
p	Pressure, N/M^2
A	Area, M^2
Fsx	Shaft force exerted upon the fluid, Newtons
U	Fluid velocity in/sec
J	778.10 n. m /Kcal
h	Specific enthalpy, Kcal
S	Specific entropy, kcal/kg ^oK
$\mathcal{E}$	Entropy production rate Kcal/sec
$\dot{Q}$	volume flow rate in^2/sec
V_o	Velocity of the moving plate, m/sec.
b	Clearance between plates, m
t	"thickness" of flow path (at right angles to flow), m
l	Length of flow path, m
μ	Fluid viscosity, average value Kg/m sec
r_j	"radius" or "location" of the moving element j from shaft center line, m
N	rpm
Vc	Clearance volume/revolution; m^3
b_{ks}	kidney-side clearance, m
N_{ovp}	Overall efficiency
Nt	Torque efficiency

continued........

A5.0 (continued)

Nv Volumetric efficiency

Rmaj Cam ring major radius,m

A 6.0 Vane Pump

L	Width of the ran, cm.
R	Major radius of the cam ring, cm.
r	Minor radius of the cam ring, cm.
ΔT	Degree of subcooling of the liquid in ^{o}C

A 7.0 Boost Pump

Δp	Pressure rise, (psi or N/M^2)
ρ	Liquid Density, (lb/ft^3 or N/M^3)
H	Pressure head, (ft or M)
ξ_H	$\dfrac{\text{Distance from center line to the hub}}{\text{Distance from center line to the tip of the leading blade edge}}$
$\beta_{I,T}$	Inducer inlet relative flow angle
$r_{I,T}$	Blade radius at inlet
$r_{I,H}$	Hub radius at inlet
	blade edge
$\beta^*_{I,T}$	Blade angle at the leading edge tip
$i_{I,T}$	Incedence angle
H_I	Inducer pressure head, (ft or M)
$\eta_{I,HYD}$	Inducer hydraulic efficiency
r_{ex}	Inducer average exit radius, (in or cm)
μ_I	slip factor
$C_{Fl,EX}$	Exit flow coefficient
δ_{ex}	Blade blockage factor
β^*_{ex}	Exit blade angle
$\beta_S{}^*$	Blade angle along the shroud
W_{EX}	Fluid relative velocity at exit, (ft/sec. or m/sec)
$W_{I,T}$	Fluid relative velocity at inlet, (ft/sec. or M/sec)
t_D	Fluid dwell time in the inducer, (sec.)
σ_1	Blade solidity of 1st boost stage
$\beta^*_{1,LE}$	1st impeller leading edge blade angle
r_T	impeller tip radius, (in. or cm)
h_T	Tip blade height, (in. or cm)
μ_T	slip factor at blade tip

continued...........

A7.0 (continued)

$C_{FL,T}$	Flow coefficient at impeller tip
ψ	Head Coefficient
$r_{2,LE}$	Leading edge radius of 2nd impeller, cm.
h_2, LE	Pressure head at 2nd stage leading edge, cm.
r_2,LE	2nd stage leading edge radius, cm.
β^*_2,LE	2nd stage leading edge blade angle
β_2, LE	Inlet flow angle
i_2,LE	2nd stage incidence angle
C_2,FL-LE	2nd stage impeller flow coefficient
W_2,T	Relative velocity at 2nd stage impeller discharge, (ft/sec. or M/sec.)
W_2,LE	Relative velocity at 2nd stage impeller inlet., (ft/sec. or M/sec.)

A 8.0 Performance Prediction

$\dot{Q}$	Discharge flow rate, GPM or Liter/Min.
ΔP	Pressure Rise, ft. or M.
η Boost	Efficiency of the centrifugal stage alone
η' Boost	Efficiency of the centrifugal stage in the entire pump package
η Vane	Efficiency of the vane stage
η' Vane	Efficiency of the vane stage in the whole pump package
η'(Boost & Vane)	Efficiency of the entire pump package
P_x	Pressure at the fictitious station X, psi or N/M^2

A 9.1

HP	Horsepower
T	Torque, in. lb. or cm. kg.
N	Speed in RPM
σ_u	Ultimate Tensile Strength, psi or N/M^2
σ_y	Tensile yield strength, psi or N/M^2
τ_y	Shear yield strength, psi or N/M^2
σ_{cy}	Compressive yield strength, psi or N/M^2
M.S.	Margin of safety
N	Safety factor
b	Key width, in or cm.
l	Key length, in. or cm.
σ_b	Bending stress, psi or N/M^2
t	Vanes thickness, in. or cm.
a	Stroke, max. vane travel, in. or cm.
w	Axial vane width, in. or cm.
h	Vane height, in. or cm.
Fc	Centrifugal force, lb. or N
F_p	Pressure force, lb. or N
δ	Poision ratio
b	Width of rectangular contact area, in. or cm.
Sc	Contact stress, psi or N/M^2

r_1	Distance from center line to the labyrinth on the inlet side of the impeller, in. or cm
r_1'	Impeller inlet radius, in. or cm.
r_3	Distance from center line to the labyrinth on the back side of the impeller, in. or cm.
r_2	Impeller discharge radius, in. or cm.
V_{m_1}	Average fluid inlet velocity, ft./sec. or M/sec.
$\dot{m}$	Mass flow rate, lb.-sec.^{2}/ft. or gm/sec.
U_t	Impeller tip velocity, ft./sec. or M/sec.
F_1	Axial thrust on first stage impeller, lb. or N.
F_2	Axial thrust on second stage impeller, lb. or N.

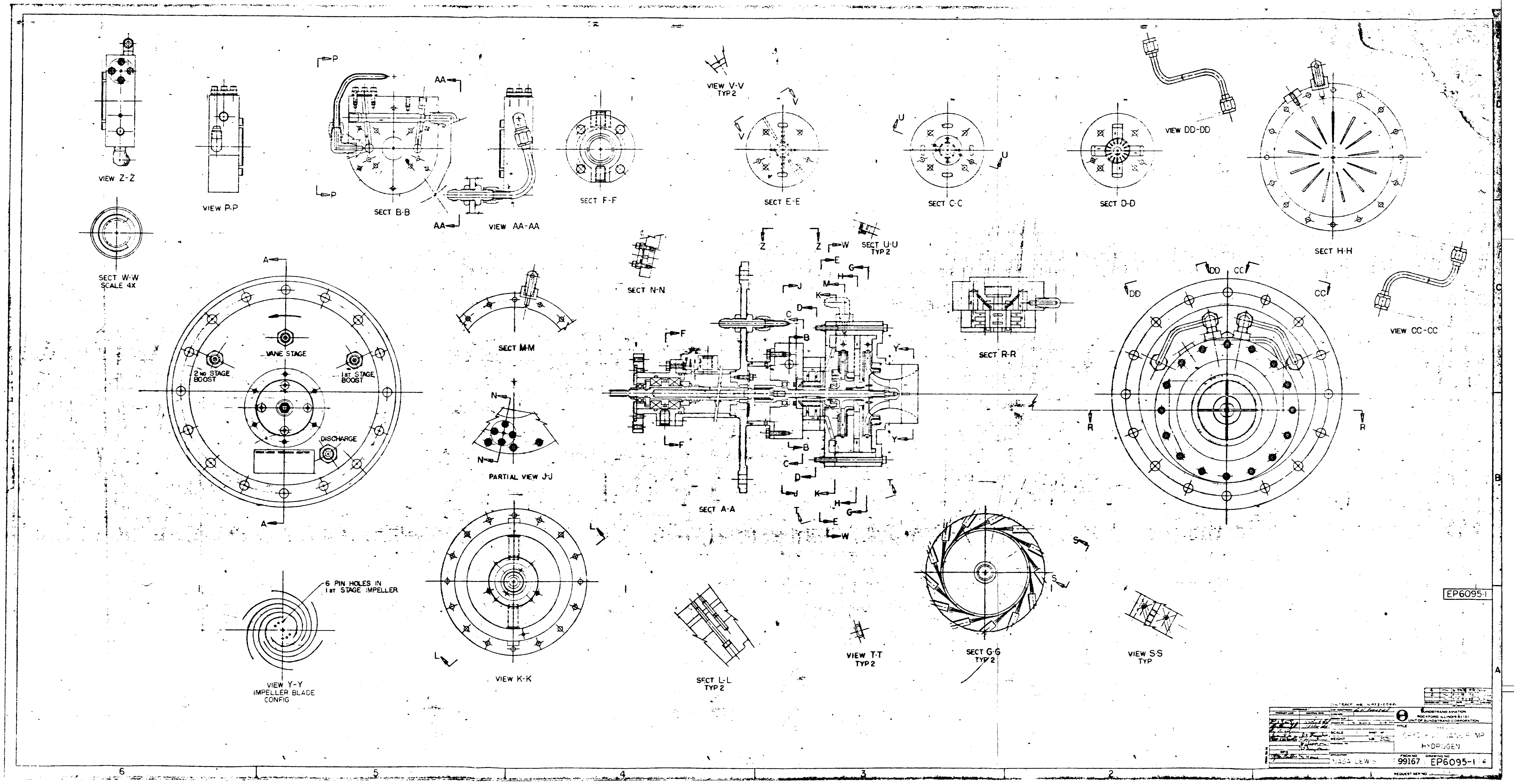

VIEW Z-Z
VIEW P-P
SECT B-B
VIEW AA-AA
SECT F-F
VIEW V-V TYP 2
SECT E-E
SECT C-C
SECT D-D
VIEW DD-DD
SECT H-H
SECT W-W SCALE 4X
SECT N-N
SECT U-U TYP 2
SECT M-M
VANE STAGE
2ND STAGE BOOST
1ST STAGE BOOST
DISCHARGE
PARTIAL VIEW J-J
SECT A-A
SECT R-R
VIEW CC-CC
6 PIN HOLES IN 1ST STAGE IMPELLER
VIEW Y-Y IMPELLER BLADE CONFIG
VIEW K-K
SECT L-L TYP 2
VIEW T-T TYP 2
SECT G-G TYP 2
VIEW S-S TYP
EP6095-1
SUNDSTRAND AVIATION
ROCKFORD ILLINOIS 61101
UNIT OF SUNDSTRAND CORPORATION
TITLE
HYDROGEN
SCALE
WEIGHT
MFG
FSCM NO
99167
DRAWING NO
EP6095-1
REQUEST SER NO

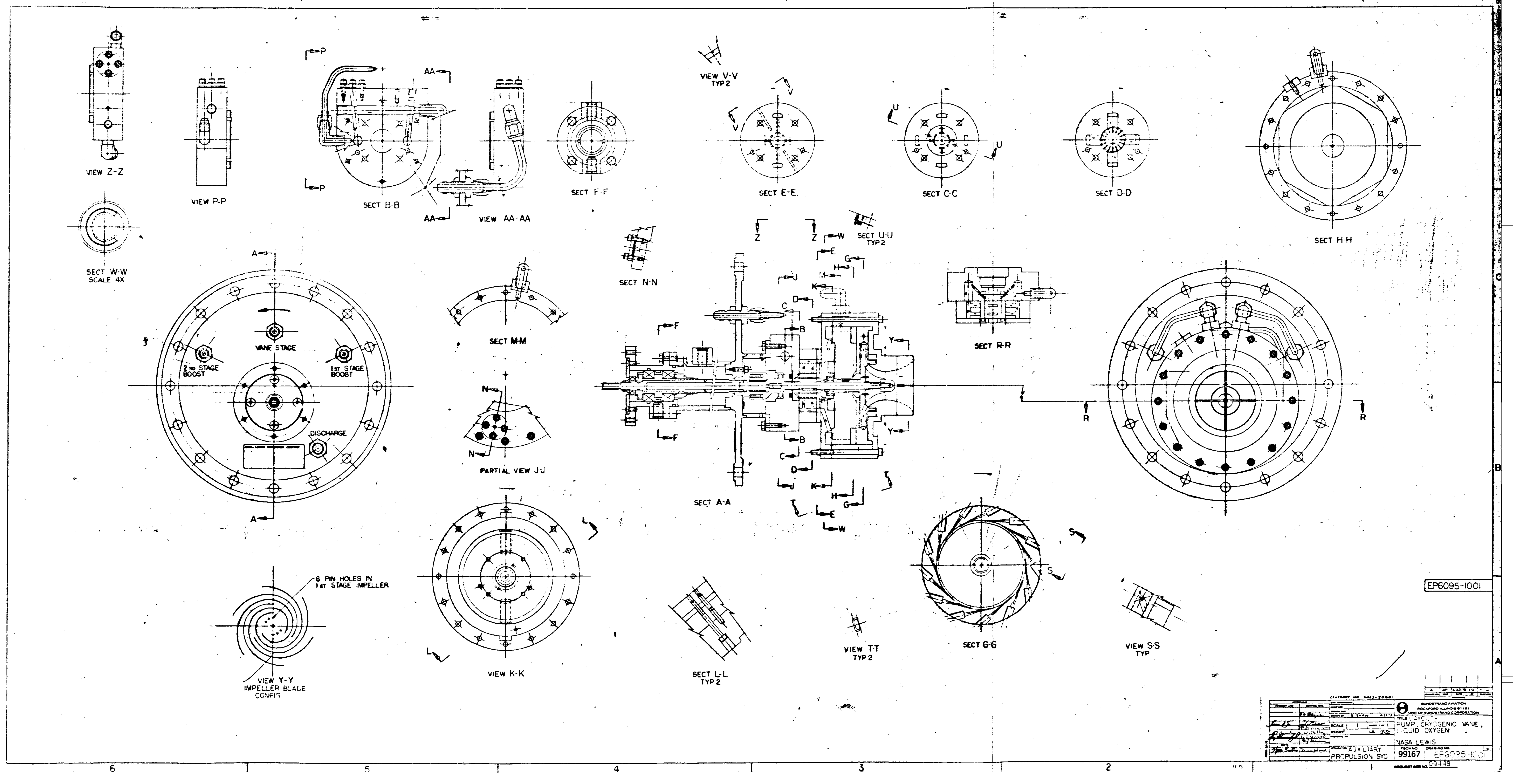

VIEW Z-Z
VIEW P-P
SECT B-B
VIEW AA-AA
SECT F-F
VIEW V-V TYP 2
SECT E-E
SECT C-C
SECT D-D
SECT H-H
SECT W-W SCALE 4X
SECT U-U TYP 2
SECT N-N
VANE STAGE
2ND STAGE BOOST
1ST STAGE BOOST
DISCHARGE
SECT M-M
PARTIAL VIEW J-J
SECT A-A
SECT R-R
6 PIN HOLES IN 1ST STAGE IMPELLER
VIEW Y-Y IMPELLER BLADE CONFIG
VIEW K-K
SECT L-L TYP 2
VIEW T-T TYP 2
SECT G-G
VIEW S-S TYP
EP6095-1001
CONTRACT NO. NAS3-20401
DRAWN BY S. SHAW
SCALE 1
SUNDSTRAND AVIATION
ROCKFORD ILLINOIS 61101
UNIT OF SUNDSTRAND CORPORATION
TITLE LAYOUT - PUMP, CRYOGENIC VANE, LIQUID OXYGEN
NASA LEWIS
APPLICATION AUXILIARY PROPULSION SYS
FSCM NO 99167
DRAWING NO. EP6095-1001
REQUEST SER NO. 09449